CYCLIC TESTS ON LARGE SCALE STEEL MOMENT CONNECTIONS

Michael D. Engelhardt

Abunnasr S. Husain

Report to the Sponsor:
The Steel Committee of California

Report No. PMFSEL 92-2
Phil M. Ferguson Structural Engineering Laboratory
The University of Texas at Austin

June 1992

ABSTRACT

Moment resisting frames are widely used in earthquake resistant steel construction. The beam-to-column connections play a crucial role in the performance of these frames. For the popular detail of the welded flange - bolted web type moment connection, the 1988 UBC requires supplemental web welds between the shear tab and the beam web for beam sections where $Z_f/Z \leq 0.70$. Z is the plastic modulus of the beam, and Z_f is the plastic modulus of the beam flanges only. Past tests have suggested that inadequate participation of the beam web connection in transferring moments may have a detrimental effect on inelastic deformation capacity of the beam, particularly for beam sections characterized by a low Z_f/Z. The supplemental web welds are intended to increase the flexural participation of the web connection for such sections.

An experimental investigation was conducted on large scale beam-column subassemblages to collect additional data on the effect of the Z_f/Z ratio and the web connection details. A total of eight specimens was tested. Three different beam sections were used: W24x55 (Z_f/Z = 0.61), W21x57 (Z_f/Z = 0.67) and W18x60 (Z_f/Z = 0.75). Web connection details included bolted webs, bolts with supplemental web welds, and a single specimen with a fully welded web connection. All connections were to the flange of a W12x136 column. The panel zone of the column was sufficiently strong so as to force inelastic deformations to occur primarily as flexural yielding of the beam at the connection. All specimens were loaded cyclically to failure. Specimens were constructed by a commercial structural steel fabricator and inspected by an independent welding inspection firm. Inspection included ultrasonic testing of all complete penetration groove welds.

Results of the testing program showed highly variable performance among the eight specimens. The primary criterion for judging performance was the plastic rotation

developed by the beam prior to connection failure. All connections failed by fracture in the vicinity of the complete penetration beam flange groove welds. Plastic rotations developed by the beams varied from ± .002 radian to ± .015 radian.

The tests showed no clear influence of the Z_f/Z ratio or web connection detail on beam plastic rotation capacity. Rather, the highly variable quality of the complete penetration beam flange groove welds appears to have dominated the response of the specimens. Nonetheless, the specimens with supplemental web welds developed somewhat larger plastic rotations than their counterparts without web welds. Consequently, no change is recommended at present in the UBC detailing requirement pertaining to supplemental web welds.

The eight specimens tested in this program showed highly variable and unpredictable behavior, and developed plastic rotations that were judged as poor to marginal for severe seismic applications. Tests by other investigators have also shown similar variable results. Some of this variability can be attributed to the influence of the Z_f/Z ratio and web connection details. However, a great deal of the variability also appears to be related to the performance of the beam flange groove welds.

The final recommendation of this investigation calls for a review of current industry practice for seismic steel moment connections. The results of this and previous test programs leads to questions on the reliability of the welded flange - bolted web detail for severe seismic applications. A thorough review of design and detailing practices, as well as welding and quality control issues is needed.

ACKNOWLEDGEMENTS

The research described herein was made possible through funding provided by the Steel Committee of California. AISC Marketing, Inc. acted as the coordinator between the Steel Committee and the researchers. Thanks are due to Messrs. Roger Ferch, Jim Malley, Jim Marsh, Hank Martin, Clarkson Pinkham, Egor Popov, Mark Saunders, Jerry Shantz, Ed Teal and the late Henry Degenkolb who acted as the advisory committee for this project. Rudy Hofer of AISC Marketing, Inc. deserves the gratitude of the authors for providing coordination of the entire project. Thanks are also due to Jim Anders of AISC Marketing, Inc. in Dallas for assisting in the project. The comments of Mr. A. L. Collin in reviewing this report are also appreciated.

The donation of steel for the columns and the beams of the test specimens by Bethlehem Steel and Nucor-Yamato Steel is gratefully acknowledged.

The authors would also like to express their gratitude to Dr. Joseph Yura and Dr. Karl Frank of The University of Texas at Austin for their interest and suggestions. Thanks are due to the Ferguson Laboratory staff for assisting in the experiments.

The opinions expressed in this report are those of the authors and do not necessarily reflect the views of the sponsor nor of the individuals noted above.

TABLE OF CONTENTS

LIST OF TABLES

LIST OF FIGURES

1 - INTRODUCTION

1.1 GENERAL

Moment Resisting Frames (MRFs) represent a widely used structural system for earthquake resistant steel construction. The popularity of MRFs lies in their recognized ability to provide ductile response to earthquake loading, as well as their architectural versatility.

Like any earthquake resistant system, there are three main issues of interest in MRF design: strength, stiffness and ductility. The required strength of the frame, as established by code specified lateral forces, is often less than that needed to remain completely elastic during a severe earthquake. Consequently, ductility must be provided in order to sustain the anticipated inelastic deformations. Stiffness requirements are established by code specified drift limits, which for MRFs, frequently control member sizes. Code based earthquake resistant design [3,10,12,23] is largely based on elastic analysis in establishing member sizes to satisfy strength and stiffness requirements. The need for ductility is treated through various detailing requirements, which are intended to ensure that adequate inelastic deformations can be developed by the frame during a severe earthquake.

A number of significant changes and additions were introduced in the detailing requirements for steel structures in the 1988 SEAOC Recommended Lateral Force Requirements [23], commonly known as the *Blue Book*. (Since then, the 1990 Blue Book has been released but contains no significant changes over the 1988 edition for steel detailing). These detailing requirements were adopted by the 1988 Uniform Building Code [12] with minor modifications. The NEHRP Recommended Provisions for the Development of Seismic Regulations for New Buildings [10] and the AISC LRFD

Seismic Provisions for Structural Steel Buildings [3] have also adopted similar provisions. The new detailing requirements introduced in the 1988 Blue Book have therefore been widely adopted by other code and model code documents, and consequently, can be expected to have an important impact on future seismic resistant steel construction. Some of the new detailing requirements pertaining to steel beam-to-column moment connections introduced in the 1988 Blue Book are the subject of the research described in this report.

1.2 MOMENT CONNECTIONS

A number of the new detailing requirements in the 1988 Blue Book pertain to the beam-column joint in steel MRFs. The joint region is critical since the ductility of MRFs is typically developed by inelastic deformations in this region, in the form of flexural yielding of the beam and/or shear yielding of the column panel zone. The beam-to-column connection must be capable of developing the strength of the beam or panel zone, and maintain that strength as the beam or panel zone undergoes large inelastic deformations.

There are two basic types of moment connections. One type occurs when the beam frames into the strong bending direction of the column i.e. the beam-to-column flange type of connection. The other type occurs when the beam frames into the weak bending direction of the column i.e. the beam-to-column web connection. This study addresses only beam-to-column flange connections. Although several details are available for beam-to-column flange moment connections, the most widely used detail in current practice is the welded flange-bolted web type connection. The flanges of the beam are welded to the column flange using complete penetration groove welds. Single bevel groove welds with backup plates are used. These welds are typically made in the field using the self shielded flux core arc welding process. Web copes are provided to accommodate the backup plate at the top flange and to permit making the continuous weld at the bottom flange. The beam web is bolted to a single plate shear tab, which is shop welded to the column flange.

The strength and ductility of this standard moment connection under cyclic loading has been studied in several experimental investigations using large scale test specimens [8,9,14-17,24]. However, considering the importance and widespread use of the welded flange-bolted web detail, the amount of experimental investigation is actually rather limited.

An investigation by Popov and Stephen [16] was one of the earliest cyclic test programs on large scale steel moment connections. This investigation (using W18x50 and W24x76 beams) compared the performance of all welded connections to the performance of welded flange-bolted web connections. The all welded connections showed outstanding performance, permitting very large inelastic beam rotations without failure. The welded flange-bolted web connections did not, in general, perform as well. These connections failed by fractures occurring in the region of the complete penetration groove welds. Further, the performance of the connections with bolted webs showed considerable variability. Nonetheless, these connections did develop substantial inelastic beam rotations, and were judged as being adequate for many seismic applications.

Subsequent tests on moment connections with bolted webs showed somewhat mixed results [15,17,24]. In some tests, the connections developed large inelastic rotations. Others showed rather poor performance, with failure of the connection occurring at fairly low levels of inelastic rotation. The predominant failure mode for the connection tests with bolted webs was fracture at or near the complete penetration beam flange welds.

An important conclusion that can be drawn by studying the available cyclic test data on welded flange-bolted web details, is that the performance of this connection has been erratic, with some specimens performing well and others performing poorly. The large variability in the experimental observations can perhaps be related to the large

number of design and detailing variables that may influence the performance of this connection. Table 1.1 provides a partial list of the factors which may have an influence on the strength and ductility of the welded flange-bolted web connection of a beam to the column flange. Additional factors could be added for moment connections to the column web, which have shown even greater variability in experimental performance [17].

TABLE 1.1

Factors Influencing the Performance of

Welded Flange - Bolted Web Moment Connections

1. Flange weld details.
   - root opening
   - bevel angles
   - welding process (SMAW, FCAW, etc.)
   - level of skill and workmanship of welder
   - thickness of beam flange and column flange
   - flanges welded before or after tensioning of bolts
   - size and method of tacking backup strip
   - use of run-out and extension plates
   - are run-out and extension plates removed after welding?
   - use of preheat for thick materials
   - type and quality of weld inspection
   - detection of possible laminations in the column flange

2. Web cope details
   - overall dimensions: length, depth and radius of web copes
   - method of cutting web copes
   - grinding of web copes

3. Beam web connection details
   - number, size and grade of bolts
   - type of hole: standard, oversize or slotted
   - bolt installation and inspection procedures
   - condition of faying surfaces
   - size and placement of supplemental web welds
   - are supplementary web welds made after flange welds have fully cooled?

4. Beam characteristics
   - value of Z_f/Z for beam section
   - grade of steel: A36, A572 Gr.50, etc.
   - flange and web slenderness
   - lateral support
   - presence of a composite deck

5. Column and column panel zone characteristics
   - the size and weld details of continuity plates, if used
   - the size and weld details of doubler plates, if used
   - column panel zone shear strength

6. Loading characteristics
   - symmetric cyclic loading vs. random cyclic loading
   - the presence of a single large pulse in the loading
   - number of applied inelastic cycles
   - location of the point of inflection in the beam
   - magnitude of gravity load on beam
   - magnitude of the applied shear force at the connection

Of the many factors listed in Table 1.1, this study addresses some of the variables related to the beam web connection details and beam characteristics.

1.3 BEAM WEB CONNECTION DETAILS

The design of welded flange-bolted web connections is usually based on the assumption that the flanges carry all the moment and the web carries all the shear. Consequently, the bolted web connection is typically designed for shear only. Its participation in resisting moments is not explicitly considered in design calculations.

Tests have shown, however, that the web participation in resisting moments may have a significant influence on overall connection performance under cyclic load [16,17,24]. Cyclic tests on all welded connections typically show significant yielding of the flanges and the web of the beam, indicating participation of the web in developing the flexural strength and ductility of the beam. Conversely, tests on connections with bolted webs typically show little or no yielding of the web, indicating that the bolted web connection does not develop the flexural capacity of the beam web. This results in increased forces in the flanges to carry the same moment, which in turn may lead to an earlier failure of the flange connection.

The fact that connections with bolted webs usually develop less ductility than connections with welded webs has generally been attributed to slip in the bolted web connection [17,24]. However, providing a bolted web connection capable of developing the flexural strength of the web without slip is neither a realistic nor a necessary requirement. This can be demonstrated by the simple example shown in Figure 1.1. This example, for a W24x76 beam with seven 7/8" A325 bolts, estimates the moment developed by the web connection when the bolts have reached their slip loads. Although based on some simplifying assumptions, this simple calculation shows that the bolted web connection can only develop approximately 22% of the beam web's flexural strength at

the slip load of the bolts. Any shear force carried by the bolts would further reduce this percentage. This example is intended to demonstrate that it would be virtually impossible to design a bolted web connection capable of developing the flexural strength of a web without slip. Slip measurements in the experiments by Popov and Stephen [16] confirmed that slip in the web connection occurred early in the cyclic loading process. Yet, despite the slip, many of the specimens showed satisfactory performance. Thus, the occurrence of slip cannot, by itself, be considered a failure condition.

In assessing the importance of the flexural capacity of the web connection, the relative contribution of the beam web towards the full moment capacity of the beam must be considered. The relative flexural contribution of the web can be evaluated in terms of the ratio M_{pf}/M_p, where M_p is the fully plastic moment of the beam and M_{pf} is the fully plastic moment of the flanges only. The theoretical upper bound for this ratio is 1.0, corresponding to a beam section with no web. As the value of M_{pf}/M_p becomes smaller, the web contributes an increasingly large share of the beam's total flexural capacity. Correspondingly, the moment carrying capacity of the web connection can be expected to exert an increasingly greater influence on the overall performance of the connection. The inability of the web connection to develop an adequate flexural capacity for sections with low values of M_{pf}/M_p results in significantly increased flange forces, with the resulting tendency for an earlier failure of the flange connection. For example, consider a beam with M_{pf}/M_p equal to 0.66 (a W18x35 or W21x57). If the web connection is unable to develop any moment, the flanges must strain harden to $1.5F_y$ just to develop M_p of the section (this may not be possible if $F_u < 1.5F_y$). Further strain hardening of the flanges may be needed to develop adequate inelastic beam rotations. This simple example demonstrates that the inability of the web connection to develop moment can result in an increase in flange forces of 50% or more. Yet, this important factor is typically neglected in the design of the web connection.

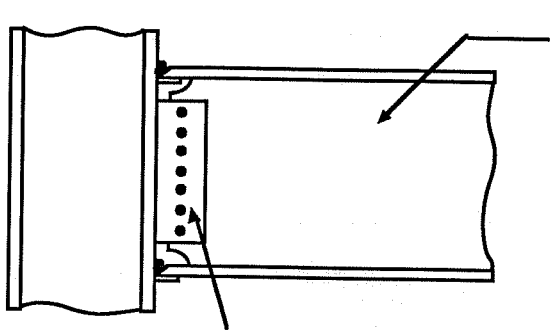

Figure 1.1 - Example of
Bending Moment Developed by Bolt Slip Loads

It should be noted that the ratio M_{pf}/M_p can be taken equal to Z_f/Z only if the yield strength of the flanges and the web are the same. Z is the plastic modulus of the entire beam and Z_f is the plastic modulus of the flanges only. Tensile coupons from test specimens typically show a higher yield strength in the web than in the flanges. Consequently, the value of M_{pf}/M_p will typically be somewhat less than the value of Z_f/Z, indicating an even greater contribution of the web in developing the actual strength of the section.

In evaluating previous experimental programs on steel moment connections, it has been recognized that the majority of the test specimens used beam sections with Z_f/Z greater than 0.7. Yet a significant number of rolled W shapes are characterized by Z_f/Z ratios less than 0.7, with some as low as 0.61 (W24x55). Based on this observation, a recent series of tests by Tsai and Popov used beam sections with Z_f/Z less than 0.70 [17,24]. These tests, conducted on W18x35 (Z_f/Z = 0.66) and on W21x44 (Z_f/Z = 0.62) beams, with specimens produced by commercial structural steel fabricators, showed several interesting trends. The specimens fabricated with the standard welded flange-bolted web detail performed poorly, failing in the usual manner by fracture of the beam flange at rather low levels of inelastic rotation. It was found, however, that the performance of this connection was substantially improved when tension control bolts were used for the web connection, or when small fillet welds were added near the top and bottom of the shear tab. These welds were sized to nominally develop 20% of $M_{p\,web}$, where $M_{p\,web}$ is the fully plastic moment of the beam web. Based on this criterion, the welds used were quite small. Yet, a remarkable improvement in performance was observed.

These tests, though on a very limited number of specimens, demonstrated the importance of the web connection for beam sections with relatively low values of Z_f/Z. These tests also suggested the possibility that adequate web participation can be achieved either through the use of supplemental web welds, or by assuring proper tensioning of the bolts combined with due care for the condition of the faying surfaces. However, the results also suggest that current fabrication and erection practices may not consistently provided properly tensioned bolts.

1.4 OBJECTIVES AND SCOPE

A new detailing requirement in the 1988 Blue Book (Section 4F.1.b.(2)) and in the 1988 UBC (Section 2722 (f) 2B) requires that any beam section with $Z_f/Z \leq 0.7$ must

be provided with welds between the shear tab and beam web with a nominal strength to develop 20% of $M_{p\,web}$, in addition to high strength, fully tensioned bolts to carry the beam shear.

The new requirement for supplemental web welds is based on a small number of tests. Accordingly, the overall objective of this study is to obtain additional experimental data on the influence of the web connection detail on the performance of welded flange-bolted web moment connections. More specifically, this study is intended to provide additional experimental data that will contribute to answering the following questions:

1. If fully tensioned high strength bolts (A325 or A490) are used, are supplemental web welds still needed?
2. What is the limiting value of Z_f/Z, below which supplemental web welds are required to develop adequate ductility of the beam without connection failure?

The focus of this research study was an experimental program involving eight large scale cantilever type test specimens. The remainder of this report describes the experimental setup and test specimens, performance of the specimens under cyclic load, and analysis of the resulting data. General observations and discussion follow at the end of the report.

2 - EXPERIMENTAL SETUP

2.1 GENERAL

The experimental program was designed to investigate the behavior of the welded flange-bolted web type moment connection based on the issues discussed in Chapter 1. The main objective was to investigate the web connection requirements for beams of varying Z_f/Z ratios. The primary variables considered in this program were:

- Beam sections with different Z_f/Z ratios, but with approximately the same M_p.
- Different amounts of bolt tension in the web bolts.
- Effect of supplementary welds between the shear tab and beam web, sized nominally to develop 20% of $M_{p\,web}$.

2.2 SUBASSEMBLAGE

The test setup is illustrated in Figure 2.1. A subassemblage was chosen as a single beam connected to the column in the strong bending direction of the column, and models a portion of a seismic resistant MRF. Boundaries of the subassemblage were chosen to approximately coincide with the inflection points in an MRF under lateral load.

The dimensions of the subassemblage were chosen to represent a frame at or near full scale. The column height of 12 ft was selected as a nominal story height with assumed inflection points at mid-height. The length of the beam in the subassemblage was selected to be 8 ft measured from the face of the column to the point of load application. The actual location of inflection points in a column varies during an earthquake. This is an important issue for column design, but should have little effect on connection behavior. The location of the inflection point in an MRF beam depends on a number of factors, including span length and the relative magnitudes of lateral and gravity loads, and would

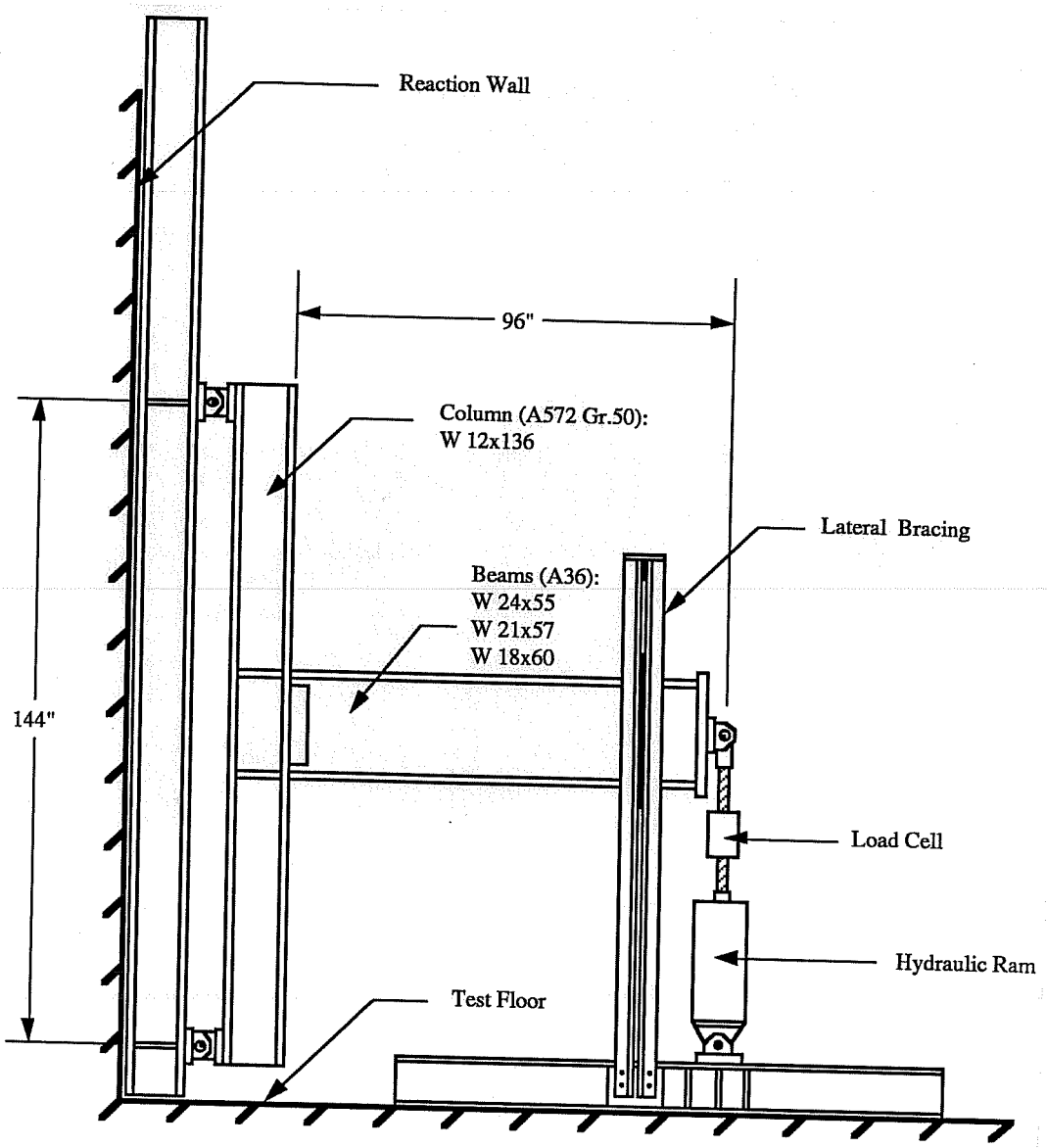

Figure 2.1 - Test Setup

also be expected to vary during the course of an earthquake. The subassemblage provides for a constant 8 ft distance from the column to the point of inflection, representing a considerable simplification compared to actual loading conditions. However, it is believed

that this subassemblage provides a reasonable simulation of the loading environment for the beam-to-column connection. This subassemblage is also consistent with previous experimental investigations [14-17,24], permitting a meaningful comparison of results.

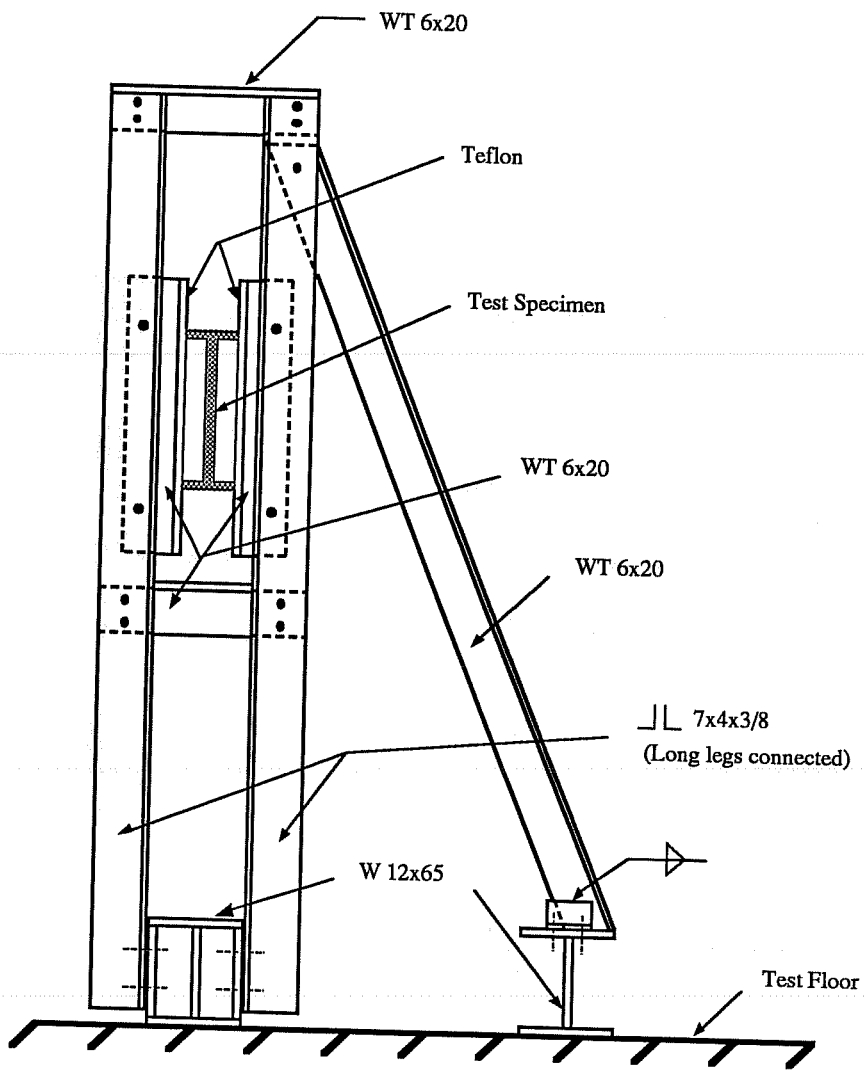

Figure 2.2 - Lateral Bracing

The column of the subassemblage was held in place by means of clevis attachments, permitting free rotations at the column ends. A cyclic load was applied to the end of the beam by a hydraulic ram.

Lateral bracing was provided for the beam near the loading point. Details of the lateral bracing are shown in Figure 2.2. Teflon was provided at points of contact between the beam and the lateral support, to permit free movement in the vertical direction.

All tests were conducted at The University of Texas Phil M. Ferguson Structural Engineering Laboratory in Austin, Texas.

2.3 DESCRIPTION OF TEST SPECIMENS

A total of eight specimens was tested. Each specimen consisted of an 8 ft beam segment connected to a 12 ft column segment, as indicated in Figure 2.1. The test specimens, as described below, were designed in consultation with the project's advisory committee.

2.3.1 Beam Sections

The beam sections used for the test specimens are listed Table 2.1. As noted earlier, a primary variable of this study was the Z_f/Z ratio of the beam section. Accordingly, three different sections, W24x55, W21x57, and W18x60 with Z_f/Z ratios of 0.61, 0.67, and 0.75 respectively, were used. These were chosen to represent Z_f/Z ratios both above and below the 0.70 value currently specified in the Blue Book for the use of supplemental web welds. Note that supplemental web welds are required on the W24x55 and W21x57 according to the 1988 Blue Book provisions. All beam sections were A36 steel. All beams of the same size were taken from the same heat of steel.

2.3.2 Column Section

The columns for all eight test specimens were W12x136 sections of A572 Gr 50 steel. This section was chosen primarily to provide a strong column panel zone. The nominal shear strength of the panel zone of the W12x136 is considerably in excess of that required to develop the nominal M_p of the test specimens' beam sections. (Data on panel zone strength is provided in Chapter 4). Consequently, little or no inelastic deformation was expected within the panel zone. The test specimens are therefore representative of beam-column joints in which ductility must be developed by flexural yielding of the beam. The W12x136 column section also satisfies the strong column-weak girder design provisions of the 1988 Blue Book. Seven of the eight W12x136 sections used for the test specimens were from the same heat of steel. (Eight W12x136 sections of the same heat were not available from the steel supplier). The single W12x136 section from a different heat was used in Specimen 8.

TABLE 2.1 - Test Specimens

Specimen	Beam	Z_f/Z	Web Connection
1	W 24x55	0.61	6 - 7/8" A325 Bolts
2	W 24x55	0.61	6 - 7/8" A490 Bolts
3	W 24x55	0.61	6 - 7/8" A325 Bolts + 20% web weld
4	W 18x60	0.75	4 - 7/8" A325 Bolts
5	W 18x60	0.75	4 - 7/8" A325 Bolts
6	W 21x57	0.67	5 - 7/8" A325 Bolts
7	W 21x57	0.67	5 - 7/8" A325 Bolts + 20% web weld
8	W 21x57	0.67	All welded, with 3 - 7/8" A325 Erection Bolts

Notes: (1) All beams A36
(2) Bolt tension : 7/8" A325 - 41k : 7/8" A490 - 51.5k

2.3.3 Connection Details

Connection details are illustrated in Figure 2.3. Complete penetration single bevel groove welds were used to connect the beam flange to the column flange in all eight specimens. Details of the flange welds are discussed in Section 2.5.

A variety of web connection details, illustrated in Figure 2.3, and summarized in Table 2.1, were used for the eight specimens. These included all bolted connections (Specimens 1, 2, 4, 5, 6), bolted connections with supplemental web welds (Specimens 3 and 7), and an all welded web connection (Specimen 8). All specimens used 7/8" A325 bolts, with the exception of Specimen 2, which used 7/8" A490 bolts. All bolts were fully tensioned, using installation methods described in Section 2.5.2. The bolts were all conventional A325 or A490 bolts, i.e. tension control bolts were not used.

For each of the beam sections used in the test program, three 7/8" A325 bolts would have been sufficient to satisfy the 1988 Blue Book connection shear strength requirements (Section 4F 1 (b)). The required connection shear strength can be taken as the shear force in the beam when M_p is developed. For the test specimens, this can be computed as the nominal M_p of the beam, divided by the cantilever length of 96 inches. This results in shear forces of 50 kips, 48 kips, and 46 kips for the W24x55, W21x57, and W18x60 sections, respectively. The shear strength of one 7/8" A325 bolt is taken as 17.3 kips. (1.7 times the allowable force for a slip critical connection with class A surface per Section 4.C.2 of the 1988 Blue Book). Consequently, three 7/8" A325 bolts provide 52 kips shear capacity, which is adequate for the required shear forces noted above.

Based on discussions with the project's advisory committee, it was judged that more than the minimum required three bolts would typically be used for these beam sections in current California practice. Thus, the number of bolts was somewhat arbitrarily increased to provide four, five, and six bolts for the W18x60, W21x57, and W24x55

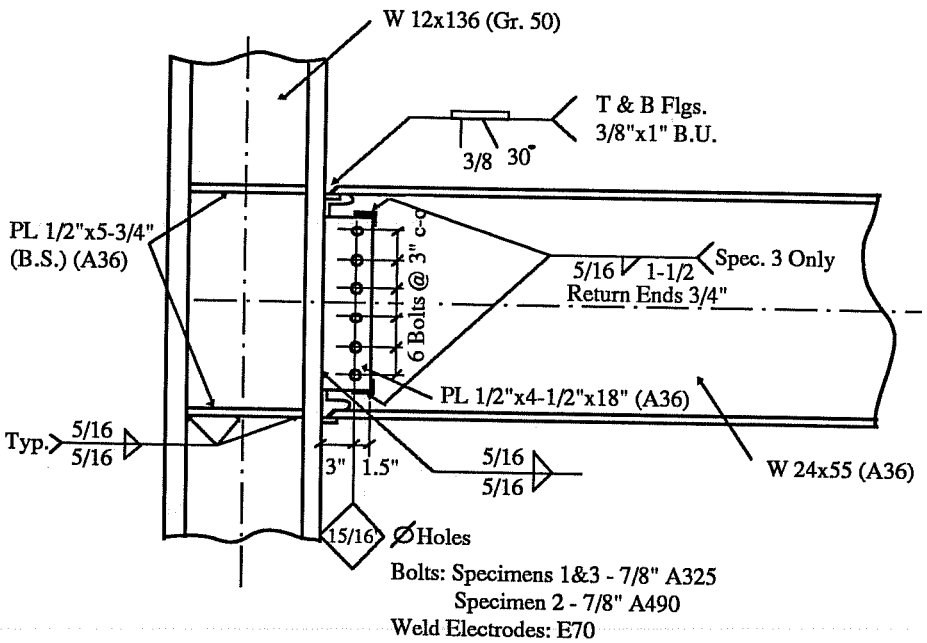

Figure 2.3(a) - Specimens 1, 2, and 3

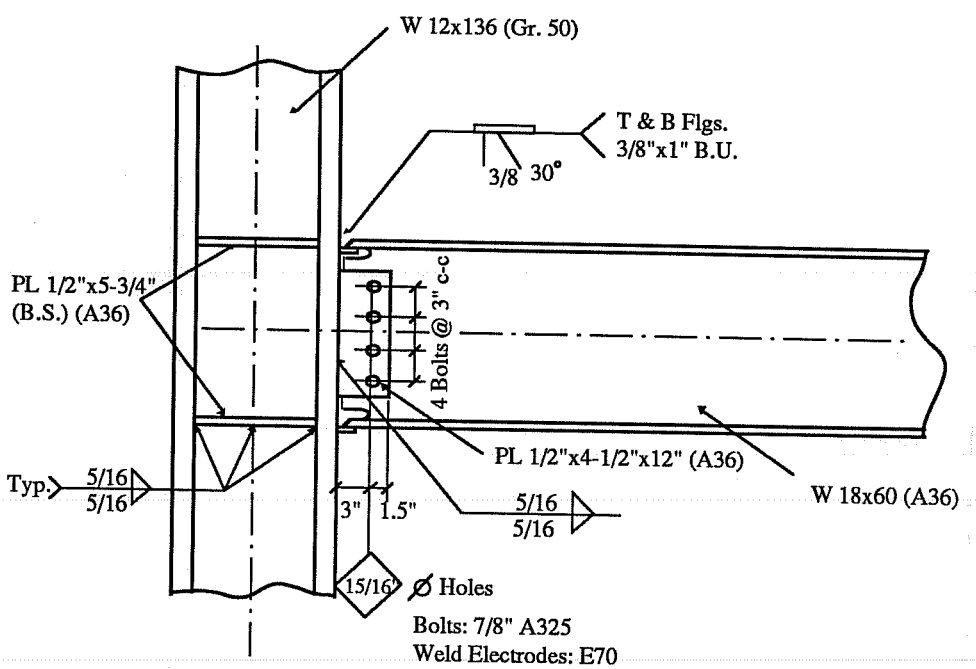

Figure 2.3(b) - Specimens 4 and 5

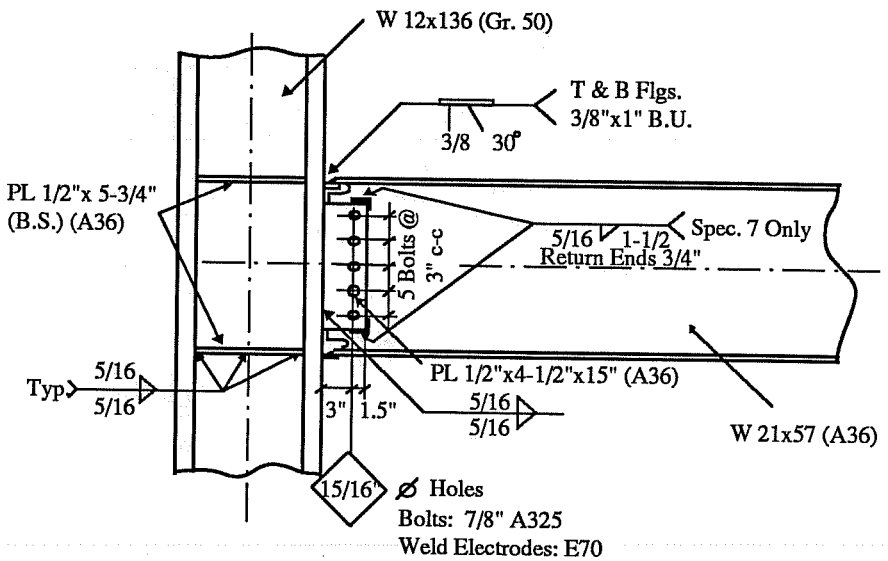

Figure 2.3(c) - Specimens 6 and 7

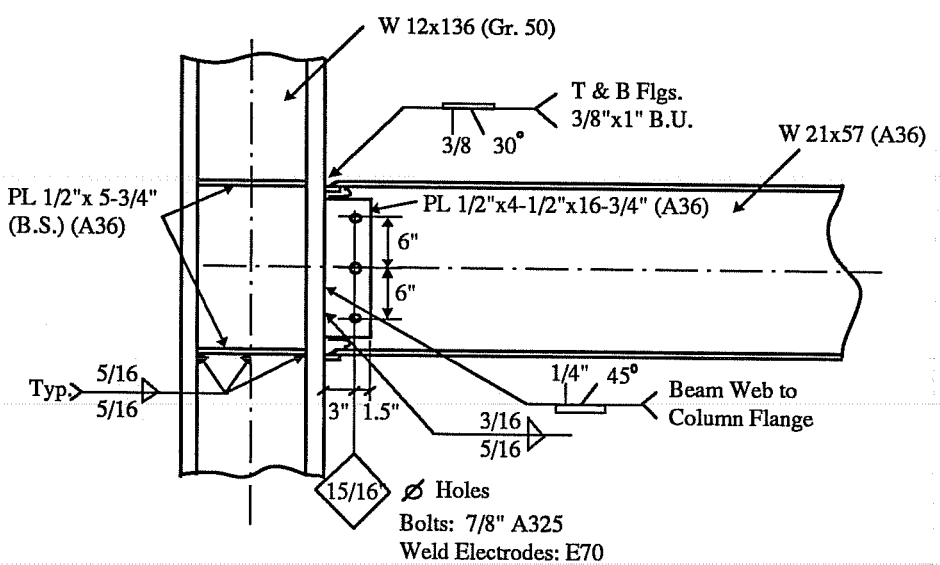

Figure 2.3(d) - Specimen 8

sections, respectively, to be more representative of typical detailing practices. Only three bolts were used on Specimen 8, to simulate erection bolts used with the all welded connection.

In addition to web bolts, Specimens 3 and 7 were provided with supplemental welds at the top and bottom of the shear tab, as indicated in Figure 2.3. These welds were sized to provide a nominal strength of 20% of $M_{p\,web}$, where $M_{p\,web}$ was computed as 36 ksi * $(d\text{-}2t_f)^2 * t_w/4$. Weld strength was computed at 1.7 times allowable, per Section 4.C.2 of the 1988 Blue Book.

All specimens were provided with 1/2 inch thick continuity plates, as shown in Figure 2.3. According to 1988 Blue Book requirements (Section 4.F.4), continuity plates are not required for any of the test connections. Continuity plates were provided, however, to eliminate the possible influence of local column flange bending as an additional variable affecting the test results. According to Section 4.F.2 of the 1988 Blue Book, no doubler plates are required for any of the test specimens, and none were provided.

The connection design for Specimens 3, 4, 5, 7, and 8 met or exceeded all 1988 Blue Book requirements. The connection design for Specimens 1, 2, and 6 intentionally violated the requirements for supplemental web welds, but satisfied or exceeded all other requirements.

2.4 SECTION AND MATERIAL PROPERTIES

2.4.1 Tensile Coupon Tests

Standard tensile coupon tests were performed on 18" long plate type coupons cut from the beam sections and from a column section. There were two coupons taken from each section, one from the flange and one from the web. The web coupons were taken

from the mid-depth of the members while the flange coupons were taken from the edge. The coupon data are reported in Table 2.2.

As noted earlier, all beam sections of the same size were taken from the same heat of steel. Seven of the eight W12x136 column sections were also from a single heat. The column coupon data was taken from one of these seven. No coupons were tested for the single W12x136 section that was from a different heat. Note that column coupon data is not of primary interest for these tests, since the beams were expected to sustain almost all of the inelastic deformations.

TABLE 2.2 - Tensile Coupon Data

Section	Location	Static Yield (ksi)	Dynamic Yield (ksi)	Static Ultimate (ksi)	Dynamic Ultimate (ksi)	Percent Elongation (%)
W24x55	Flange	41.6	44.8	59.6	63.9	29.3
W24x55	Web	42.3	45.3	58.6	62.5	30.6
W21x57	Flange	38.4	40.8	56.1	60.2	25.4
W21x57	Web	36.5	40.8	54.7	58.2	33.0
W18x60	Flange	40.9	43.9	59.9	63.7	29.8
W18x60	Web	43.0	44.9	59.9	62.6	31.6
W12x136	Flange	52.0	57.1	70.4	78.5	27.3
W12x136	Web	54.9	59.6	73.7	82.1	35.9

Notes: Rate of loading = 0.1 in/min. upto yield; 0.2 in/min. after yield for dynamic yield values
Percent elongation based on 8" gage length

2.4.2 Beam Section Properties

The nominal dimensions and properties of the beam sections are listed in Table 2.3. For each specimen, actual dimensions were measured at a number of locations. Their average appears in Table 2.4 along with the estimated actual M_p based on tensile coupon data.

TABLE 2.3

Nominal Section Dimensions and Properties

Section	d (in.)	b_f (in.)	t_w (in.)	t_f (in.)	Z (in.^{3})	M_p (k-in.)
W 24x55	23.57	7.005	0.395	0.505	134	4824
W 21x57	21.06	6.555	0.405	0.650	129	4644
W 18x60	18.24	7.555	0.415	0.695	123	4428

Notes : M_p based on nominal F_y
$M_p = Z * 36$ ksi

TABLE 2.4

Actual Section Dimensions and Properties

Section	d (in.)	b_f (in.)	t_w (in.)	t_f (in.)	Z_f (in.^{3})	Z_w (in.^{3})	M_p (k-in.)
W 24x55	23.58	7.06	0.416	0.499	82.39	54.11	6142
W 21x57	21.06	6.59	0.413	0.638	87.12	41.67	5255
W 18x60	18.22	7.63	0.437	0.699	94.15	31.62	5553

Notes : M_p based on coupon data
$M_p = Z_f * F_{y\,flg.} + Z_w * F_{y\,web}$ (Based on Dynamic yield)

2.4.3 Slip Tests

Tests were conducted to characterize the slip coefficient between the shear tab and the beam web. A test procedure similar to that specified in the "Specifications for Structural Joints using ASTM A325 or A490 Bolts" [20] was followed. As described in the above reference, the specimens consisted of two outer and one inner plate. Pieces cut from the shear tab were used as the inner plates while pieces from the beam web were used as the outer plates. Three tests were conducted for each beam section. The results are reported in Table 2.5. The slip coefficients are based on the load at first slip of the specimens. None of the specimens were painted. There was little loose rust, loose mill scale, or grease on the beam or shear tab material. Consequently, no cleaning or surface preparation was done by the fabricator for the test specimens. Similarly, no cleaning or

surface preparation was done for the slip tests. The slip coefficients reported in Table 2.5 vary from approximately 0.3 to 0.4, which is typical for class A ("clean mill scale") surfaces.

TABLE 2.5

Measured Slip Coefficients Between Shear Tab and Beam Web

No.	W 24x55	W 21x57	W 18x60
1	0.343	0.326	0.401
2	0.355	0.315	0.374
3	0.358	0.370	0.394
Average	0.352	0.337	0.390

2.5 FABRICATION

The specimens were fabricated by a commercial structural steel fabricator in Austin, Texas. The fabricator is experienced in structural steel building fabrication, and maintains AISC Catergory II (Complex Steel Building Structures) certification.

The entire operation of material procurement, fabrication, and delivery to the laboratory was conducted in two stages. The first stage included procurement of all material, and fabrication and delivery of Specimens 1 to 4. The second stage involved fabrication and delivery of Specimens 5 to 8. This arrangement allowed for design changes in the final four specimens, based on results of the first four specimens.

2.5.1 Fabrication Sequence

A six step fabrication sequence was specified for the connections. The first step was to weld the continuity plates to the column. The shear tab was then welded to the column flange. After that, the beam web was bolted to the shear tab, and the bolts were

fully tightened. The top and the bottom flanges of the beam were welded to the column flange respectively as the fourth and fifth steps. Finally, supplementary web welds to the shear tab were provided where required after the flange welds had cooled.

2.5.2 Bolt Installation

Considerable care was taken to assure proper tightening of the bolts. This was done in an attempt to better relate the web participation in resisting moments to the tension in web bolts.

The goal of the bolt installation process was to develop a bolt tension as close as possible to the value required by the Specification for Structural Joints Using ASTM A325 or A490 Bolts [20], for slip critical connections. The tension values specified for 7/8" A325 and A490 bolts are 39 kips and 49 kips, respectively. The specification also requires that bolt installation methods must develop a tension at least five percent greater than the above specified values. Consequently, target tension values of 41 kips and 51.5 kips were set for A325 and A490 bolts in the test specimens.

Bolt installation was accomplished by a carefully controlled calibrated wrench method. Bolts were first tightened in a Skidmore-Wilhelm bolt tension calibrator using a torque wrench. For each type of bolt used, a sample of five bolts were tightened to develop a torque-tension relationship. A hardened washer was used under the nut. Lubricated nuts were used to obtain a more consistent torque- tension relationship. The results of the calibration process are shown in the plots in Figure 2.4. These plots show that a consistent torque-tension relationship was developed for the bolts used in the project.

After the calibration process, the bolts were installed in the test specimens. Bolts, nuts, and washers used for the specimens were taken from the same lot as those used in

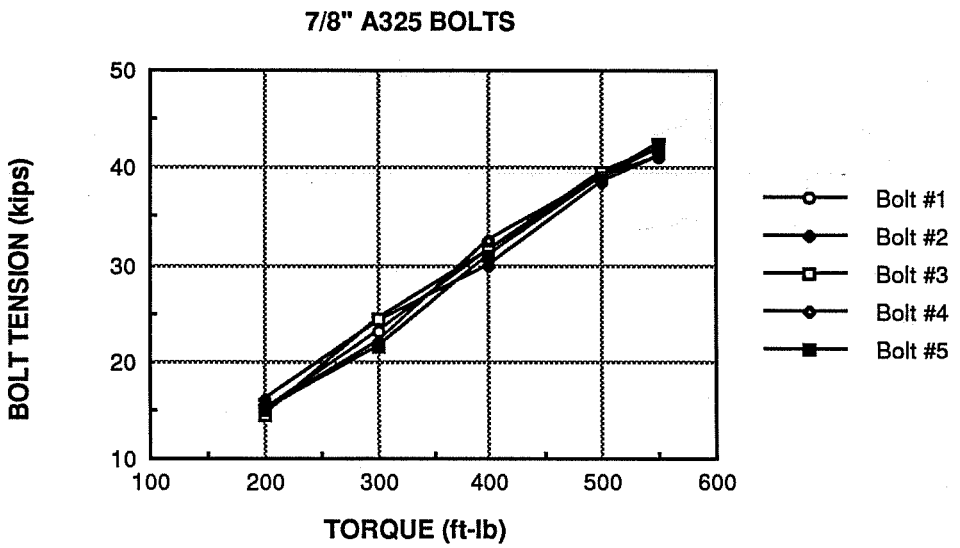

Figure 2.4 (a) - Torque-Tension Relationship of A325 Bolts for Specs. 1, 3, and 4

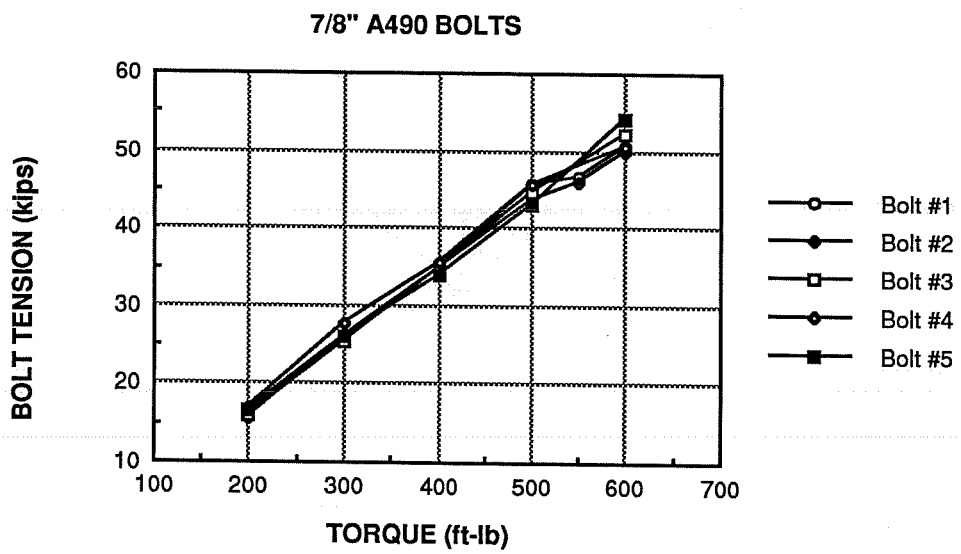

Figure 2.4 (b) - Torque-Tension Relationship of A490 Bolts for Spec. 2

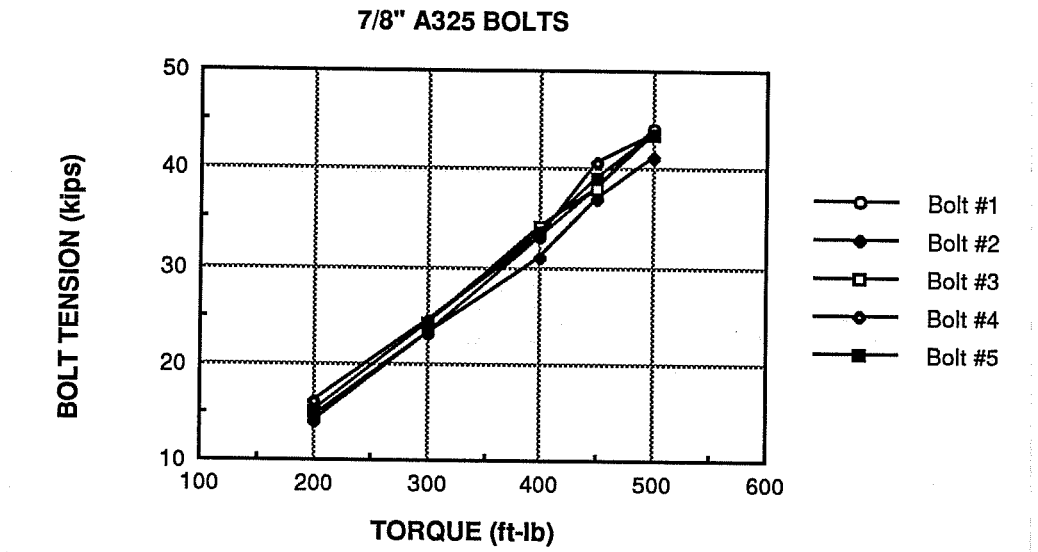

Figure 2.4 (c) - Torque-Tension Relationship of A325 Bolts for Specs. 5 to 8

the calibration process. In the specimens, the bolts were first brought to a snug-tight condition, and then were torqued to values established by the torque-tension calibration to achieve the target tension values. The bolts were torqued several times to compensate for any relaxation due to subsequent tightening of adjacent bolts.

2.5.3 Web Cope and Flange Weld Details

Details of the web copes and of the complete penetration groove welds used for the beam flanges are shown in Figure 2.5. The shape and dimensions of the web copes for Specimens 1-4 were chosen to be generally in conformance with AISC recommendations (Section J 1.11 of reference 11). Based on experience with the first four specimens, the size of the web copes was increased for Specimens 5-8, as indicated in Figure 2.5. For all specimens, the copes were torch cut, and then ground smooth.

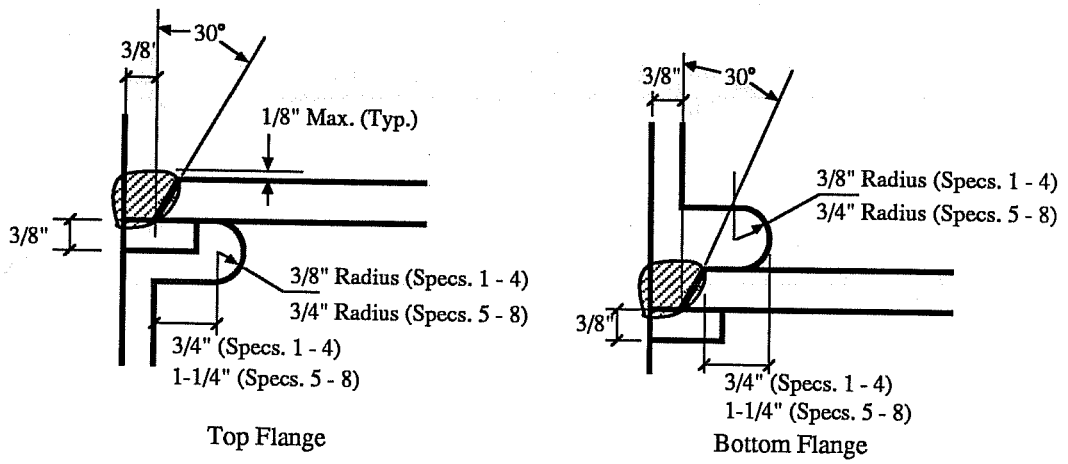

Figure 2.5 - Web Cope Details

The complete penetration single bevel groove welds were detailed with a 3/8" root opening and a 30° bevel; a prequalified detail, per AWS D1.1-88 [7]. All flange groove welds were provided with a 3/8"x1" backup strip. The backup strips extended approximately 1" beyond the edges of the beam flange. For the flange welds on Specimens 5, 6, and 8, extension plates were used to extend the bevel beyond the edge of the beam flange. Extension plates were not used on the other specimens. All backup strips and extension plates were of A36 steel, and remained in place after the welds were completed.

Welding was accomplished by self shielded FCAW process, using an E70T-7 3/32" diameter electrode. All welds on Specimens 1 to 4 were made by one welder. Welds on Specimens 5, 6, and 8 were made by a second welder, and those on Specimen 7, by a third welder. All welders were qualified per AWS D1.1-88 for the weld types, positions and processes used for the test specimens. All groove welds were made with the specimens in an upright position to simulate field welding positions.

2.5.4 Weld Inspection

Inspection was provided by an independent welding inspection firm. The individual performing the inspection maintained Level II and Level III NDT qualifications [5] as well as AWS Certified Welding Inspector qualifications [6]. Three separate inspections were provided for each specimen as described below. Tests and inspection were specified to be in compliance with AWS D 1.1 [7].

The first inspection consisted of ultrasonically testing the column flanges for the presence of large laminations. A region extending for three inches below to three inches above the groove weld locations were tested. No laminations were detected within this region on any of the column sections.

The second inspection consisted of a pre-weld fitup check. After the beam was bolted to the shear tab, the root opening and bevel angle was checked. Both were within AWS D1.1-88 tolerances for all specimens.

The final inspection consisted of ultrasonic tests of all groove welds. Testing was performed in accordance with AWS D1.1-88, Section 6, Part C. Acceptance criteria were in accordance with Table 8.2 of AWS D1.1-88. All welds passed this inspection, with the exception of Specimen 3. Problems encountered with Specimen 3 are described below.

2.5.5 Specimen 3 Welding Repairs

In the fabrication sequence for Specimen 3, the beam flanges were welded (top flange was welded before bottom flange), and on the following day, the welds between the shear tab and the beam web were made. Shortly after these web welds were made (and were still cooling), the flange groove welds were ultrasonically tested. The groove welds passed this inspection. Within minutes of completing the ultrasonic testing, a loud

"pop" was heard from the specimen. The welds were retested, and a large flaw was detected in the bottom flange weld.

The backup strip and a portion of the groove weld were removed from below the connection by air-arc gouge. The weld was then repaired, from below, using SMAW process with E7018 electrodes. The groove welds were then retested, and a new flaw was discovered in the top flange weld. A portion of the top weld was then removed by air-arc gouge from above, and rewelded. Retesting indicated a new flaw in the previously repaired bottom flange weld. The bottom flange weld was then repaired a second time. However, while rewelding the bottom flange, preheat was maintained on the top flange. A final ultrasonic test showed both welds to be satisfactory. In summary, the bottom flange weld in Specimen 3 was repaired twice, and the top flange weld was repaired once. These extensive repairs must be considered when interpreting the test results for this specimen.

2.6 INSTRUMENTATION

Each specimen was instrumented with a load cell to monitor the applied load at the end of the cantilever and seven displacement transducers. Two transducers were provided to measure tip displacement, two to measure slip between the shear tab and the beam web parallel to the beam axis, one to measure slip between the shear tab and the beam web perpendicular to the beam axis, and two to measure column panel zone rotations. The rotations of the panel zone were measured by attaching a rigid bar to the continuity plates and measuring the displacements at its ends. These displacements were measured by transducers rigidly supported by the laboratory reaction wall. Locations of transducers are shown in Figure 2.6. All data was recorded using a computer based electronic data acquisition system. For each specimen, whitewash was applied to the beam in the connection region, and also to the column panel zone and continuity plates, to detect yielding.

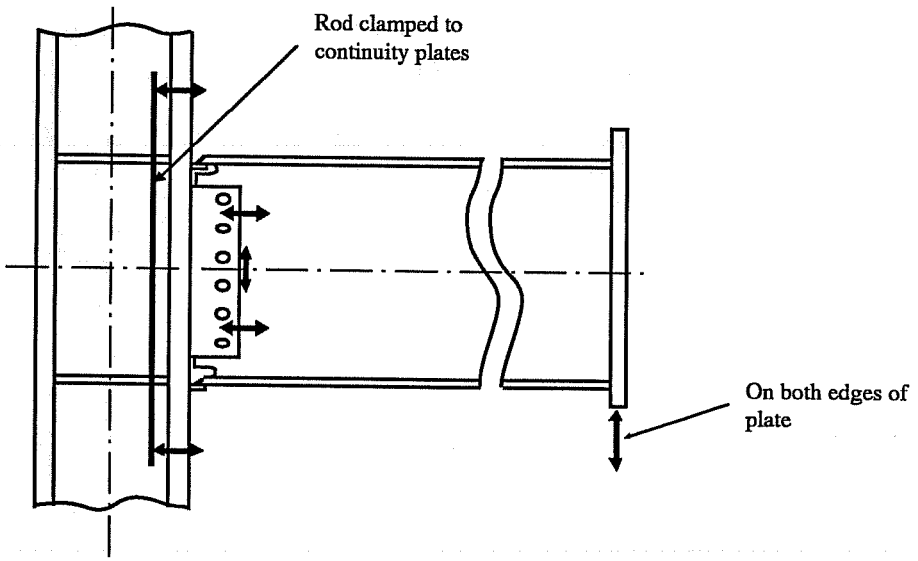

Figure 2.6 - Location of Displacement Transducers

3 - EXPERIMENTAL RESULTS

3.1 GENERAL

The experimental performance of the eight test specimens is presented in this chapter. The response is shown in the form of plots of load vs. deflection at the tip of the cantilever (the load was applied at 96" from the face of the column; displacement transducers measured deflections at the end plate located at 91 inches from the face of the column) and plots of moment vs. plastic rotation angle at the connection. A description of the failure of each specimen is also provided.

Additional experimental data, including displacements measured at the shear tab and column panel zone, are presented in Chapter 4. General observations and discussion of the experimental results are provided in Chapter 5.

3.1.1 Loading Sequence

All specimens were subject to slowly applied cyclic loads up to failure. A similar loading sequence was used for each specimen, as described below.

A zero reading was assigned to all instruments before the specimens were loaded. Subsequently, the specimens were loaded in the elastic range to ±15 kips, ±30 kips, and then to ±45 kips. Beyond ±45 kips, significant yielding occurred for all specimens. The loading was then switched from load control to displacement control, with displacements increasing in 1/4" increments up to failure. Increments of 1/4" were chosen to provide a reasonable number of loading cycles in the inelastic range. (Approximately 6 inelastic cycles to achieve 0.015 radian plastic rotation). Some cycles in the inelastic range were repeated. Tables 3.1 to 3.3 provide a listing of the nominal loads and displacements applied to each test specimen. A positive sign corresponds to upward load or upward displacement of the tip of the cantilever.

TABLE 3.1

Nominal Loading Sequence (Specimens 1 to 3, W24x55)

Cycle	Spec. # 1	Spec. # 2	Spec. # 3
1	±15 k	±15 k	±15 k
2	± 30 k	± 30 k	± 30 k
3	± 45 k	± 45 k	± 45 k
4	± 0.75 in.	± 0.75 in.	± 0.75 in.
5	± 1 in.	± 1 in.	± 1 in.
6	Failure	Failure	±1.25 in.
7			± 1.5 in.
8			± 1.5 in.
9			± 1.75 in.
10			Failure

TABLE 3.2

Nominal Loading Sequence (Specimens 4 & 5, W18x60)

Cycle	Spec. # 4	Spec. # 5
1	±15 k	±15 k
2	± 30 k	± 30 k
3	± 45 k	± 45 k
4	± 1 in.	± 1 in.
5	Failure	±1.25 in.
6		± 1.5 in.
7		± 1.75 in.
8		± 2 in.
9		± 2 in.
10		± 2.25 in.
11		Failure

TABLE 3.3

Nominal Loading Sequence (Specimens 6 to 8, W21x57)

Cycle	Spec. # 6	Spec. # 7	Spec. # 8
1	±15 k	±15 k	±15 k
2	± 30 k	± 30 k	± 30 k
3	± 45 k	± 45 k	± 45 k
4	± 1 in.	± 1 in.	± 1 in.
5	± 1.25 in.	± 1.25 in.	± 1.25 in.
6	± 1.5 in.	± 1.5 in.	± 1.5 in.
7	± 1.75 in.	± 1.75 in.	± 1.75 in.
8	± 2 in.	± 2 in.	± 2 in.
9	Failure	± 2 in.	± 2 in.
10		± 2.25 in.	Failure
11		+ 2.5 in. / Failure	

Notes:
(1) Loads measured at 96" and displacements measured at 91" from the face of the column.
(2) + = Upward load or displacement

3.1.2 Calculation of Moment and Plastic Rotation

In addition to the plot of load vs. displacement, a plot of moment vs. plastic rotation is provided for each specimen.

The moment at the connection was computed simply as the load multiplied by the cantilever length of 96 inches. The plastic rotation, θ_p, was computed as follows:

$$\theta_p = \Delta_p / 91 \text{ inches}$$
$$\Delta_p = \Delta - \Delta_e$$
$$\Delta_e = P/k_e$$

where:

Δ = Measured tip deflection

Δ_p = Tip deflection due to plastic deformations

Δ_e = Recoverable, elastic tip deflection

P = Load at which Δ_p is being calculated

k_e = Elastic stiffness of the specimen (taken as the slope of the elastic portion of the load-displacement plot)

The value of θ_p, as computed above, can be interpreted as the rotation of a plastic hinge of zero length, located at the face of the column. This represents an idealization for the actual specimens, since yielding occurs over some length of the beam. This method of computing θ_p is consistent, however, with previous experimental investigations [14-17,24], and therefore provides a meaningful basis for comparison.

The plastic rotation of the test specimens can be attributed primarily to flexural yielding of the beams. Yielding was observed in the column panel zone of the specimens. However, measurements at the column panel zone (presented in Chapter 4) generally indicate that little inelastic deformation was contributed by the panel zones.

On the load-displacement and moment-plastic rotation plots for each specimen, dashed lines are used for a portion of the plot. The dashed lines indicate the response of the specimens after fracture occurred at a beam flange to column flange connection.

3.2 RESPONSE OF SPECIMENS 1 TO 4

Specimen 1

Specimen 1 was a W24x55 beam (Z_f/Z = 0.61) with six 7/8" A325 bolts in the web. The hysteretic response of the specimen is shown in Figure 3.1.

Slight yield lines were first noted on the beam flanges during the 2nd cycle. During the 3rd and 4th cycles, the yielding became more pronounced. During the 5th cycle, with a peak displacement of ±1.0 in., slip between the shear tab and the beam web was clearly visible. The beam flanges showed significant yielding. No yielding, however, was visible in the beam web or the column panel zone. During the 6th cycle, at about +1.2 in. displacement and +57 kips load, a sudden failure occurred at the bottom flange. Fracture occurred at the interface of the weld and the column flange. This fracture occurred over the full width of the weld nearly instantaneously. Figure 3.2 shows this fracture at a tip displacement of +2.0 in.

After failure at the bottom flange, the load was reversed, and downward displacement was applied until failure occurred at the top flange. During this final cycle (dashed lines in Figure 3.1), the top flange fractured at about -2.6 inches displacement. The fracture occurred within the beam flange, initiating in the region of the web cope, and gradually spreading over the width of the flange. Figure 3.3 shows the top flange failure.

After completion of the test, the beam was completely removed from the column to permit examination of the failure at the bottom flange. The region of the column at the bottom flange weld is shown in Figure 3.4. Examination of the failure at the weld-column interface revealed two observations of interest. First, in a small region near the bottom middle portion of the weld (the portion of the weld adjacent to the beam web), it appeared that the weld did not fuse with the column flange. Secondly, portions of the fracture within the column flange had a fibrous appearance, suggesting the possibility of some lamellar tearing in the column flange.

Specimen 2

Specimen 2 was a W24x55 beam (Z_f/Z = 0.61) with six 7/8" A490 bolts in the web. Specimen 2 was nominally identical to Specimen 1, except that A490 bolts were used instead of A325 bolts. The hysteretic response of the specimen is shown in Figure 3.5.

The behavior of this specimen was very similar to the behavior of the first specimen. Slight yield lines appeared in the beam flanges during the 2nd cycle and increased during the following cycles. The web, as with Specimen 1, showed no yielding. Panel zone yield lines formed in the 5th cycle but were barely noticeable at the time. The specimen failed in the 6th cycle by a sudden fracture at the bottom flange connection. The load at failure was approximately +56 kips with an accompanied tip displacement of about +1.2 in. Fracture occurred at the interface of the weld and the column flange, and travelled across the entire width of the weld nearly instantaneously. Figure 3.6 shows the fracture from beneath the bottom flange at a tip displacement of 2 inches. Note the separation of the backup plate from the column flange, indicating a separation of the weld from the column flange. Figure 3.7 shows the same fracture from the top of the bottom flange. Figure 3.8 shows a photograph of the connection, taken just after the bottom flange failure. It can be seen that the web apparently did not participate in developing inelastic deformations, as indicated by the absence of yield lines in the web.

After failure at the bottom flange, the load was reversed, and downward displacement applied until failure occurred at the top flange (dashed lines in Figure 3.5). Fracture at the beam's top flange occurred at a displacement of about -3.5 inches. As with Specimen 1, the fracture was within the beam flange, initiating near the web cope.

As with Specimen 1, the beam was completely removed from the column after completion of the test, to permit examination of the failure at the bottom flange. The

fracture surface at the weld-column interface was very similar to that of Specimen 1. There were small regions where the weld apparently did not fuse with the column flange. There were also some portions of the fracture surface in the column flange with the appearance of lamellar tearing.

Specimen 3

Specimen 3 was also a W24x55 beam with a Z_f/Z = 0.61. This specimen was provided with six 7/8" A325 bolts and with supplementary web welds on the shear tab to nominally develop 20% of the plastic moment capacity of the beam web. The complete penetration groove welds on this specimen had been repaired as described in Chapter 2. The hysteretic response is shown in Figure 3.9. The performance of this specimen was significantly better than the earlier ones.

The yielding in the beam flanges was pronounced by the end of the 5th cycle, which attained a peak displacement of ±1.0 in. Some yielding was observed in the column panel zone and the region of the web welds at the end of the 7th cycle. The first crack appeared at the edge of the bottom beam flange during the 9th cycle. Another crack appeared on the top flange in the other half of the same cycle. This was accompanied by slight bottom flange buckling. The specimen started dropping load sharply in the early part of the 10th cycle as the bottom flange crack propagated across the beam flange (Figure 3.10). The tip displacement at this point was about +1.6 in. The yielding in the beam web was still restricted to the region around the supplementary welds, which appeared to fracture simultaneously with the flange. Panel zone yielding was also at about the same level as in the 7th cycle. The loading was continued until about +2.6 in. when the fracture was complete across the entire width of the beam flange.

The loading, as with earlier specimens, was continued in the other direction until complete fracture of the top flange (dashed lines in Figure 3.9). The fracture occurred at about the same load and tip displacement as for the bottom flange. The fracture initiated at one edge of the beam flange and propagated through the flange metal. Figure 3.11 shows the top flange after its fracture. The supplementary welds at the top of the shear tab after failure are shown in Figure 3.12.

Specimen 4

This specimen was a W18x60 beam with a Z_f/Z = 0.75. Four 7/8" A325 bolts were provided for the web connection. The hysteretic response of this specimen is shown in Figure 3.13. The Z_f/Z ratio of this beam section was the highest of all sections used in this testing program, but the performance of the specimen was very poor. Figure 3.14 shows the size of web copes of the specimen, which was typical of the cope sizes in Specimens 1 to 4.

Some yield lines formed in the beam flanges during the 2nd cycle and increased during the 3rd cycle. The 4th cycle was the last stable cycle. A sudden fracture at the bottom flange weld occurred during the 5th cycle, at a load of about +48.0 kips and a tip displacement of +1.1 in. The fracture occurred at the interface of the weld and the column flange as with Specimens 1 and 2. Figure 3.15 shows the fracture from beneath the bottom flange. It can be seen in the photograph that the backup plate was separated from the column flange, indicating a separation of the weld from the column flange. The failure appeared to initiate in the middle portion of weld. There were essentially no yield lines in the beam web at the time of the failure, and very slight yield lines in the panel zone.

The loading was reversed and continued in the other direction producing a tip deflection of about -4.8 in., at which point the hydraulic ram ran out of stroke and the test

was ended. Yielding in the beam web and the column panel zone was significant at this point, indicating their participation in developing inelastic deformations in this final half cycle of loading. There was no sign of any fracture initiating in the top flange at the end of the test.

After the test, the top flange was torch cut and the beam completely removed from the column. Examination of the bottom flange failure revealed the fracture surface to be similar to those of Specimens 1 and 2. Their were regions with apparent lack of fusion and some portions with the fibrous appearance of lamellar tearing in the column. Figure 3.16 shows the region of the bottom flange weld on the column.

3.3 DESIGN CONSIDERATIONS FOR SPECIMENS 5 TO 8

As discussed in Chapter 2, the specimens were fabricated in two groups: first Specimens 1 to 4, and then Specimens 5 to 8. Based on an evaluation of the performance of Specimens 1 to 4, modifications were made to the design and fabrication of Specimens 5 to 8. A discussion of these issues is presented in the following sections.

3.3.1 Behavior of Specimens 1 - 4

Overall, the performance of Specimens 1 to 4 was poor. With the exception of Specimen 3 (which had repaired flange welds, and supplementary web welds), very little plastic rotation was developed by the specimens. Specimens 1, 2, and 4 were particularly poor, barely exceeding the range of elastic behavior at the point of failure.

Specimens 1, 2, and 4 failed in a nearly identical manner. In each specimen, a fracture occurred at the interface of the column flange and the bottom beam flange weld. Examination of the fracture surfaces suggested two possible causes of failure. First, there was a small region at the bottom of each weld, where the weld apparently did not fuse

with the column flange. Secondly, in each case, the fracture surface extended into the column flange and exhibited a fibrous appearance, characteristic of lamellar tearing [1]. It should be noted that whatever problem caused the early failures at the bottom flange welds, the same problem apparently was not present at the top flange welds. In each of Specimens 1, 2, and 4, the top flange performed well in the final half cycle of loading. In no case did a failure occur at the weld-column interface at the top flange.

Two possible explanations can be given for the different behavior at the top and bottom flanges of Specimens 1, 2, and 4. First, placement of the bottom flange weld must always be interrupted in the region of the beam web. In contrast, the top flange weld can be placed continuously, without interruption, across the width of the flange. Thus, it may be argued that the bottom flange weld is more difficult to place for the welder, and therefore, more likely to contain defects. The rather small web copes in Specimens 1 to 4 may have also contributed to increased difficulty in making a sound weld at the bottom flange.

There is also a difference in the degree of shrinkage restraint at the top flange and bottom flange welds. In the fabrication sequence used for these specimens, the web bolts were first fully tensioned, then the top flange was welded, and then finally the bottom flange was welded. Shrinkage at the bottom flange weld was therefore restrained by both the tensioned web bolts and by the top flange weld. This high level of restraint at the bottom flange weld may have contributed to an increased likelihood of lamellar tearing.

3.3.2 Investigation of Column Steel

Based on observations of the fracture surfaces at the bottom flanges of Specimens 1, 2, and 4, it appeared that inadequate fusion of the weld into the column contributed significantly to the early failures of these specimens. Several measures were taken to assure better welds on the final four specimens, as described later. In addition, a brief

investigation was conducted on the properties of the column steel, to assure that the mechanical and chemical properties were within specified limits of A572 Gr. 50 steel. The purpose of this investigation was to determine if there was anything unusual about these particular columns that might preclude their use in the final four specimens.

As a first step, the mill certificate for the columns was obtained. The mechanical properties (yield point, tensile strength, and percent elongation) and the chemical analysis were within specified limits for ASTM A572 Gr. 50 steel. This was confirmed by independent tensile coupon tests (data presented in Chapter 2) and independent chemical analysis of the column steel (data presented in Chapter 4).

Testing of Charpy V-Notch specimens, as recommended by the project's advisory committee, was also undertaken at Ferguson Laboratory. Specimens were taken from the column flange, at the location specified in Supplement No. 1 to the LRFD Specification [4], and also from the outer surface of the column flange. The absorbed energy of all specimens significantly exceeded 20 ft-lb. at 70°F, as required in this supplement. The complete Charpy V-Notch data is presented in Chapter 4.

In addition to the above tests, a portion of the column and the beam from one of the failed specimens was sent to the metallurgical laboratory of the steel mill that supplied the columns. Metallurgical and welding specialists examined the failure surfaces. Their opinion was that even though some lamellar tearing was present on the fracture surface, poor welding was likely the primary cause of the failure.

Based on the above information, the decision was made to continue with the same column sections for Specimens 5 to 8. It should be noted that the mechanical tests (tensile coupons and Charpy V-Notch) and chemical analysis conducted on the columns do not provide any direct data on the susceptibility of the steel to lamellar tearing. The data

indicate, however, that the columns meet standard material acceptance tests, and consequently, there was no justification to preclude their continued use for the remaining test specimens.

As a final point of information on the columns, two special tensile coupons were prepared and tested. For each coupon, sections of steel were welded to a section of the column flange, such that the column flange steel could be loaded in the through-thickness direction. These coupons were welded under conditions providing no restraint to weld shrinkage. Both coupons failed due to apparent poor welds to the column flange sections. These "through-thickness" coupons emphasized the role of poor welding in the failures. The testing of these coupons is described in Chapter 4.

3.3.3 Modifications for Specimens 5 - 8

In the light of above discussion, some modifications were made to the design and fabrication of Specimens 5 to 8, in an attempt to avoid the early failures that characterized Specimens 1, 2, and 4. First, the size of the web copes was substantially increased, as shown in Figure 2.5. It was believed that larger copes would permit easier welding on the bottom flange, and therefore would promote better welds. Secondly, extension plates were used to extend the bevel beyond the outer edges of the beam flanges. Extension plates were not used in the first four specimens. Although the previous failures did not appear to initiate at the flange edges, it was believed that the use of extension plates was consistent with good welding practice. Note that these plates were inadvertently left off of Specimen 7.

Finally, the welder for Specimens 1 to 4 was not used for the final four specimens. A second welder was used for Specimens 5, 6, and 8, and a third welder was used for Specimen 7. The performance of Specimens 5 to 8 is described in the following section.

3.4 RESPONSE OF SPECIMENS 5 - 8

Specimen 5

Except for the modifications noted above (cope size, welder, extension plates), this specimen was a replica of Specimen 4. (W18x60 with four 7/8" A325 bolts). The hysteretic response of Specimen 5 is shown in Figure 3.17. The performance of this specimen was significantly better than its predecessor. Figure 3.18 shows the web copes where the considerable increase in size is apparent (compare with Figure 3.14).

Yield lines first appeared in the beam flanges during the 3rd cycle. Substantial yielding was developed by the end of the 4th cycle. Some panel zone and beam web yielding was also visible by this time. During the 5th cycle, with a peak displacement of ±1 in., the shear tab started showing clearly visible signs of slip. The cycles progressed steadily in a stable manner until the 9th cycle. During the 10th cycle, cracks appeared on both the bottom and the top flanges, at the weld-beam interface. They initiated on opposite edges of the top and bottom flanges, at the extension plates. The load carrying capacity of the specimen, however, did not deteriorate. Further yielding in the panel zone was noted. In the positive half of the 11th cycle, the specimen failed at about +0.75 in. and +50 kips, due to the fracture propagating across the bottom flange. The fracture occurred at the weld-beam interface, and followed the original line of the bevel in the beam flange quite closely. Figure 3.19 shows the initiation of fracture at the bottom flange.

After failure of the specimen by bottom flange fracture, the loading was reversed and downward tip displacement applied until the top flange was completely fractured. The fracture initiated at the flange edge and progressed into the flange metal away from the weld-beam interface. The ductility achieved in the other half cycle was, as usual, excellent with a tip displacement of about -4.5 in. when the load started dropping. Figure 3.20

shows the torn top flange. A general view of Specimen 5 after failure is shown in Figure 3.21.

Specimen 6

Specimen 6 was a W21x57 beam with a Z_f/Z = 0.67. The web connection was made by using five 7/8" A325 bolts. The hysteretic response of this specimen is shown in Figure 3.22.

The specimen started to move into the inelastic region by the end of 3rd cycle, whereby yielding was visible on the beam flanges. A few yield lines also appeared in the column panel zone. A small crack was observed at the bottom flange, next to the extension plate, on one edge of the beam flange in the 4th cycle. This crack kept propagating in the future cycles. The hysteretic loops were stable until the 8th cycle, with a peak tip displacement of ±2 in. The specimen started dropping load early in the 9th cycle, and failed by fracture of the bottom flange. Figure 3.23 shows the fractured bottom flange. It can be seen that the fracture originally initiated at the weld-beam interface at the extension plate, but then propagated into the flange metal.

The loading was continued in the other direction, as usual, after the bottom flange failure. Good ductility was observed in this final half cycle of loading. The failure of the top flange occurred at a tip displacement of about -5 inches. Figure 3.24 shows the fractured top flange. As in the bottom flange, the fracture initiated at the weld-beam interface at the outer edge of the flange and then propagated into the flange metal.

Specimen 7

Specimen 7 was also a W21x57 beam with a Z_f/Z = 0.67. Five 7/8" A325 bolts along with supplementary web welds on the shear tab provided the web connection. The hysteretic response of Specimen 7 is shown in Figure 3.25. The performance of this

specimen in terms of the plastic rotation capacity, was better than all other specimens in the testing program. This was also the only specimen where failure occurred first at the top flange.

Yielding occurred as early as the 2nd cycle on the bottom flange. Pronounced yielding was observed on both flanges by the end of the 3rd cycle. Slight yielding was also observed in the beam web, near the web welds, and also on the column panel zone in this cycle. In the second half of the 5th cycle, when the tip displacement was downward, the vertical part of the top web weld cracked over approximately half of its length. During the first half of the 6th cycle, the vertical part of the bottom web weld cracked in a similar manner. At the end of the 8th cycle, with a maximum deflection of ±2 inches, a crack was observed at the top flange. The crack initiated at the beam-weld interface, at the outer edge of the flange. During the 9th cycle, the vertical portions of both the top and bottom web welds completely cracked. The horizontal portions of these welds were still intact. The hysteretic loops remained stable until the 11th cycle. Extensive yielding in the flanges and the web had occurred by this time. Slight flange buckling was observed at the top flange in the positive half of the 11th cycle.

During the negative half of the 11th cycle, failure of the specimen occurred, as the fracture propagated across the top flange. As with Specimen 6, the fracture initiated at the weld-beam interface at the outer edge of the flange and then propagated into the flange metal. As the top flange fractured, the horizontal portion of the top supplementary web weld also fractured. The loading was reversed, as usual, and upward tip displacement applied until fracture occurred at the bottom flange. Substantial ductility was observed in the reverse direction during this final half cycle. The bottom flange failed in a manner similar to the top flange. A crack initiated at the edge of the flange at the weld-beam interface, and propagated through the flange. As the bottom flange fractured, the horizontal portion of the bottom web weld also fractured.

Figures 3.26 and 3.27 show yielding in the beam web and the column panel zone as well as the top flange after failure. Figure 3.28 shows another view of the top flange fracture. The yield line pattern in the web indicates that it did take part in developing inelastic deformations. Figure 3.29 shows the cracked supplementary web weld at the bottom of the shear tab.

Specimen 8

Specimen 8 was also a W21x57 beam with a Z_f/Z = 0.67. Three 7/8" A325 bolts were used in the shear tab as erection bolts. The specimen was an all-welded connection, with both the beam flanges and the beam web welded directly to the column flange. The shear tab served as an erection plate and as a backup plate for the beam web's complete penetration weld. The hysteretic response of this specimen is shown in Figure 3.30. Figure 3.31 shows a general view of the connection before testing. The slip measuring transducers at the shear tab are visible in this photograph.

Yielding was observed in the beam flanges during the 2nd and 3rd cycles. Some yielding was observed in the beam web and in the column panel zone during the 4th cycle. Slight cracks were observed in both flanges during the 4th cycle. These cracks were located at the outer edges of the flanges, at the weld-beam interface. These cracks, however, did not grow in size for several cycles. During the 5th through 9th cycles, the hysteretic loops remained stable. Yielding at the beam flanges and beam web increased substantially during these cycles. The degree of yielding observed in the beam web was significantly greater than that observed in any previous specimen. The specimen failed during the 10th cycle, as the fracture propagated across the bottom flange. The fracture appeared to follow the weld-beam interface over the full width of the flange. Figure 3.32 shows the crack initiation on the bottom flange. After the bottom flange fractured, the lower portion of the beam web also fractured. This fracture extended from the cope, through the lower bolt hole in the web. After the failure at the bottom flange, the loading

was reversed and downward tip displacement applied. This monotonic loading was stopped after achieving about -4.5 in. displacement. At this point, a fracture had propagated across a portion of the top flange. Figures 3.33 and 3.34 show the connection after testing.

3.5 SUMMARY OF PLASTIC ROTATIONS

Table 3.4 summarizes the plastic rotation and failure mechanism for each test specimen. The tabulated value of θ_p is the maximum plastic rotation attained before failure, as measured from the beam's original undeformed position. Most specimens were loaded until fracture occurred at both the top and bottom flange connections. However, the point at which the first flange fractured is taken as the actual "failure" for each specimen, since beyond this point, the ability to resist cyclic loading is exhausted. Discussion of this data is presented in Chapter 5.

TABLE 3.4

Summary of Plastic Rotations and Failure Mechanisms

Specimen	θ_p (radian)	Failure Mechanism
1	0.004	Sudden fracture at weld-column interface at bottom flange
2	0.003	Sudden fracture at weld-column interface at bottom flange
3	0.009	Gradual fracture through bottom beam flange
4	0.002	Sudden fracture at weld-column interface at bottom flange
5	0.013	Gradual fracture at bottom beam flange; fracture initiated at weld-beam interface at edge of flange and propagated along interface
6	0.013	Gradual fracture at bottom beam flange; fracture initiated at weld-beam interface at edge of flange and propagated through flange metal
7	0.015	Gradual fracture at top beam flange; fracture initiated at weld-beam interface at edge of flange and propagated through flange metal
8	0.012	Gradual fracture at bottom beam flange; fracture initiated at weld-beam interface at edge of flange and propagated along interface

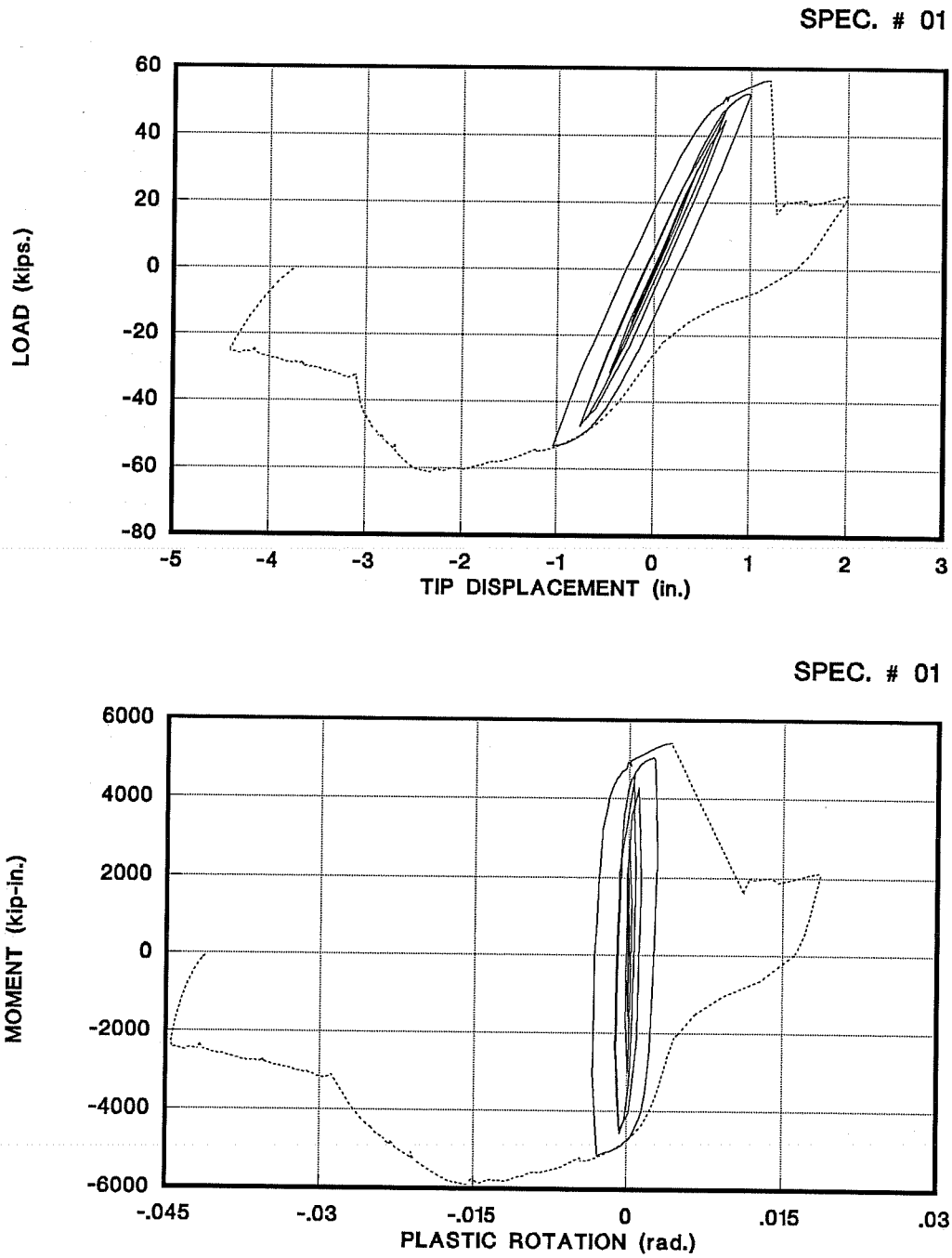

Figure 3.1 - Hysteretic Response of Specimen 1

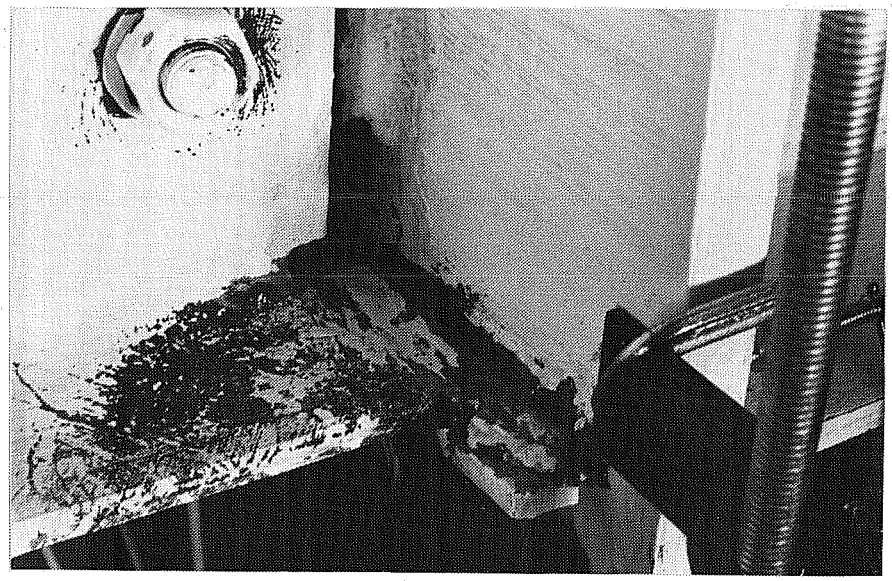

Figure 3.2 - Bottom Flange Failure in Specimen 1

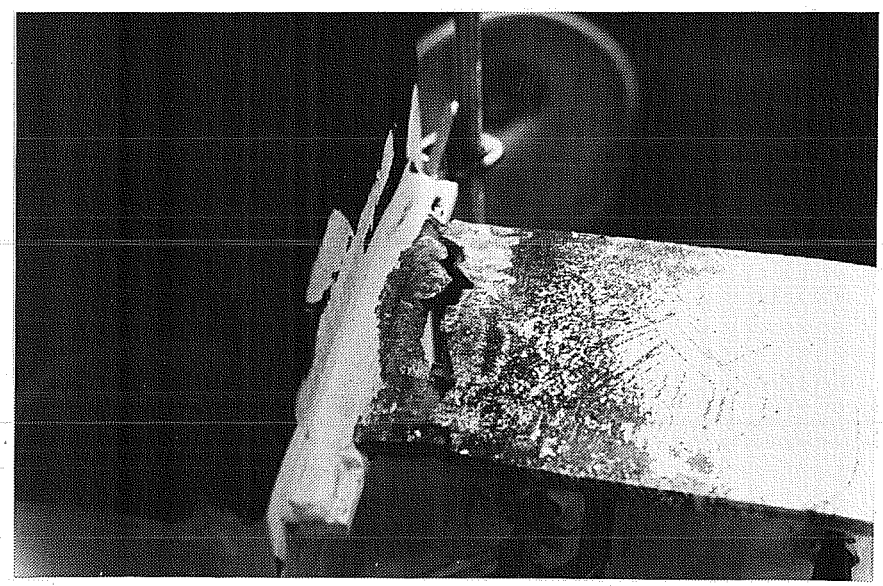

Figure 3.3 - Top Flange Failure in Specimen 1

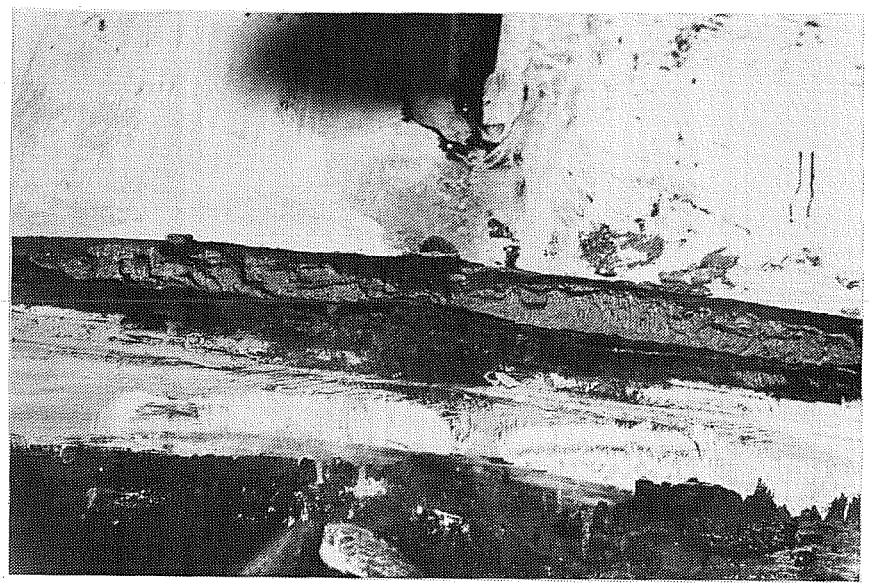

Figure 3.4 - Fracture Surface in Column of Specimen 1

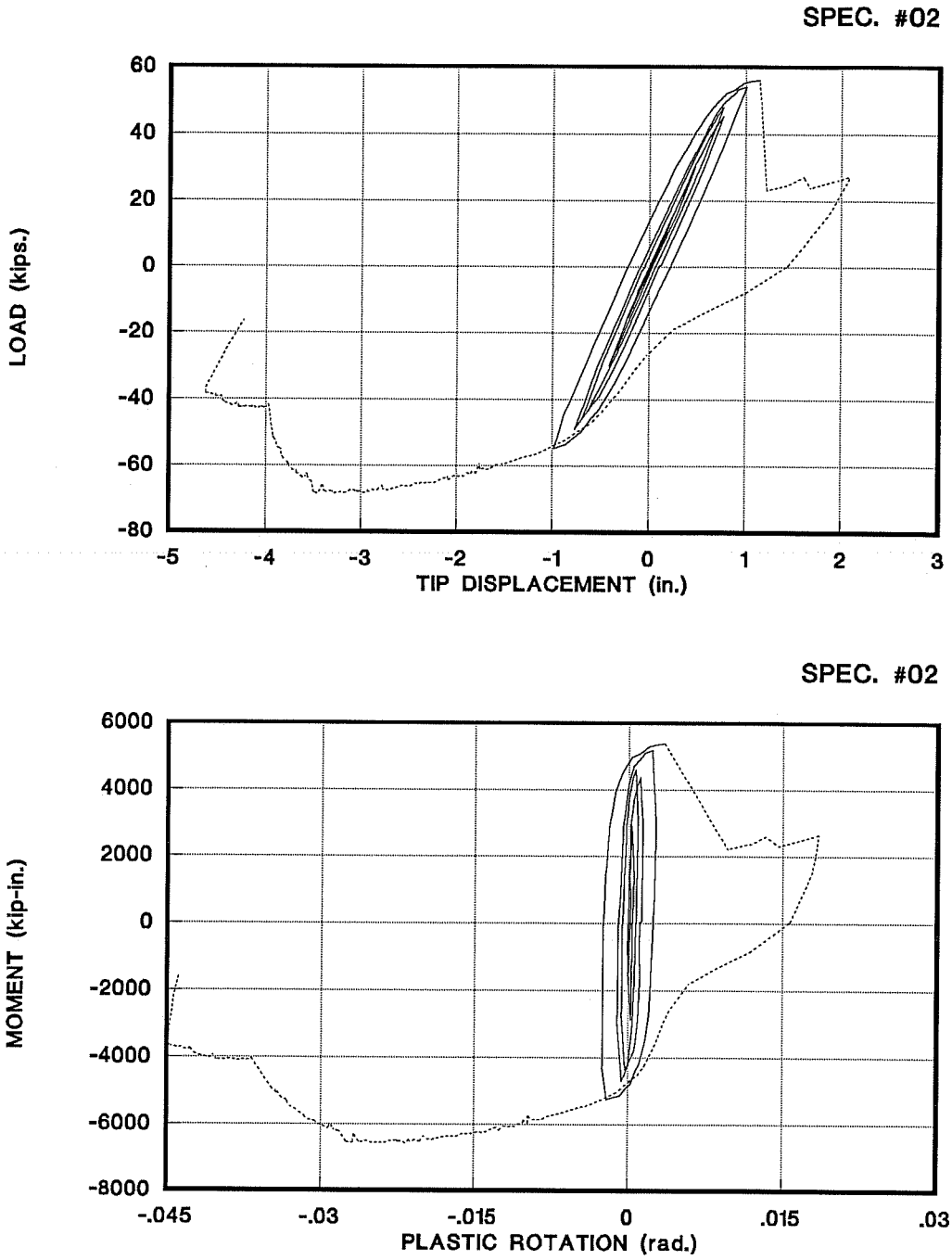

Figure 3.5 - Hysteretic Response of Specimen 2

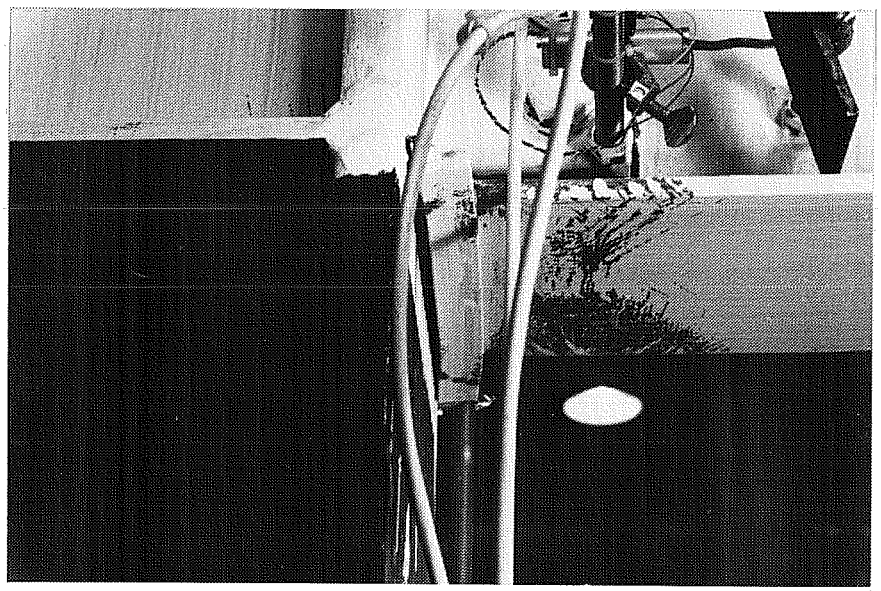

Figure 3.6 - Bottom Flange Failure in Specimen 2

Figure 3.7 - Bottom Flange Failure in Specimen 2

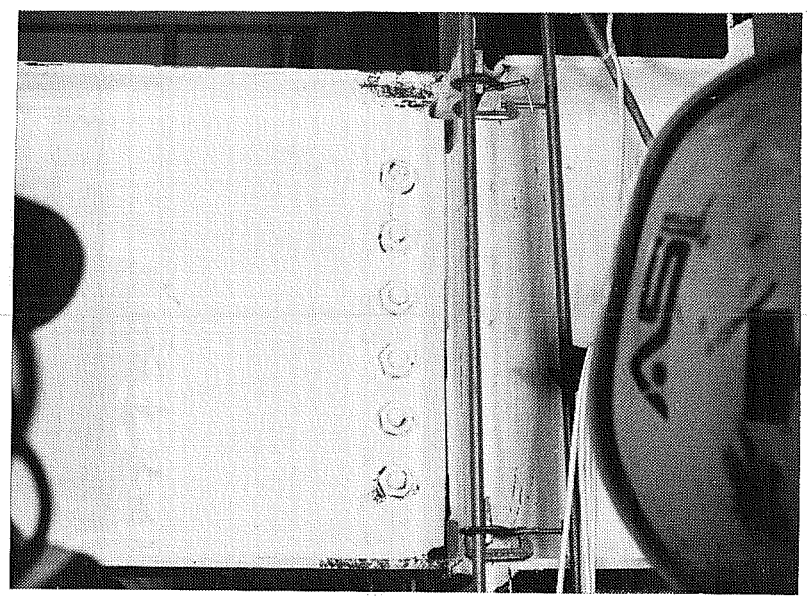

Figure 3.8 - Specimen 2 After Failure

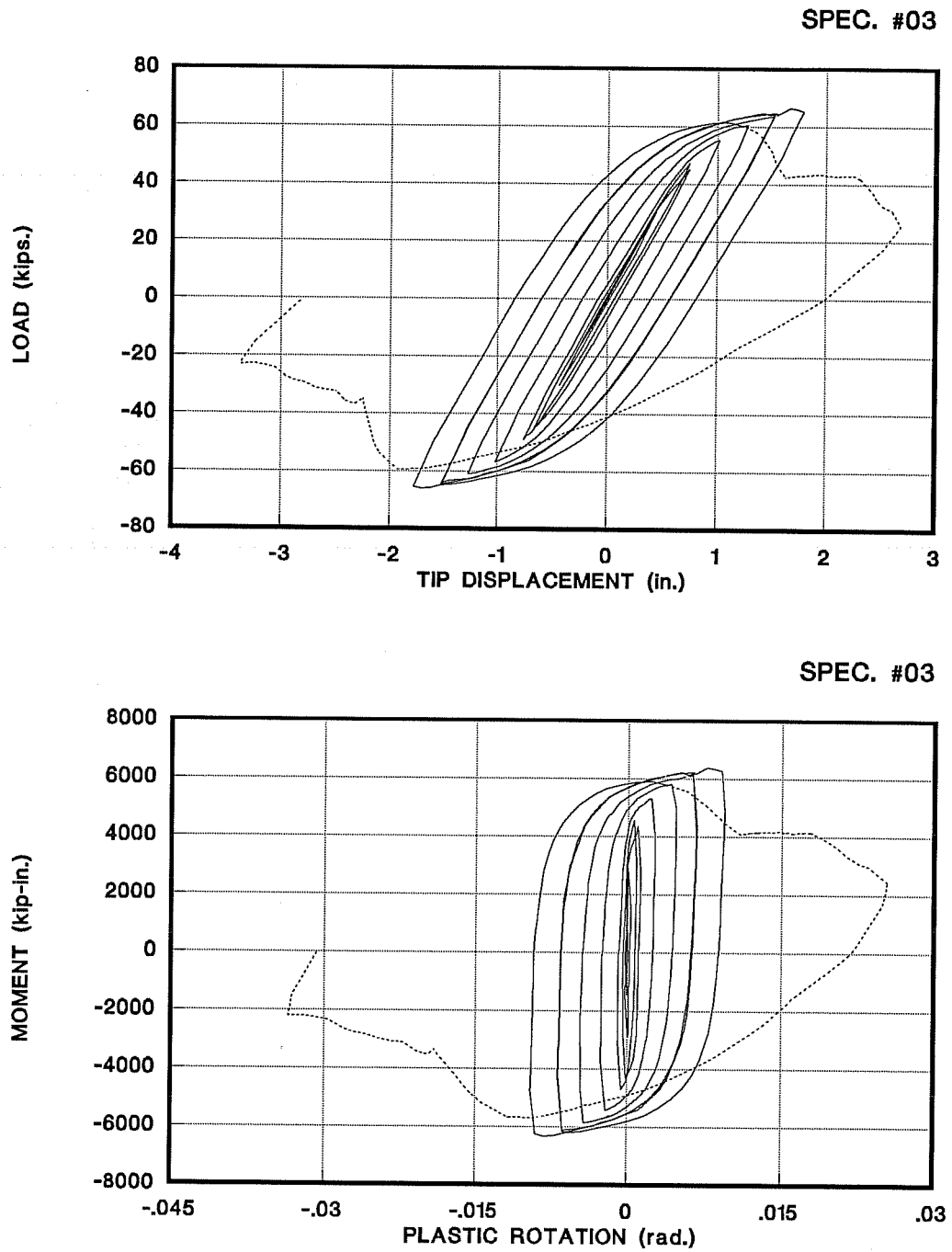

Figure 3.9 - Hysteretic Response of Specimen 3

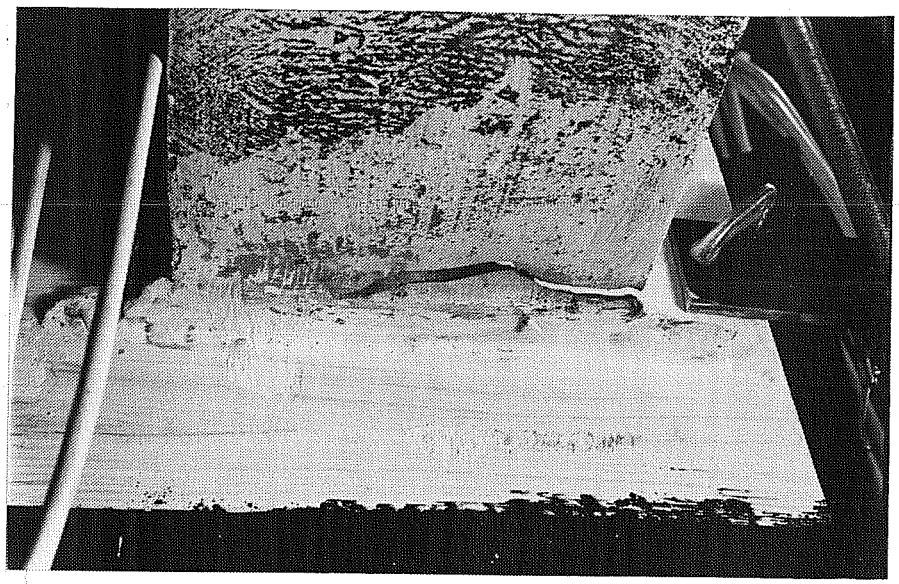

Figure 3.10 - Crack Initiation at Bottom Flange of Specimen 3

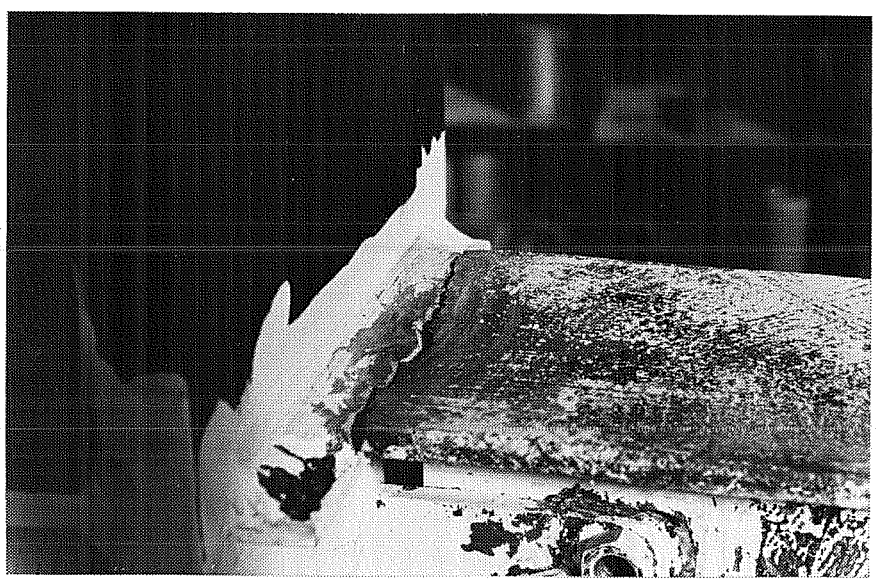

Figure 3.11 - Top Flange Failure in Specimen 3

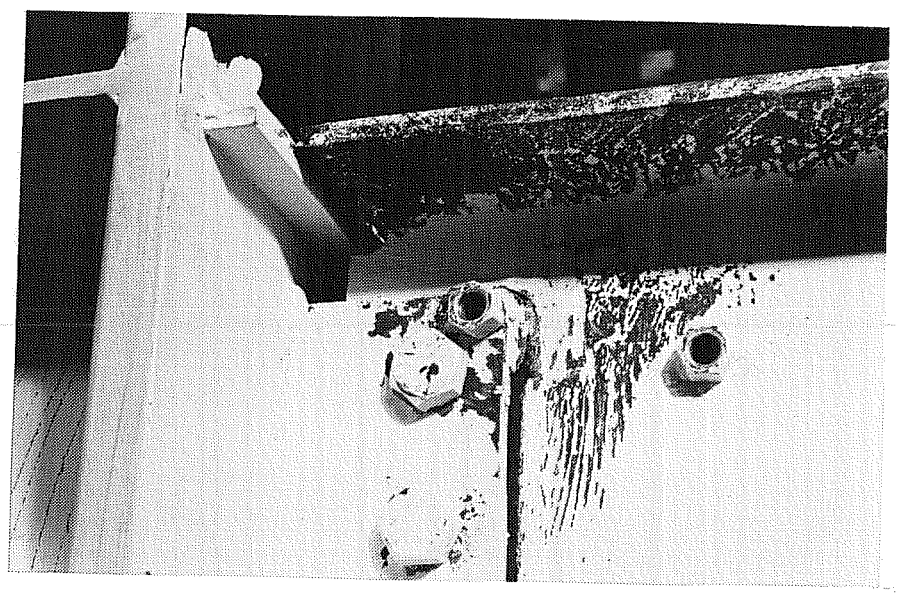

Figure 3.12 - Supplementary Web Weld Fracture in Specimen 3

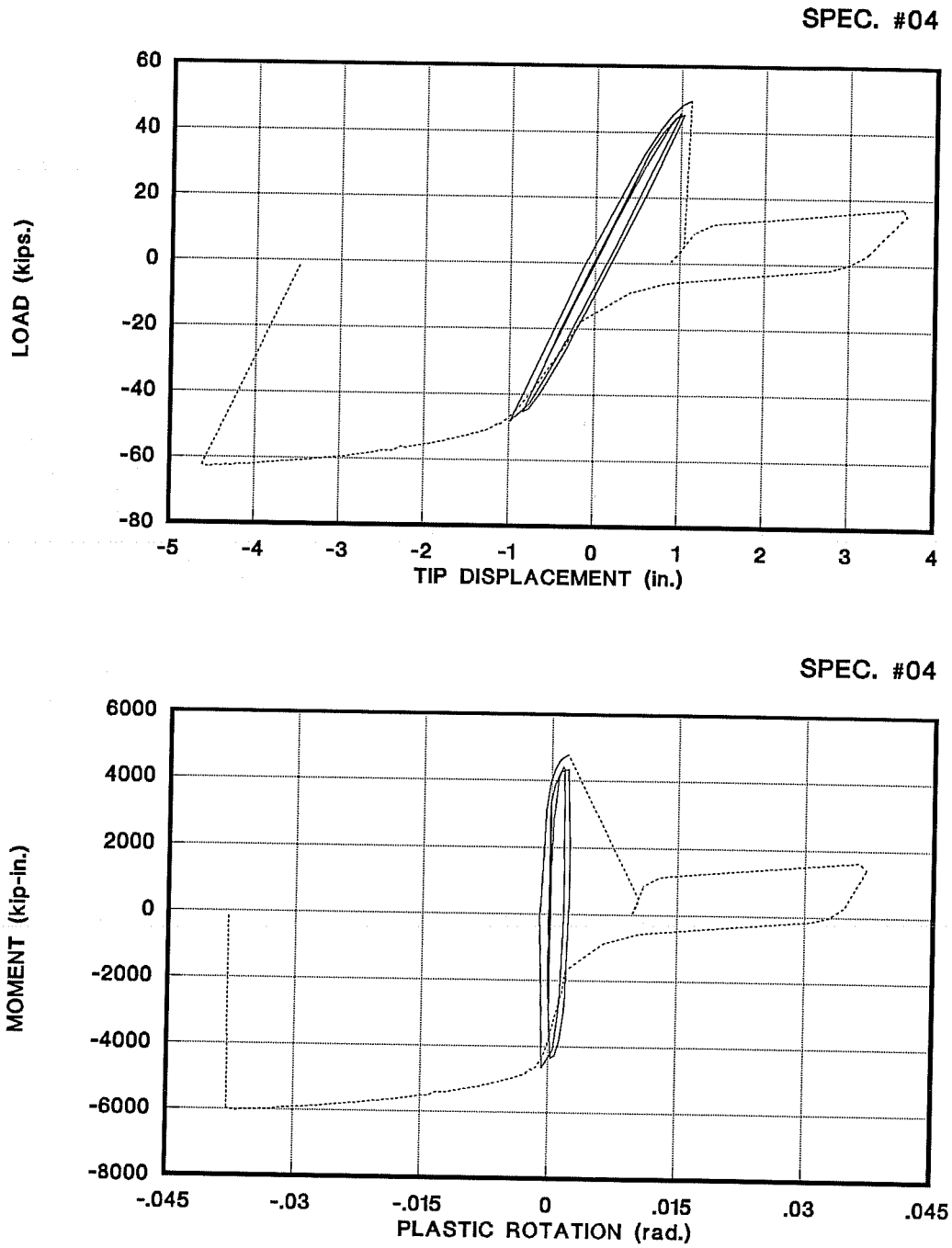

Figure 3.13 - Hysteretic Response of Specimen 4

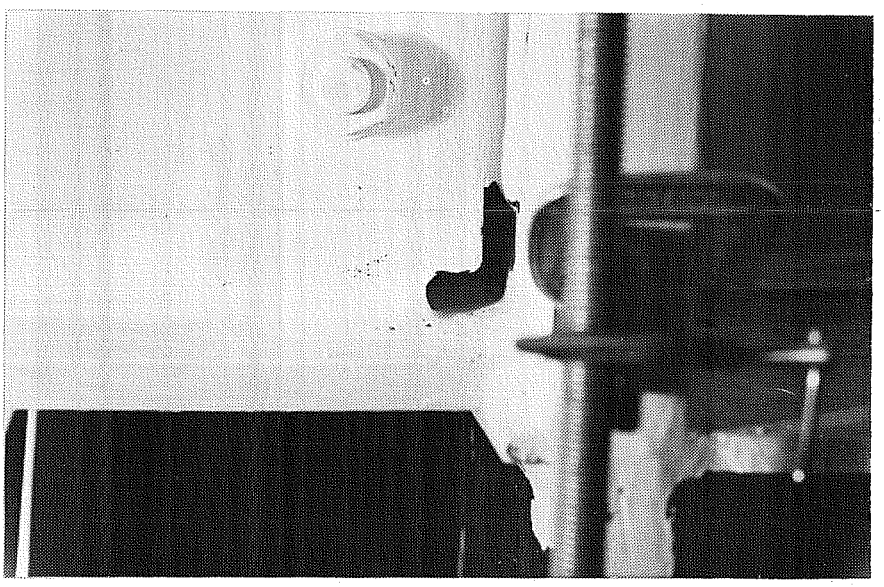

Figure 3.14 - Specimen 4 Showing Size of Web Cope

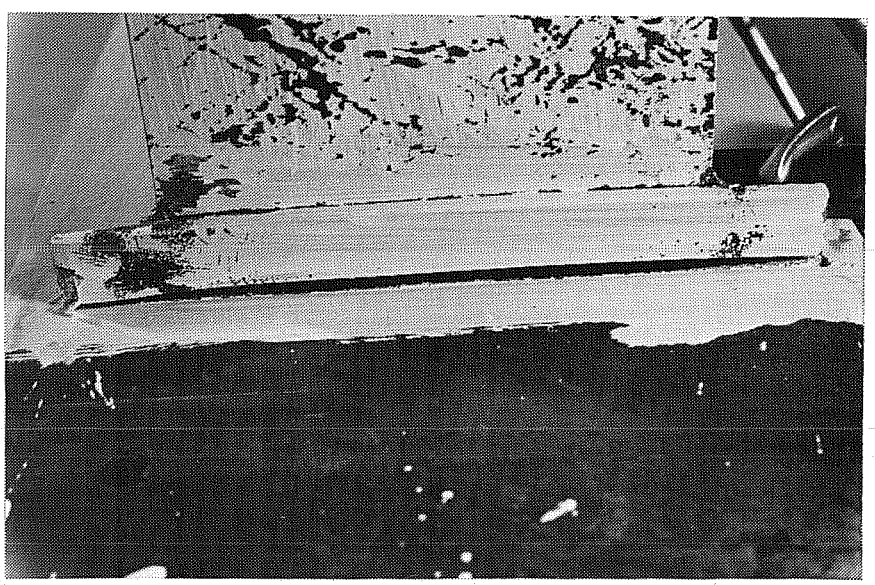

Figure 3.15 - Bottom Flange Failure in Specimen 4

Figure 3.16 - Fracture Surface in Column of Specimen 4

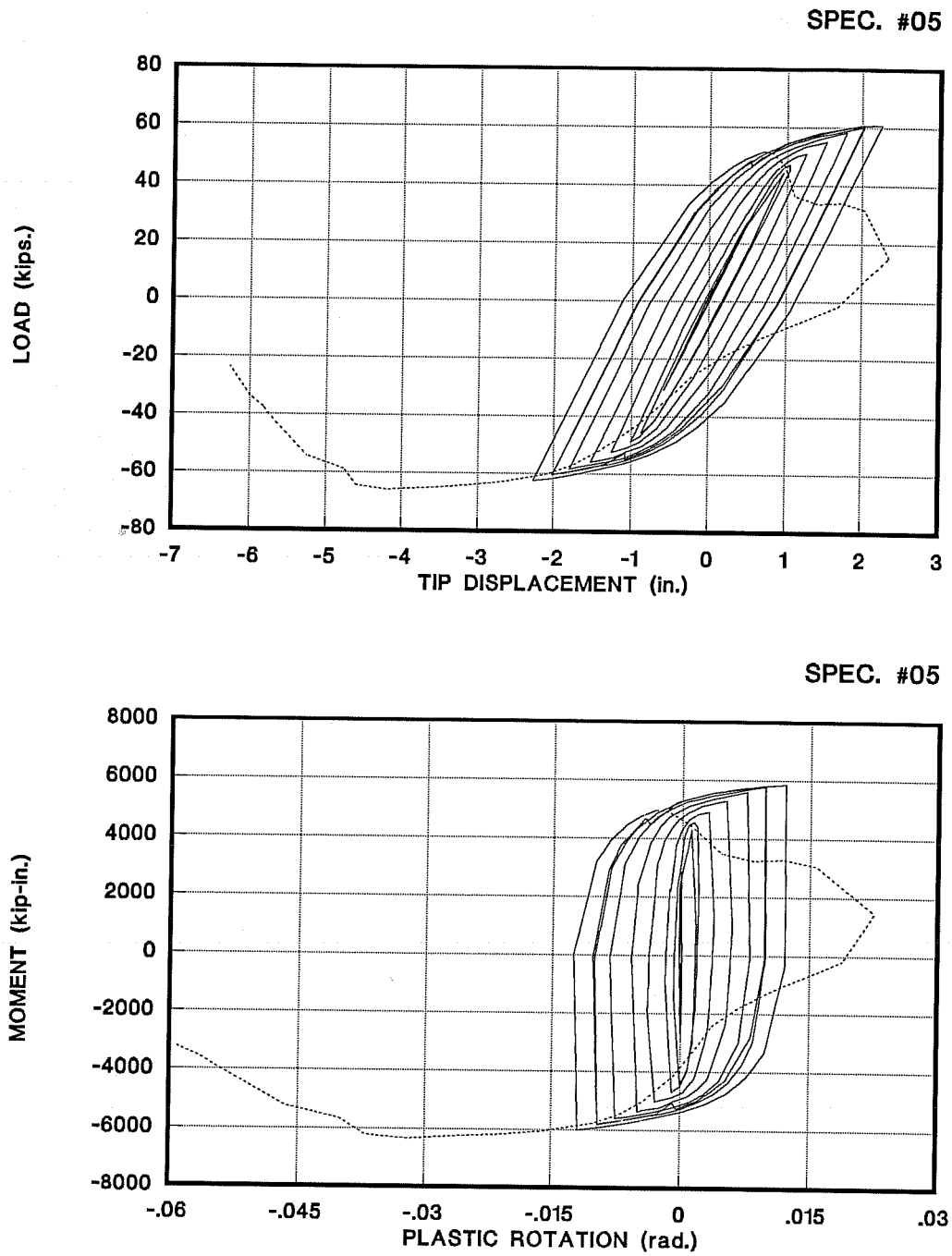

Figure 3.17 - Hysteretic Response of Specimen 5

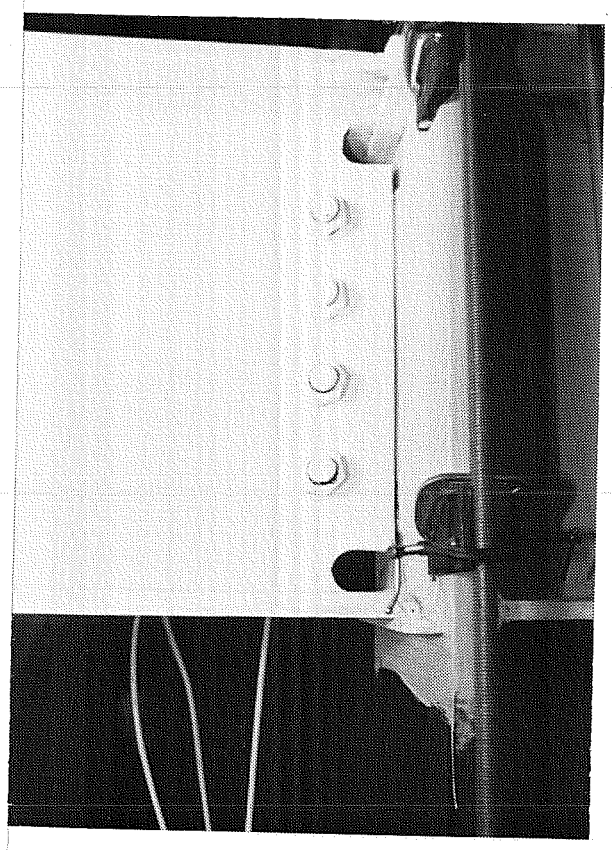

Figure 3.18 - Specimen 5 Showing Size of Web Copes

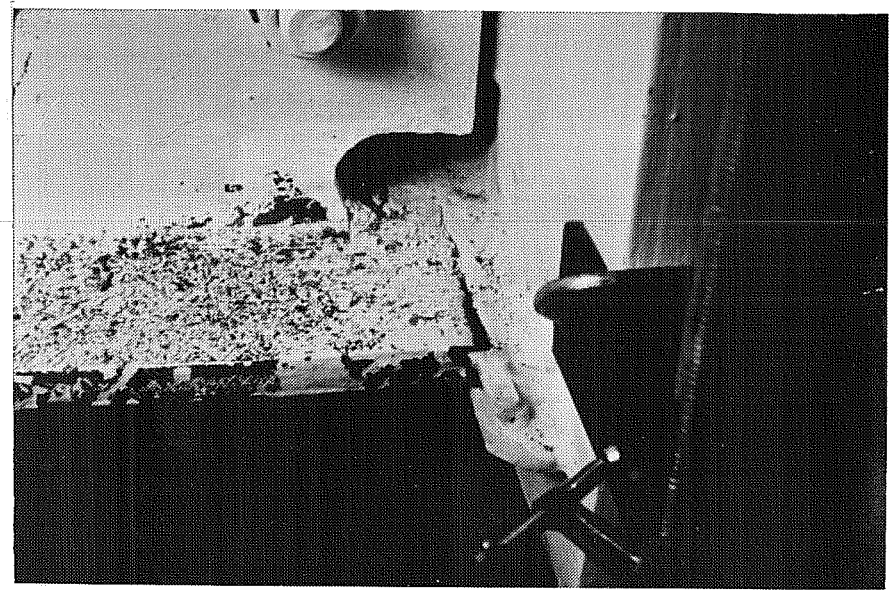

Figure 3.19 - Bottom Flange Crack Initiation in Specimen 5

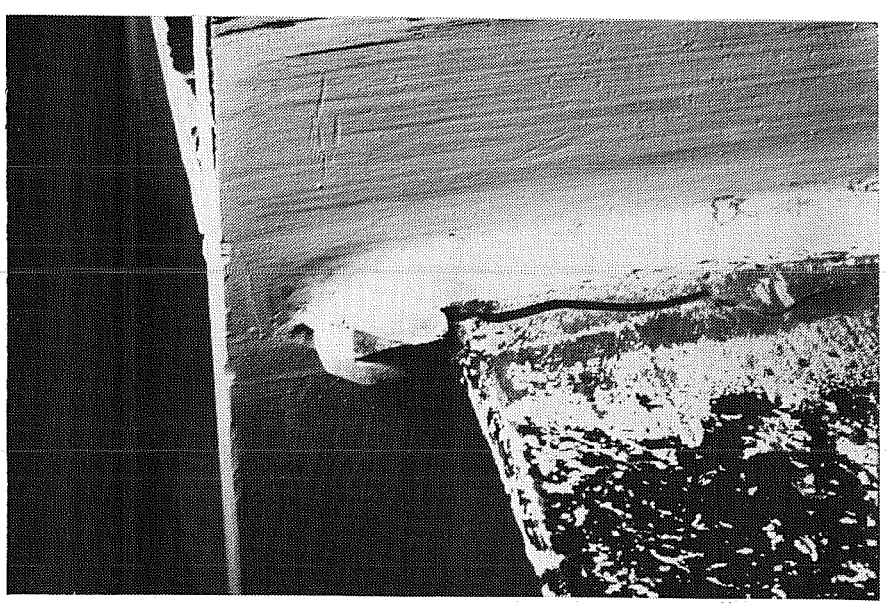

Figure 3.20 - Top Flange Failure in Specimen 5

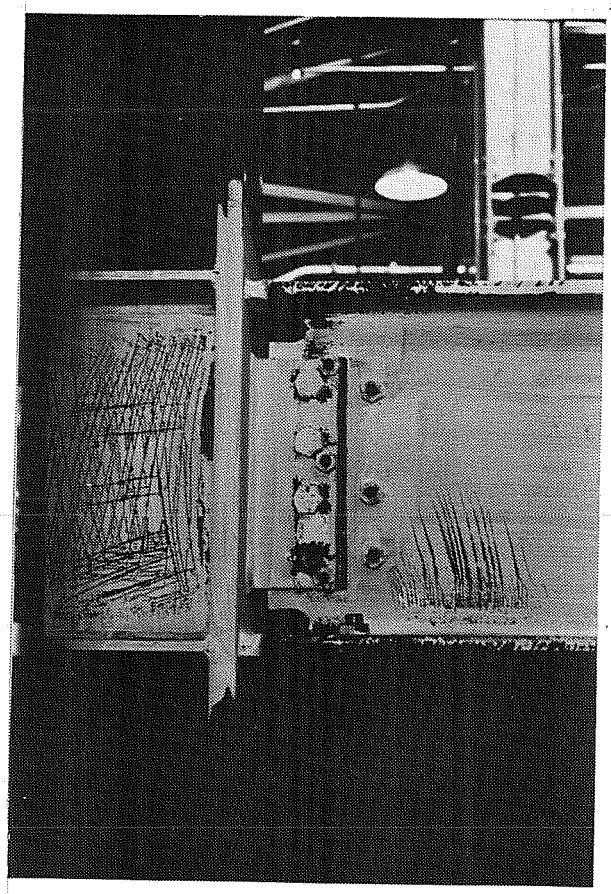

Figure 3.21 - Specimen 5 After Test

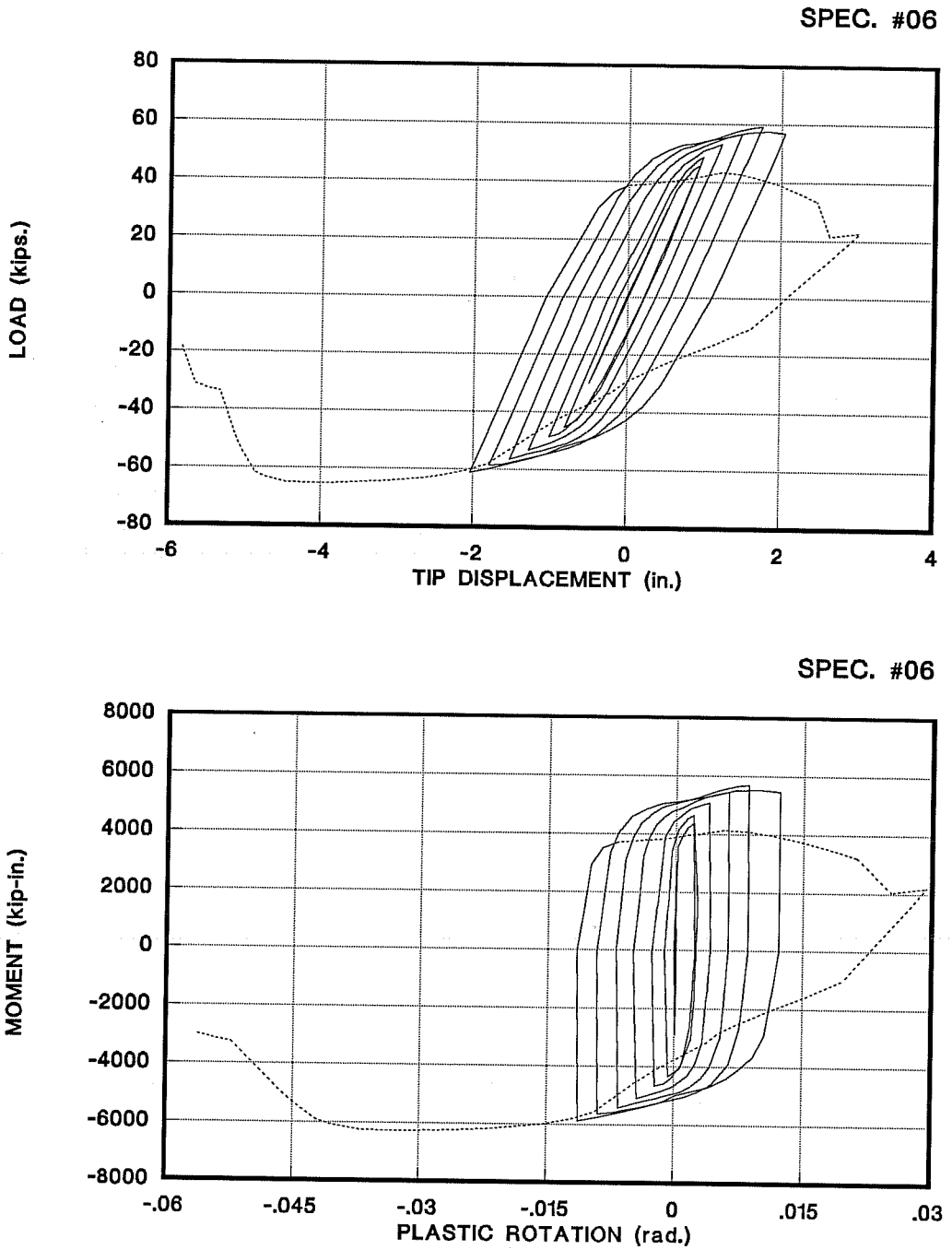

Figure 3.22 - Hysteretic Response of Specimen 6

Figure 3.23 - Bottom Flange Failure in Specimen 6

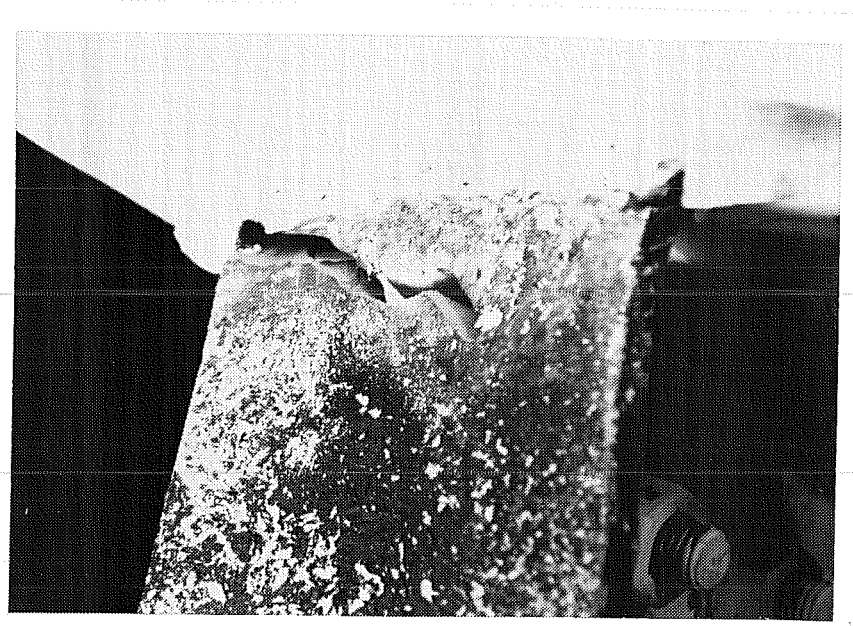

Figure 3.24 - Top Flange Failure in Specimen 6

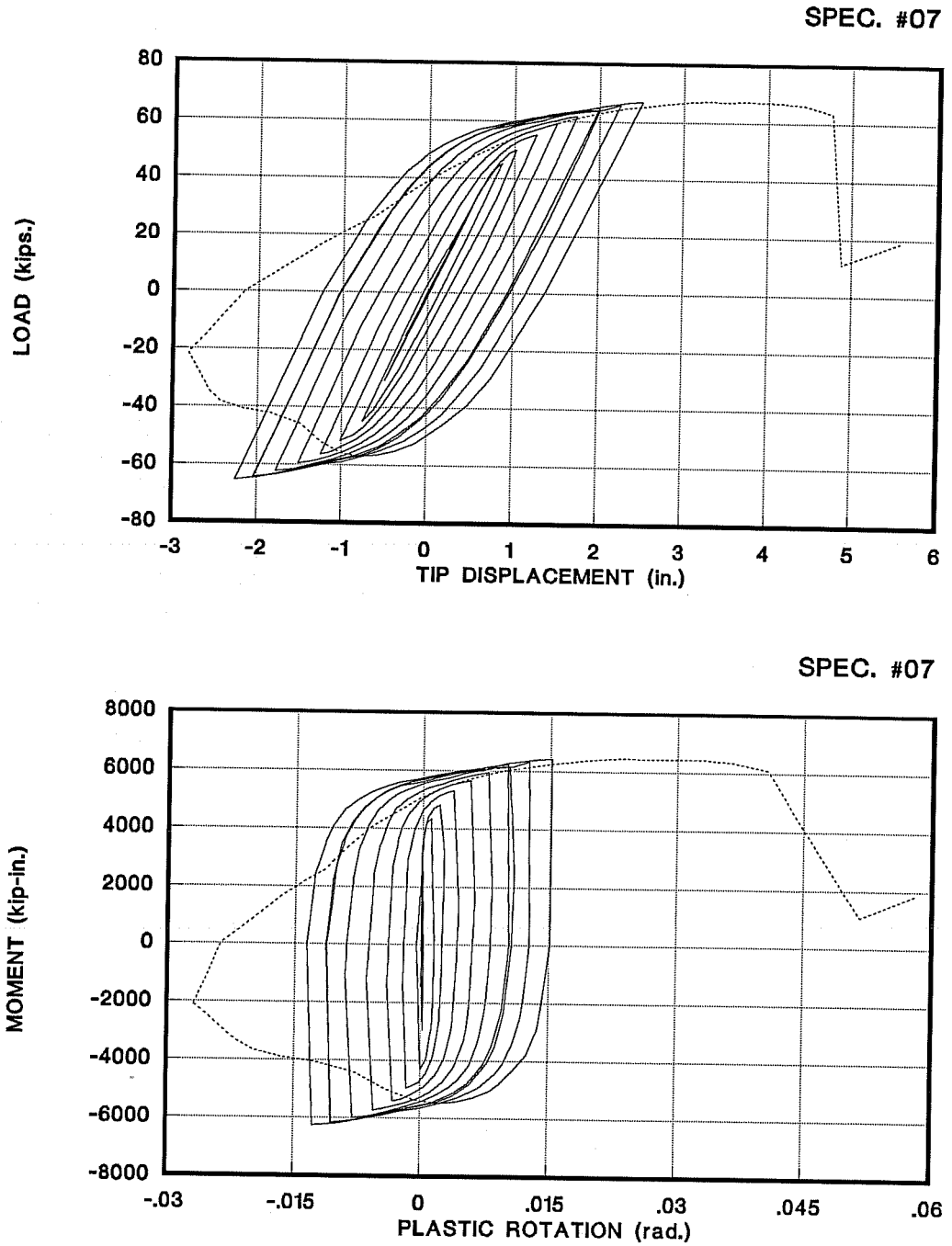

Figure 3.25 - Hysteretic Response of Specimen 7

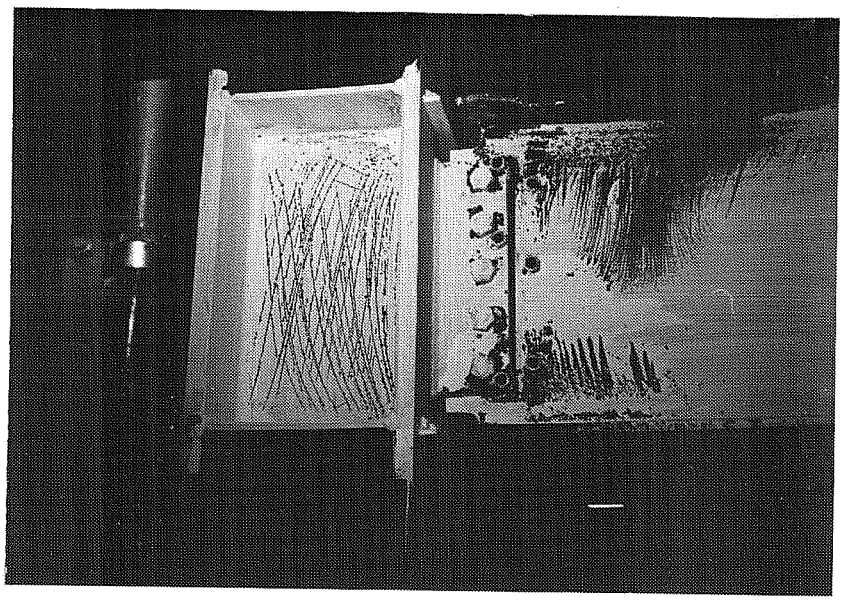

Figure 3.26 - Specimen 7 After Test

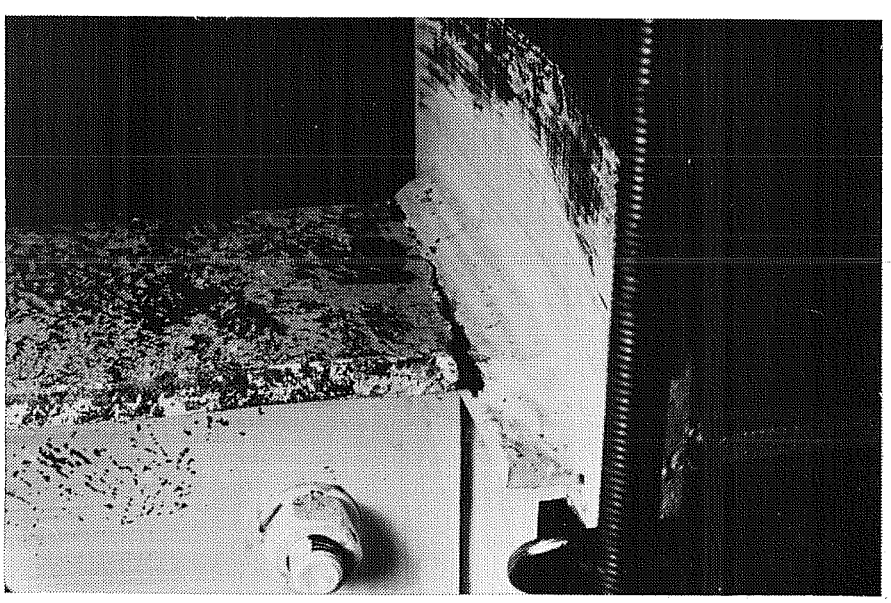

Figure 3.27 - Top Flange Failure in Specimen 7

Figure 3.28 - Top Flange Failure in Specimen 7

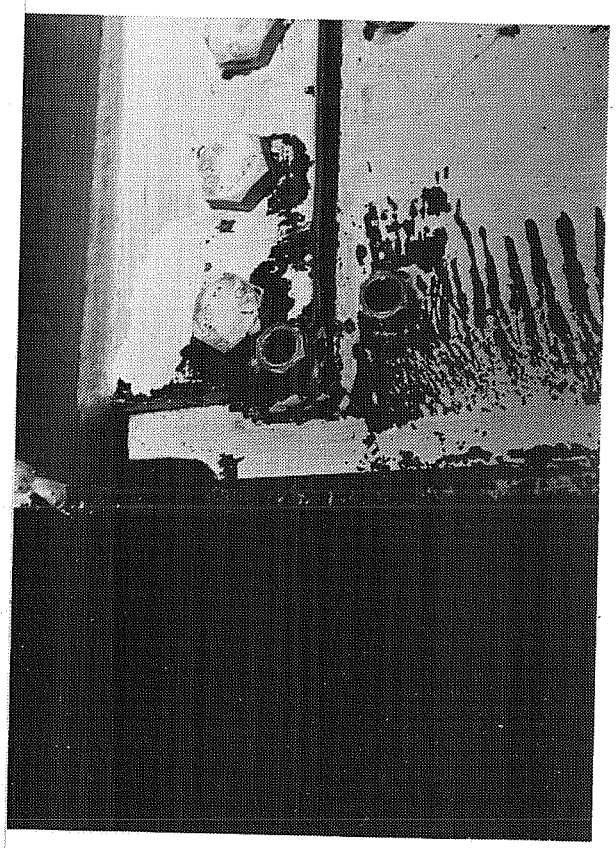

Figure 3.29 - Cracked Supplementary Web Weld in Specimen 7

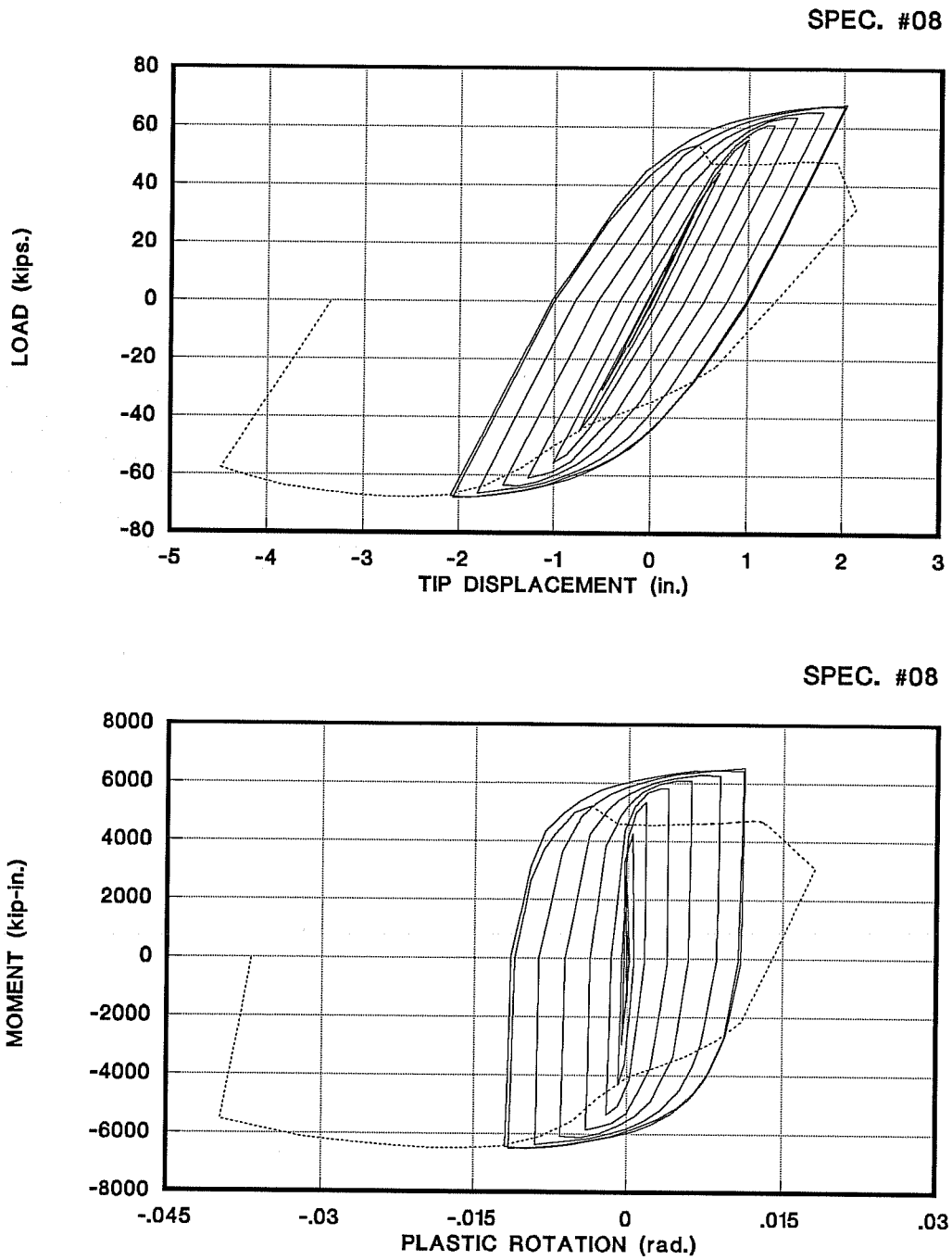

Figure 3.30 - Hysteretic Response of Specimen 8

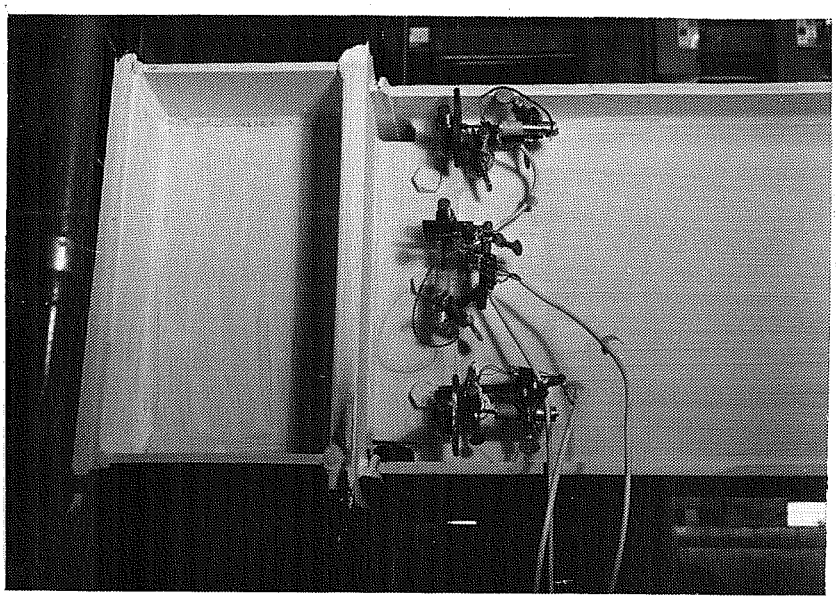

Figure 3.31 - Specimen 8 Before Testing

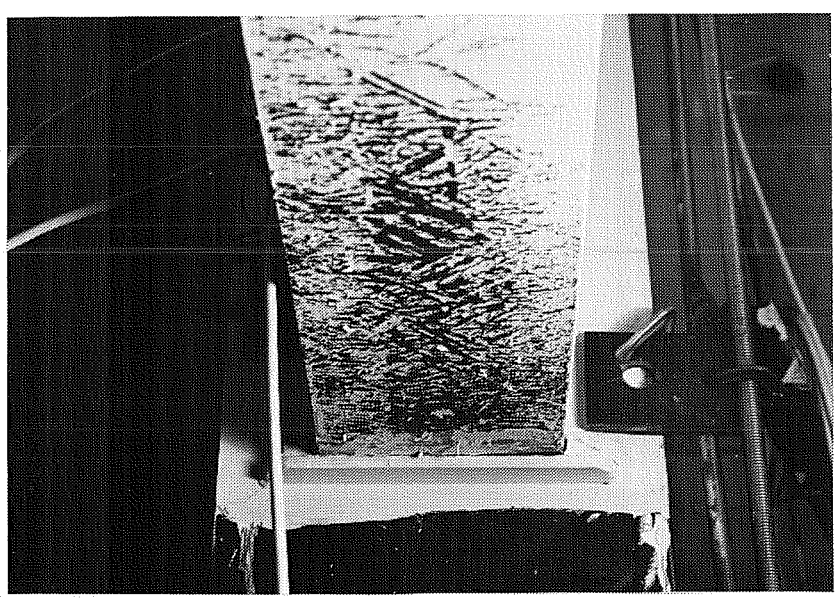

Figure 3.32 - Crack Initiation at Bottom Flange of Specimen 8

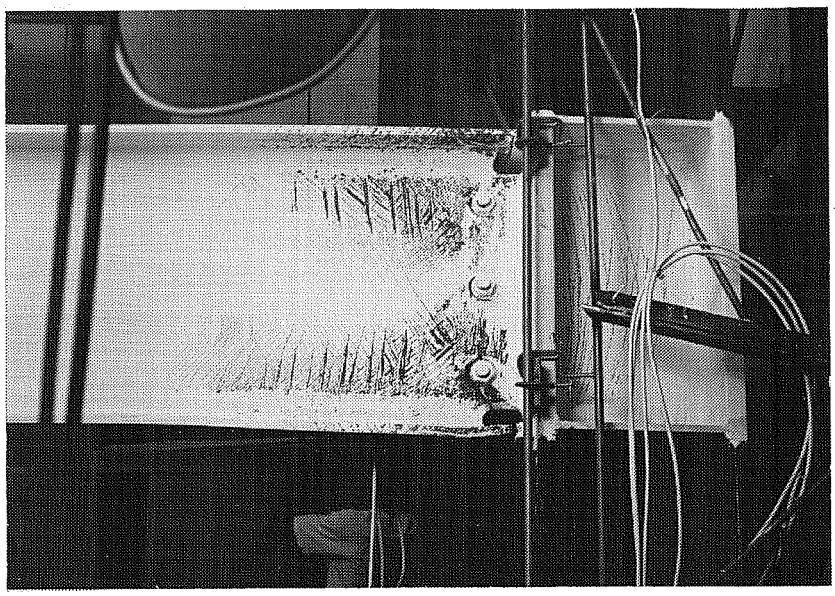

Figure 3.33 - Specimen 8 After Test

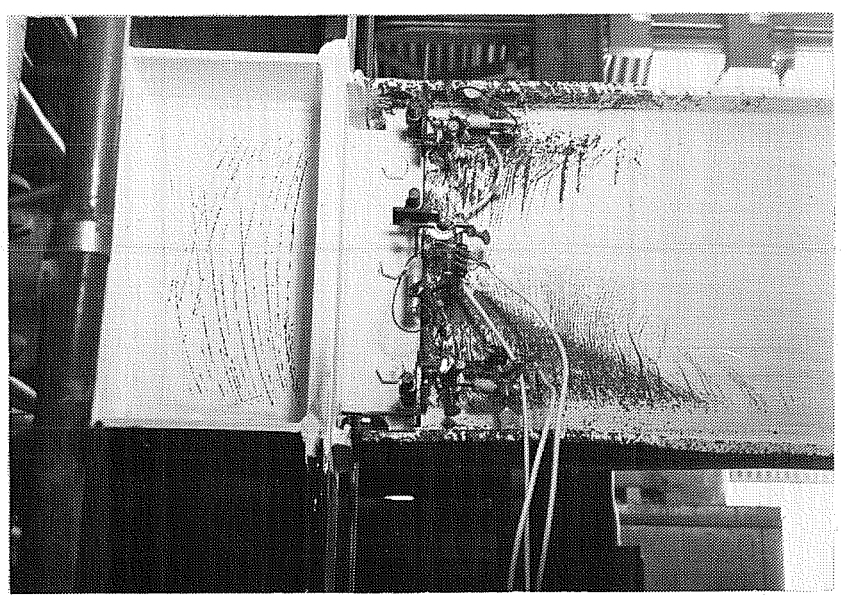

Figure 3.34 - Specimen 8 After Test

4 - ADDITIONAL EXPERIMENTAL DATA

4.1 GENERAL

The basic data consisting of the load-deformation history of the specimens were presented in Chapter 3. This chapter presents additional information and data that may provide some further insight into the overall behavior of the specimens.

4.2 BENDING MOMENTS

Although inelastic deformation capacity is the primary criterion for judging the performance of the test specimens, it is also useful to consider the maximum bending moments developed by the beam of each specimen at the connection. The maximum moment (M_{max}) developed by each beam at the column face prior to failure of the specimen is reported in Table 4.1. For comparison, the nominal plastic moment (M_p) and the estimated actual plastic moment (M_p^*) of each section are also listed. The comparison between M_{max} and M_p^* must be considered approximate, since these quantities were not necessarily measured at the same strain rate.

Several observations can be made from Table 4.1. All specimens developed their nominal plastic moments. Further, all specimens, except Nos. 1, 2, and 4, developed their estimated actual plastic moments. The poor ductility of Specimens 1, 2, and 4 has already been noted in Chapter 3. Table 4.1 indicates that these specimens also performed very poorly from a strength point of view.

A few comparisons between the performance of specimens with the same Z_f/Z ratios can also be made. Specimens 1 to 3, 4 and 5, and 6 to 8 can be grouped together on this basis. In the first group, however, Specimen 3 cannot be compared directly to Specimens 1 and 2 because it had repaired flange welds. Looking at the close

resemblance of the performance of Specimens 1 and 2, it becomes apparent that the amount of bolt tension in the beam web had little effect on strength. (Specimens 1 and 2 had A325 and A490 bolts respectively). Rather, the poor quality of the flange welds appear to have completely controlled the performance of these specimens. The importance of the flange welds is also evident in the second group (Specimens 4 and 5). Specimen 5, with identical web connection details as Specimen 4, developed substantially greater strength.

TABLE 4.1

Comparison of Nominal and Maximum Moments

Specimen	M_{max}	M_p	M_p^*	M_{max}/M_p	M_{max}/M_p^*
1	5420	4820	6140	1.12	0.88
2	5400	4820	6140	1.12	0.88
3	6390	4820	6140	1.33	1.04
4	4780	4430	5550	1.08	0.86
5	5930	4430	5550	1.34	1.07
6	5880	4640	5260	1.27	1.12
7	6340	4640	5260	1.37	1.21
8	6520	4640	5260	1.40	1.24

Notes:
M_{max} = Maximum moment in beam prior to failure
M_p = Nominal plastic moment based on F_y = 36 ksi
M_p^* = Estimated actual M_p based on coupon data (Dynamic F_y)

Perhaps the most interesting trend in behavior can be observed in the final group (Specimens 6, 7, and 8). Within this group, Specimen 6 had only a bolted web, and therefore provided the smallest degree of flexural capacity in the web connection. Specimen 7, with the supplemental web welds provided greater web participation. Finally, Specimen 8, with the all-welded web, provided the greatest degree of web participation. The data in Table 4.1 show increasing strengths progressing from Specimen 6 to 8. This

suggests that when reasonably good quality flange welds are provided, the web connection details do have a significant effect on strength. Note that a similar effect of web connection details on plastic rotation capacity was not observed (Table 3.4).

Finally, it is of interest to compare Specimens 5 and 6. These specimens each had only a bolted web, but had different Z_f/Z ratios. The data in the last column of Table 4.1 suggests that the Z_f/Z ratio, by itself, may have little impact on the maximum moment that can be developed by the section.

4.3 COLUMN PANEL ZONE SHEAR

As noted in Chapter 2, a primary criterion for choosing the W12x136, A572 Gr. 50 column was to minimize shear yielding of the panel zone, thereby forcing inelastic rotation to occur primarily by flexural yielding of the beam. This section presents various data on the shear strength of and shear forces developed within the panel zone.

In Table 4.2, panel zone data based on nominal section properties and nominal F_y's (F_y = 50 ksi for columns, F_y = 36 ksi for beams) are presented. The nominal strength of the column panel zone, as defined by Equation 4-1 of the 1988 Blue Book [23], is computed as follows:

$$V_n = 0.55 F_{yc} d_c t \left[1 + \frac{3 b_c t_{cf}^2}{d_b d_c t} \right]$$

This equation, based on Krawinkler [13], provides an estimate of the strength developed at moderately large inelastic shear deformations of the panel zone. Also tabulated in Table 4.2 is the quantity V_y, which is defined as follows:

$$V_y = 0.55 F_{yc} d_c t$$

AISC plastic design rules [2] use V_y to determine panel zone shear strength. V_y is based on the shear yield stress of $0.577F_y$ acting on an effective shear area of $0.95d_c t$. Finally, an estimate of the design shear force in the panel zone, when the nominal M_p of the beam is developed, is computed as follows:

$$V_{des} = \frac{M_p}{0.95 d_b} - V_c$$

In the above equations, the symbols are defined as:

F_{yc}	=	yield strength of column web
d_c	=	depth of column
t	=	thickness of column web
b_c	=	width of column flange
t_{cf}	=	thickness of column flange
d_b	=	depth of beam section
M_p	=	nominal plastic moment of beam
V_c	=	column shear force (outside of panel zone) when beam moment is M_p

The data in Table 4.2 show that both measures of panel zone strength, V_n and V_y are greatly in excess of the design panel zone shear force. Based on his panel zone experiments, Krawinkler indicated that yielding of the panel zone initiated at about 75 percent of V_y [13]. In Table 4.2, V_{des} is less than or equal to 75 percent of V_y for all specimens. Consequently, no yielding would be anticipated for any of the test specimens.

TABLE 4.2

Panel Zone Shear Data Based on Nominal Properties

Spec. No.	V_n (kips)	V_y (kips)	V_{des} (kips)
1	359	291	175
2	359	291	175
3	359	291	175
4	379	291	219
5	379	291	219
6	367	291	194
7	367	291	194
8	367	291	194

Table 4.3 presents panel zone data based on measured properties and forces. Estimates of panel zone strength, V_n and V_y, are computed as above, except that is F_{yc} is based on the column web coupon yield strength (estimated for Specimen 8). An estimate of the actual panel zone shear force is computed as follows:

$$V_{actual} = \frac{M_{\max}}{0.95\, d_b} - V_c$$

where:

M_{max} = maximum moment in beam prior to failure (Table 4.1)

V_c = column shear force (outside of panel zone) when beam moment is M_{max}

The comparison between V_{actual} and the quantities V_n and V_y in Table 4.3 must be considered approximate, since they were not necessarily measured at the same strain rate.

TABLE 4.3

Panel Zone Shear Data Based on Measured Properties

Spec. No.	V_n (kips)	V_y (kips)	V_{act} (kips)
1	428	347	197
2	428	347	196
3	428	347	233
4	452	347	236
5	452	347	293
6	437	347	245
7	437	347	265
8	437	347	272

The data in Table 4.3, with the exception of Specimen 5, again indicate that yielding would not be anticipated in the panel zones of the test specimens. Some yielding was, in fact, observed in all test specimens. For most specimens, the observed yielding was slight. However, somewhat more substantial yielding was observed in Specimen 5. Table 4.3 shows that Specimen 5 produced the highest panel zone shear among all the test specimens. But even for this specimen, V_{actual} was only 85 percent of V_y. Note also that the shear force in the panel zone of Specimen 5 would need to increase by an additional 50 percent before V_n is achieved.

As noted in Chapter 2, rotations were measured at the column during the tests. These rotations were measured at points where the column flange attaches to the beam flanges, as shown in Figure 2.6. These measurements include overall bending rotations of the column, as well as panel zone deformations. Figure 4.1 shows the measured rotations, plotted against bending moment in the beam. Examination of the column rotation measurements indicate that errors in the measurement system were rather large

compared to the small rotations occurring at the column. The data in Figure 4.1 should therefore be viewed only for qualitative trends in behavior.

The plots in Figure 4.1 suggest that no significant inelastic deformation was contributed by the panel zones of the test specimens. Specimen 5 was an exception. A greater degree of hysteresis is apparent in the column rotation measurements for this specimen, which is consistent with observed yielding patterns.

4.4 MEASUREMENTS AT SHEAR TAB

As shown in Figure 2.6, 3 displacement transducers were employed to measure the displacement of the beam web relative to the shear tab. A photograph of these transducers is shown in Figure 3.31. The object of measuring these displacements was to collect data that may shed some light on the effect of various details on participation of the web in resisting moments. The data collected are reported in Figures 4.2 to 4.9. The displacements were measured from the original undeformed position. Horizontal displacements were measured at the top and bottom of the shear tab. For these transducers, positive displacements are defined as the relative movement of the beam web *away* from the shear tab. A tensile deformation, therefore, corresponds to a positive displacement. Vertical displacement was measured at midheight of the shear tab. For this transducer, positive displacement corresponds to the beam web moving downward relative to the shear tab. As in Chapter 3, dashed lines show the behavior of the specimen after fracture of a flange connection occurred. The dashed portion of the plots in Figures 4.2 to 4.9, however, are terminated earlier than those in Chapter 3. This was done because, after failure, the transducers at the shear tab usually either were shook loose from their supports or exhausted their capacity.

A close look at these hysteretic loops suggests that initial slip occurred in the early cycles as the specimens were still in the elastic range. This initial slip was usually spread

over two cycles and can be spotted as sudden, jerky changes in the load-displacement plots. It can also be noticed that during this initial slip the beam web always slipped *away* from the shear tab, never *into* it. After this initiation of slip was complete in about two cycles, usually by the end of 4th cycle, the continued slip showed smoother hysteretic response.

The horizontal displacement of the beam web relative to the shear tab showed a very interesting trend. Tensile deformation was accumulated at both the top and the bottom of the shear tab as indicated by the loops leaning to the positive displacement side. A possible explanation of this phenomenon is the apparent shifting of the center of beam rotation. The beam evidently rotated about its centerline until the initial slip was complete. After that, the movement of the beam web *away* from the shear tab in the first half of a load cycle was greater than the movement *into* the tab in the second half of the cycle. In the half cycles during which the beam web was moving towards the shear tab, further movement *into* the tab was very limited after closing of the gap which was formed in the earlier half cycle. The center of rotation at this point would apparently shift to just above the shear tab bottom or just below the shear tab top. This shifting of the center of rotation was apparently leading to hysteresis that would otherwise be symmetric. Thus, the major reason for the observed hysteresis in the shear tab displacements appears to be slip accompanied by this shifting of the center of rotation and *not* due to inelastic deformations in the beam web. This observation is supported by the fact that almost no yield lines were formed on the beam web in Specimens 1, 2, and 4 at failure, yet the magnitude of hysteresis on the plots of these specimens is of the same general order as the other specimens. Only very slight yield lines formed on the beam web at failure on other specimens as well, indicating that the cause of hysteresis likely related to slip.

The vertical displacement plots generally show symmetric behavior. Where present, the asymmetry is very small. These plots reflect the vertical movement of the

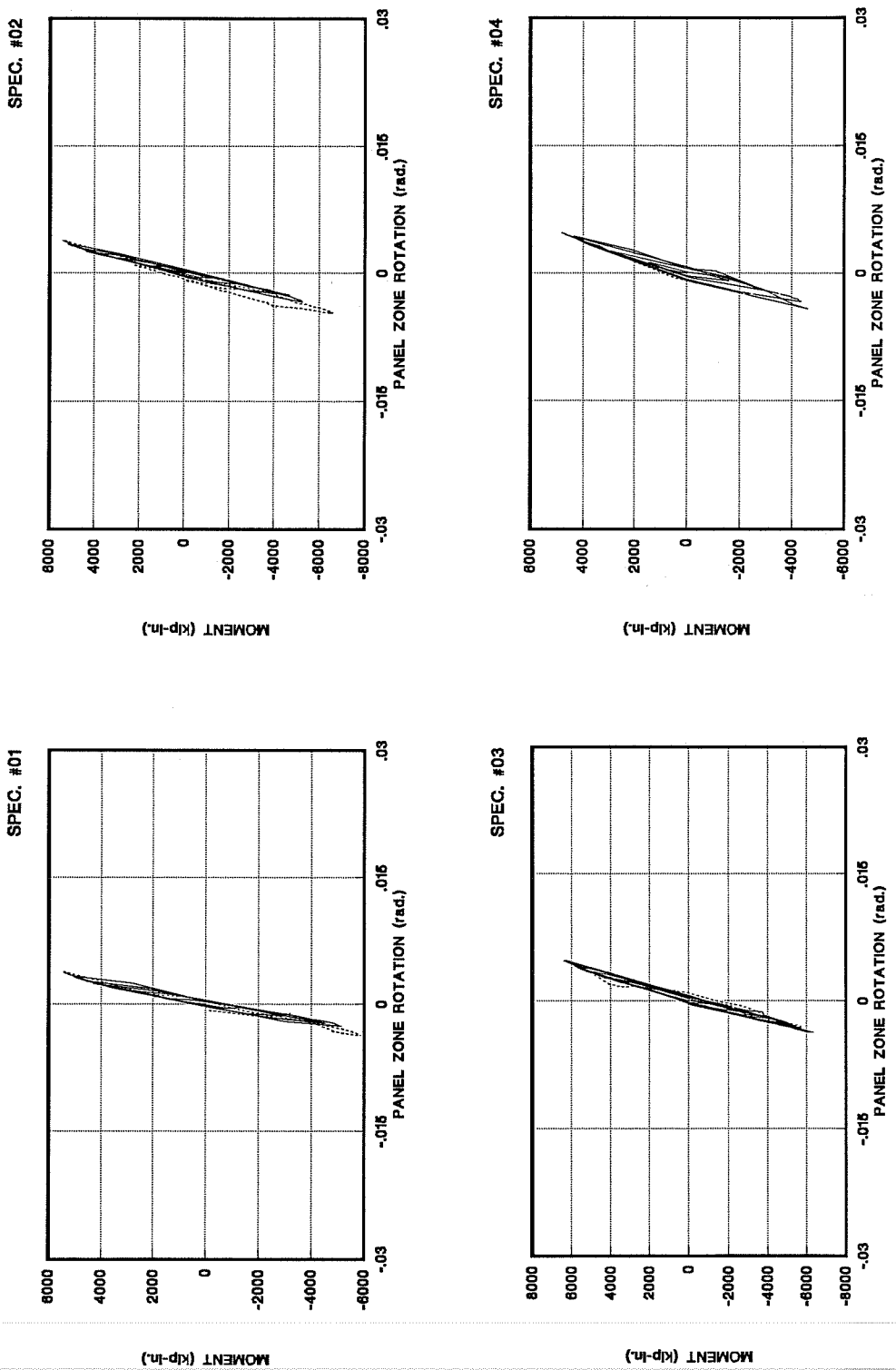

Figure 4.1 - Panel Zone Rotation vs. Moment for Specimens 1 to 8

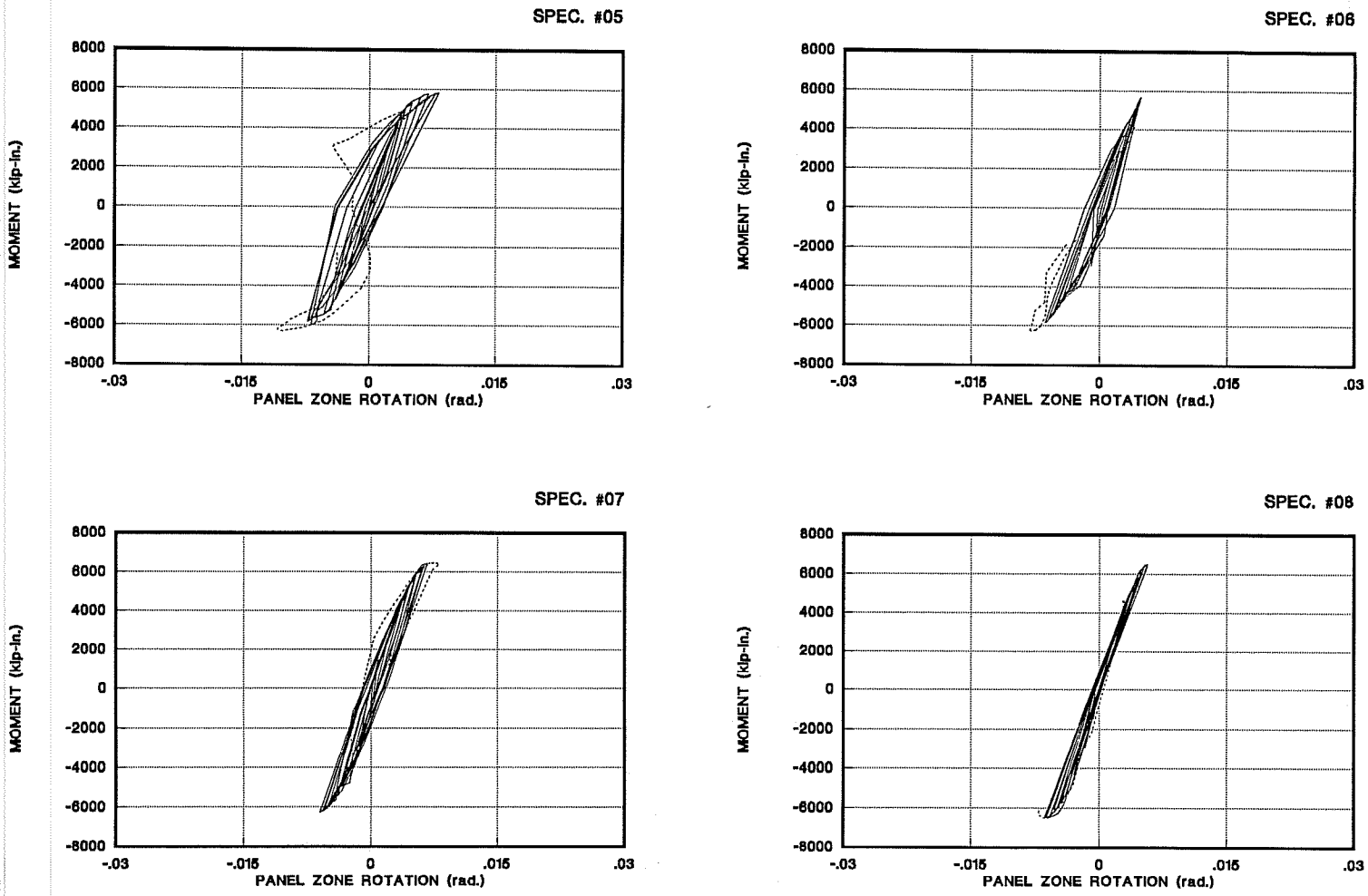

Figure 4.1 (contd.) - Panel Zone Rotation vs. Moment for Specimens 1 to 8

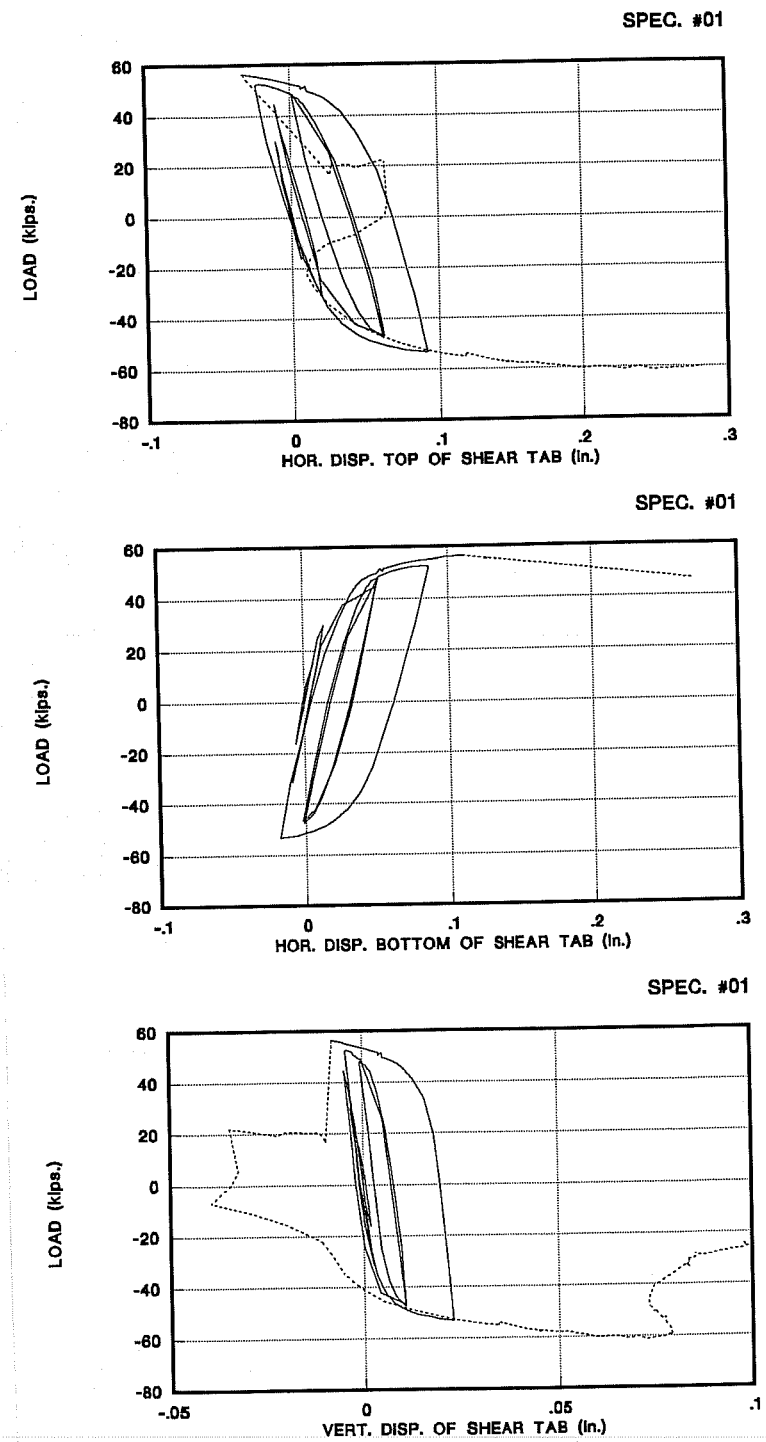

Figure 4.2 - Load vs. Displacements at Shear Tab for Specimen 1

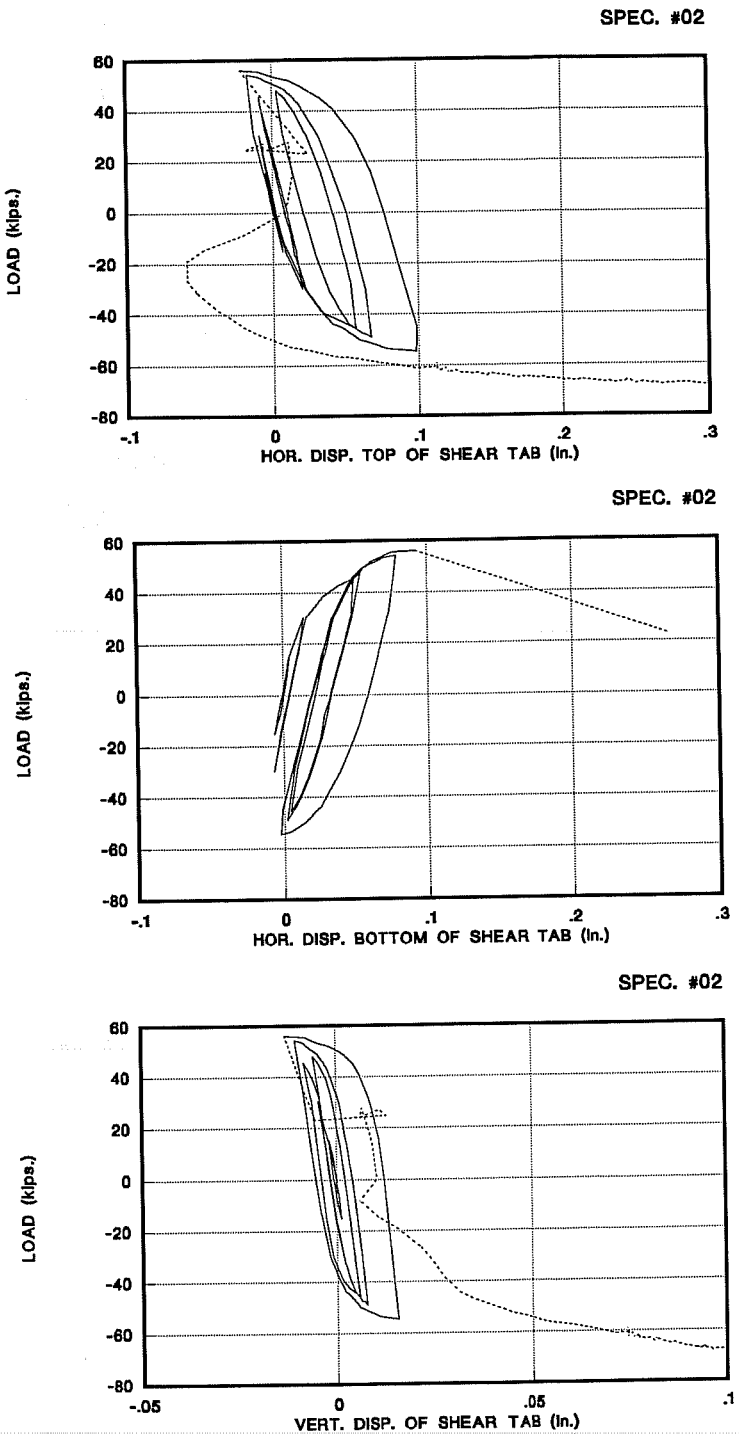

Figure 4.3 - Load vs. Displacements at Shear Tab for Specimen 2

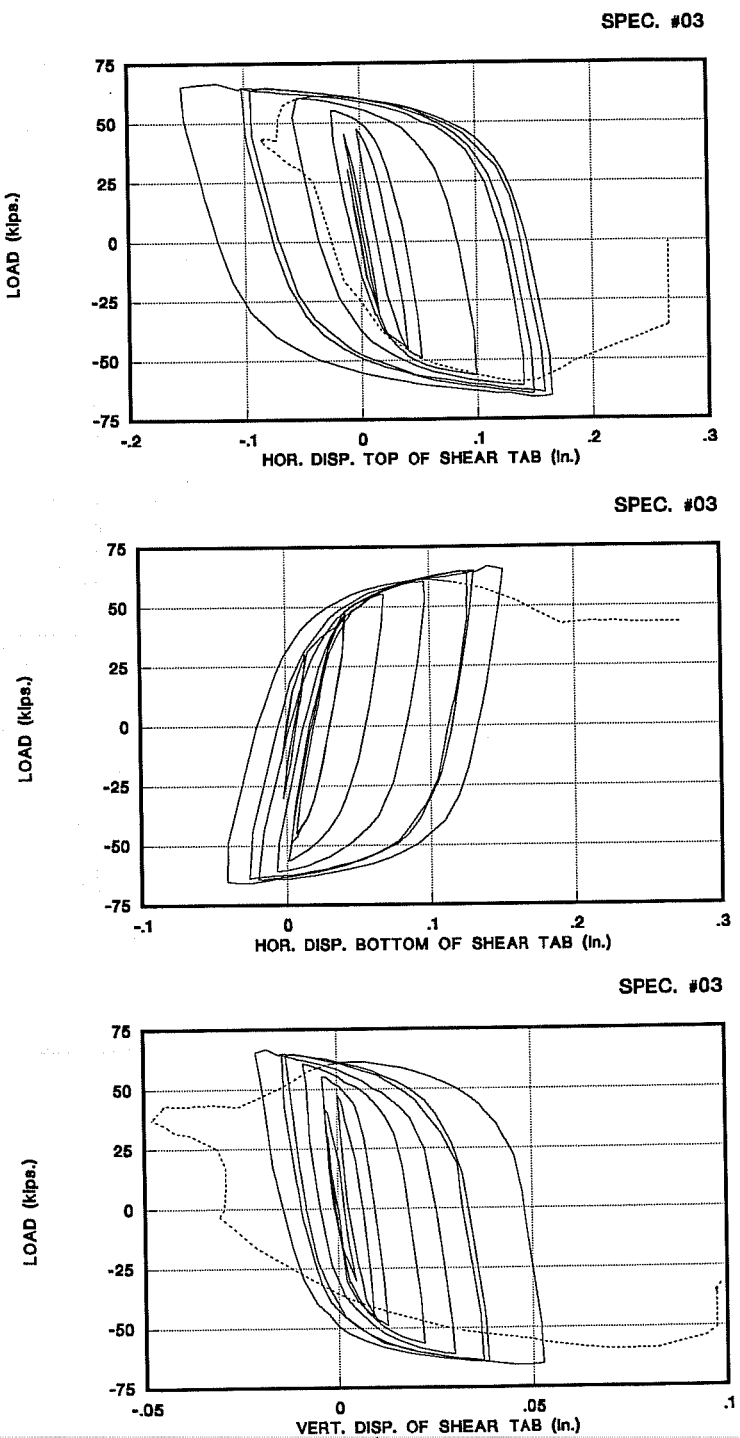

Figure 4.4 - Load vs. Displacements at Shear Tab for Specimen 3

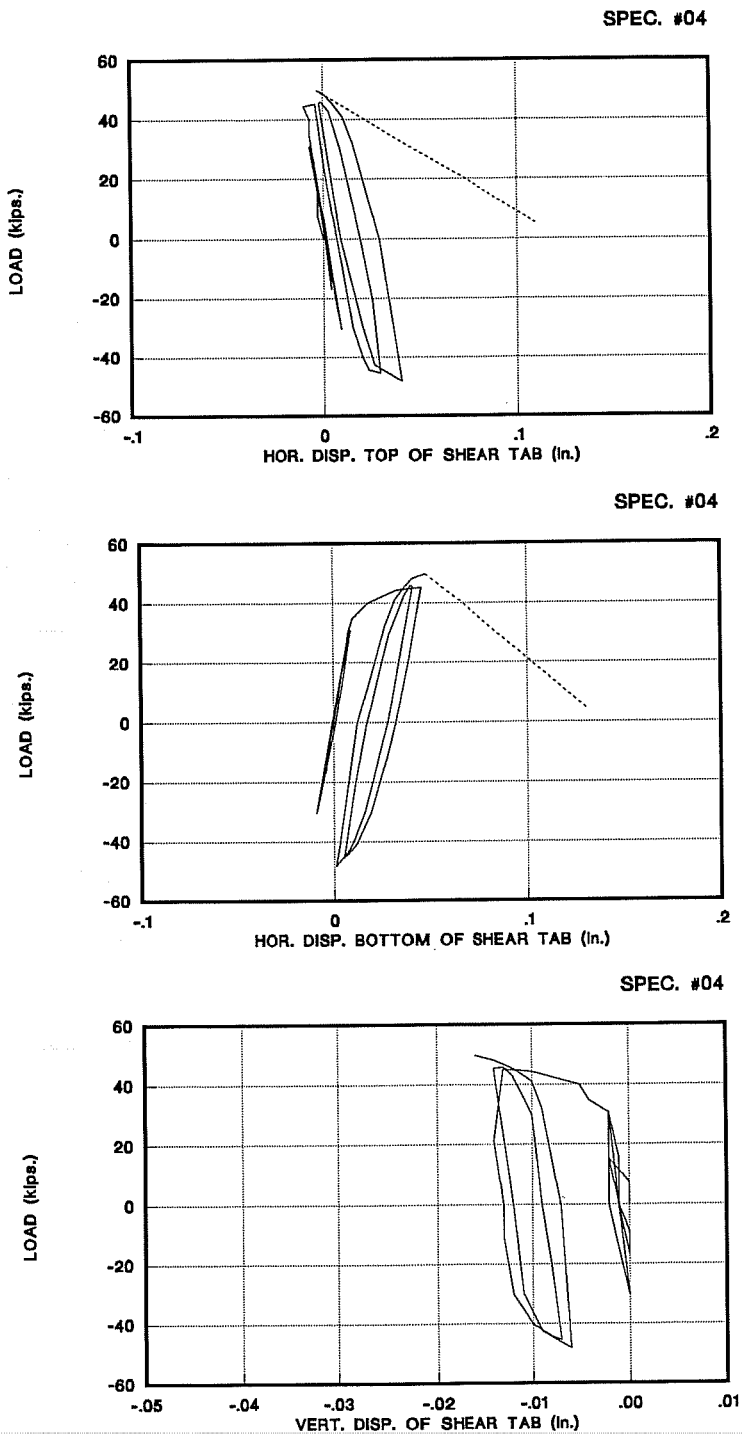

Figure 4.5 - Load vs. Displacements at Shear Tab for Specimen 4

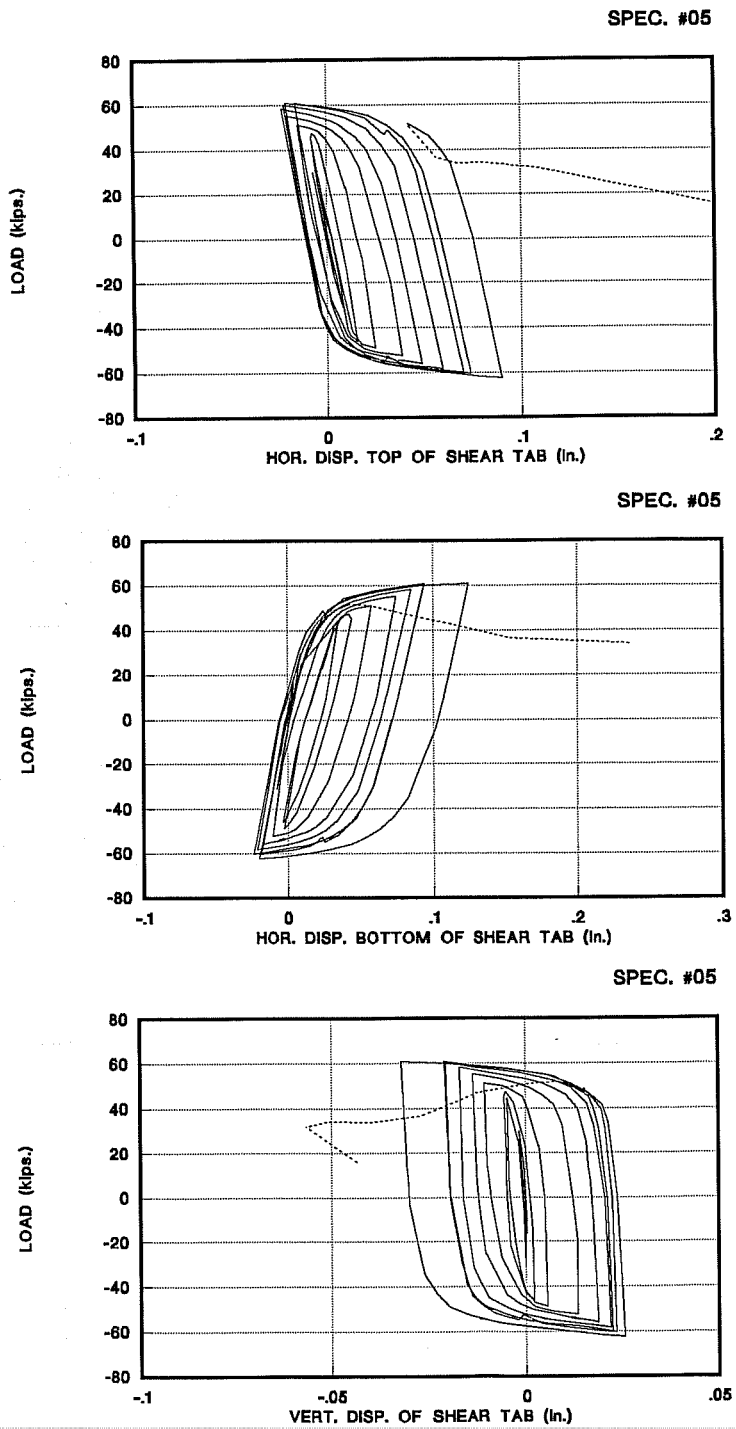

Figure 4.6 - Load vs. Displacements at Shear Tab for Specimen 5

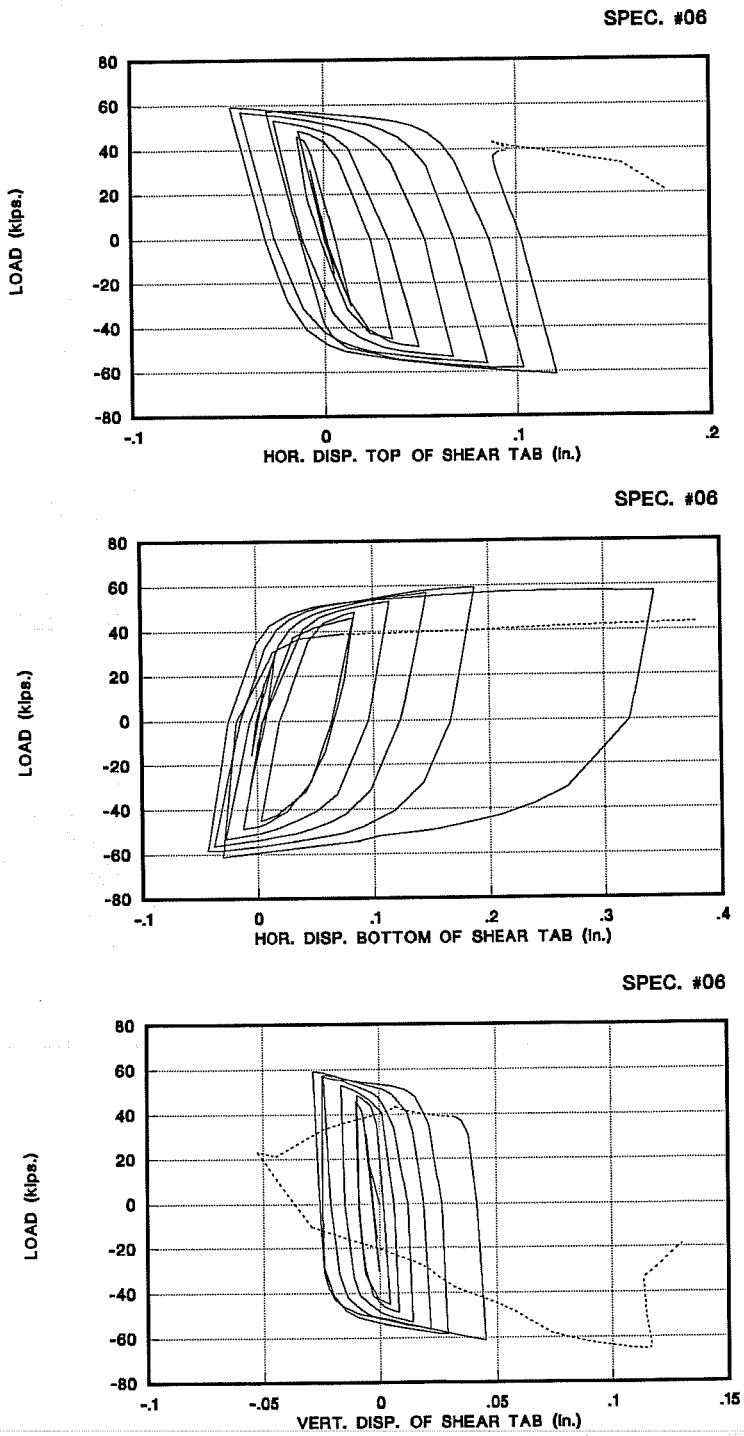

Figure 4.7 - Load vs. Displacements at Shear Tab for Specimen 6

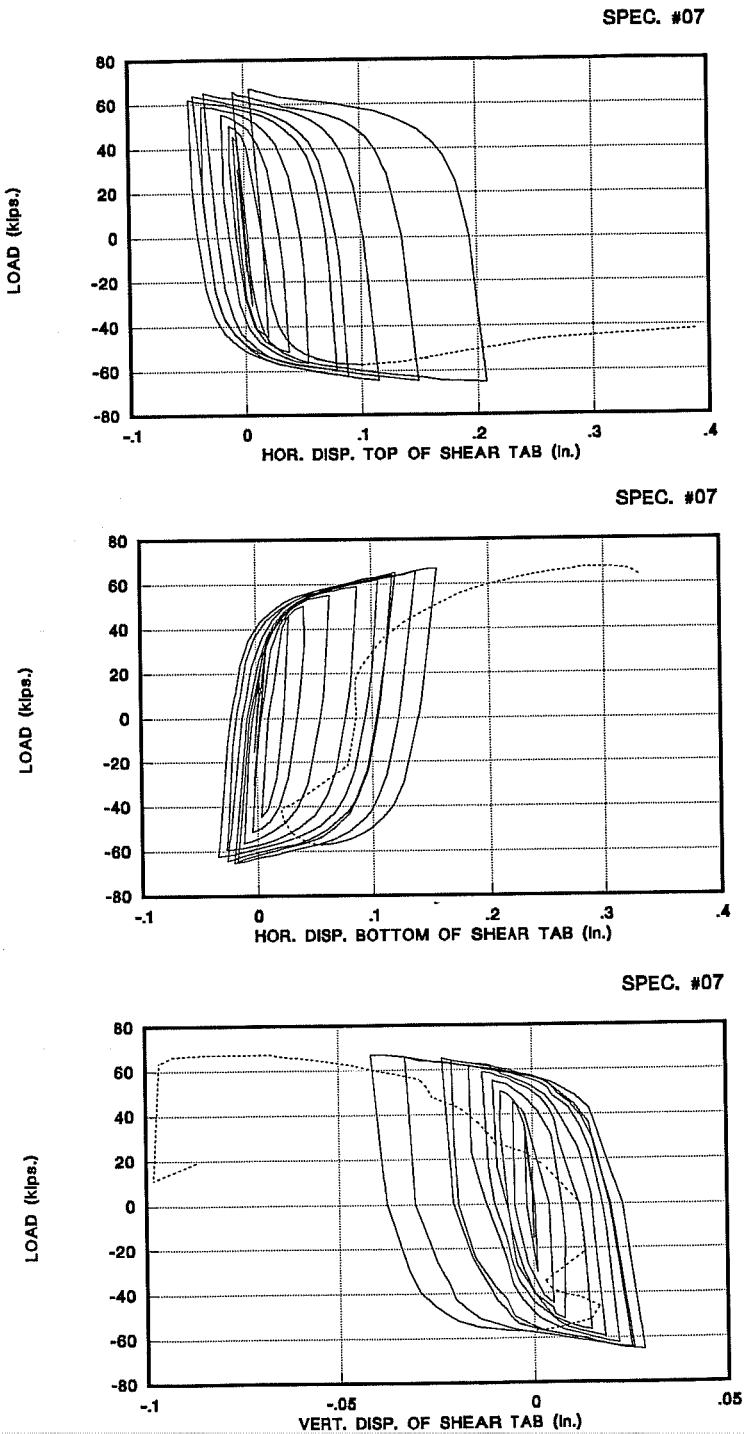

Figure 4.8 - Load vs. Displacements at Shear Tab for Specimen 7

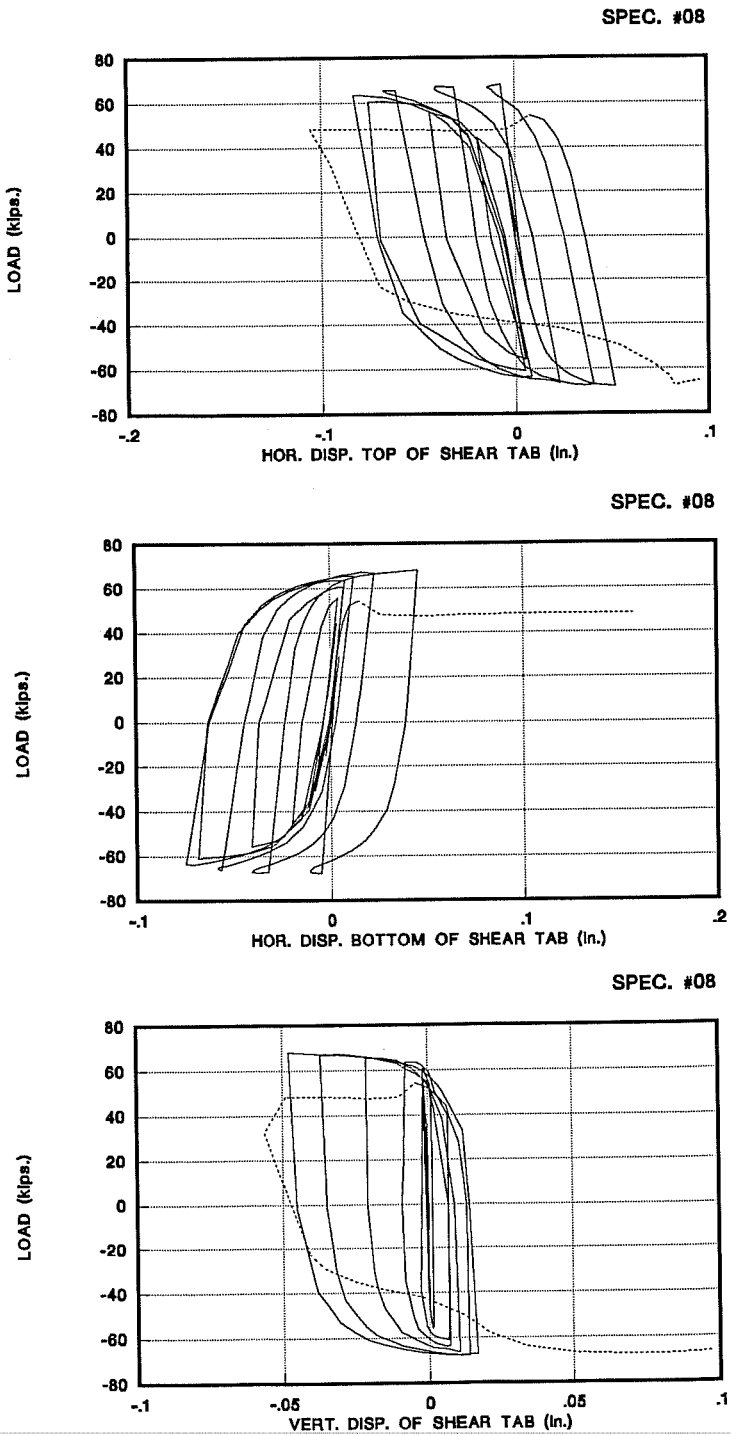

Figure 4.9 - Load vs. Displacements at Shear Tab for Specimen 8

beam web relative to the shear tab due to shear. The magnitude of vertical displacements is generally significantly smaller than the horizontal displacements.

An interesting observation can be made regarding the behavior shown by these plots for the specimens with supplemental web welds. It would be expected that these welds would effectively resist any slip between the shear tab and the beam web. This is not, however, evident from the plots of shear tab displacements. The general magnitude of these displacements on Specimens 3 and 7 with supplementary web welds is similar to that on other specimens. However, some effect of the web welds can be observed. Compare the horizontal displacement at the bottom of the shear tab for Specimen 6 (no web welds) with Specimen 7 (with web welds). More load was required for the same slip on Specimen 7 as compared to Specimen 6. This suggests that the web welds permitted greater participation of the web connection in resisting moments.

An exception to the general behavior was Specimen 8, the all-welded connection, where a little accumulation of compressive deformation is exhibited by the plots of the horizontal displacements. It is to be remembered though that this specimen is not directly comparable to others because of its different web connection detail. It can be seen that just before failure, there was actually an accumulation of tensile deformation. The strange sudden jerks visible at the tips of the loops during the final cycles were because of lateral twisting of the beam as well as web buckling witnessed in the final cycles of the test. Photographs for this specimen shown in Chapter 3 show the rather pronounced lateral twist in the beam near the connection.

4.5 ADDITIONAL COLUMN DATA

4.5.1 Charpy V-Notch Test Data

It was mentioned in Chapter 3 that an investigation was carried out to assess the quality of the column steel after the poor performance of Specimens 1, 2, and 4. The

different measures taken were discussed in that chapter. The complete data for the Charpy V-Notch tests discussed there is given in Table 4.4 below. Specimens were taken from the column flange, at the location specified in Supplement No. 1 to the LRFD Specification [4], and also from the outer surface of the column flange. The specimens numbered with the suffix 'A' were taken from the surface of the column flange. The locations of these specimens within a flange are shown in Figure 4.10. It can be seen from Table 4.4 that the absorbed energy in all cases significantly exceeded 20 ft-lb. at 70° F as required by the Supplement No.1 to the LRFD Specification.

TABLE 4.4

Charpy V-Notch Test Data

Specimen	Energy (ft-lb.)	Temp. (°F)
1	54.3	80
1A	54.3	80
2	34.2	60
2A	42.0	60
3	36.0	40
4	22.5	40
4A	21.5	40

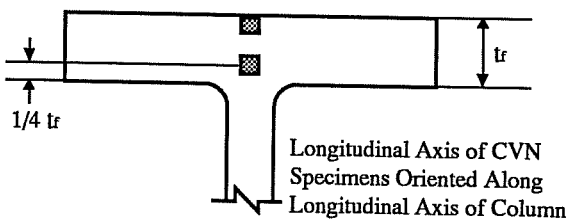

Figure 4.10 - Location of CVN Specimens Within Column Flange

4.5.2 Through-Thickness Coupons for Column Steel

Two special tensile coupons were prepared to assess the through-thickness properties of the column steel. Designated 'A' and 'B', these coupons are shown in Figures 4.11 and 4.12. The coupons were prepared by welding sections of a W18x60 beam flange in the case of coupon 'A' and sections of column flange in case of coupon 'B' to each side of a section of column flange, such that this section can be loaded in tension in the through-thickness direction. There was essentially no weld shrinkage restraint in these coupons.

Coupon 'A' was similar to the actual specimens because a beam flange was welded to the column flange in through-thickness direction. The weld detail was also similar. These coupons were prepared by a welder different from the those who did the welding on the actual specimens. Further, these welds were not ultrasonically tested.

Coupon 'A' failed in a manner similar to Specimens 1, 2, and 4. The failure occurred at the interface of the weld and the column flange in a sudden manner. Visual inspection of the failure surface showed lack of weld penetration and lack of fusion which was more severe than that on the actual specimens. The maximum stress achieved was 45.7 ksi in the beam flange material compared to 43.9 ksi yield and 63.7 ksi ultimate stress observed in the regular coupon of the W18x60 flange. The elongation achieved was negligible (less than 1%) compared to 29.8% in the regular coupon. Figure 4.13 shows the coupon after failure.

The failure of coupon 'B' was similar to coupon 'A'. A sudden failure occurred at the interface of the weld and the through-thickness segment of the column flange. Severe lack of weld penetration and a fibrous appearance were present on the failure surface. The maximum stress achieved was 63.9 ksi, compared to 57.1 ksi yield and 78.5 ksi ultimate stress observed in the regular column flange coupon. The elongation was

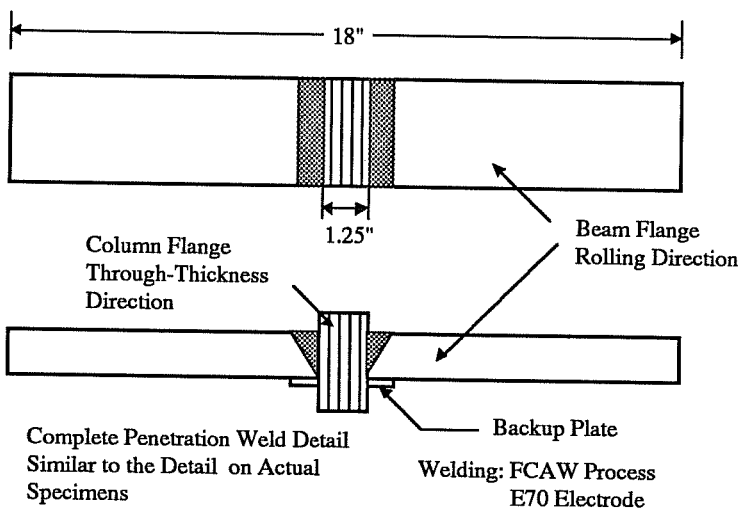

Figure 4.11 - Coupon 'A' for Testing Through-Thickness Properties of Column Flange

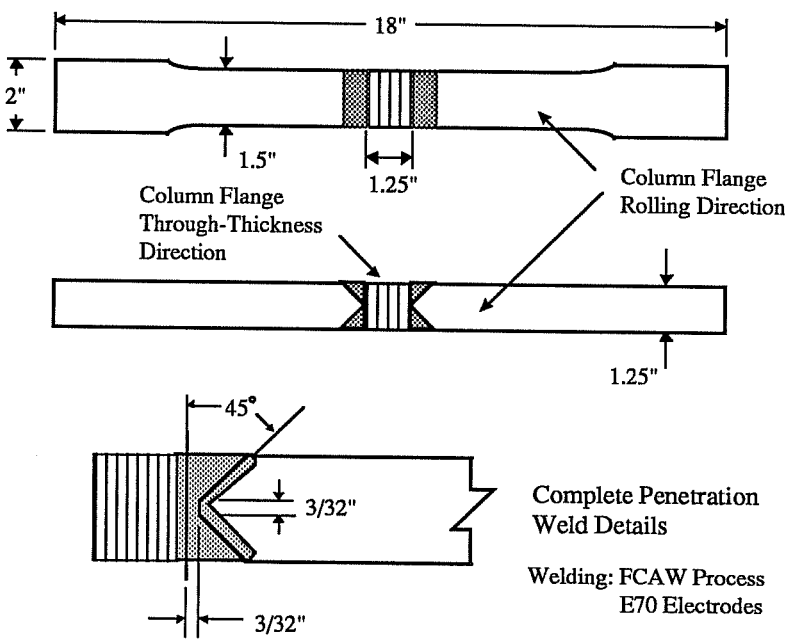

Figure 4.12 - Coupon 'B' for Testing Through-Thickness Properties of Column Flange

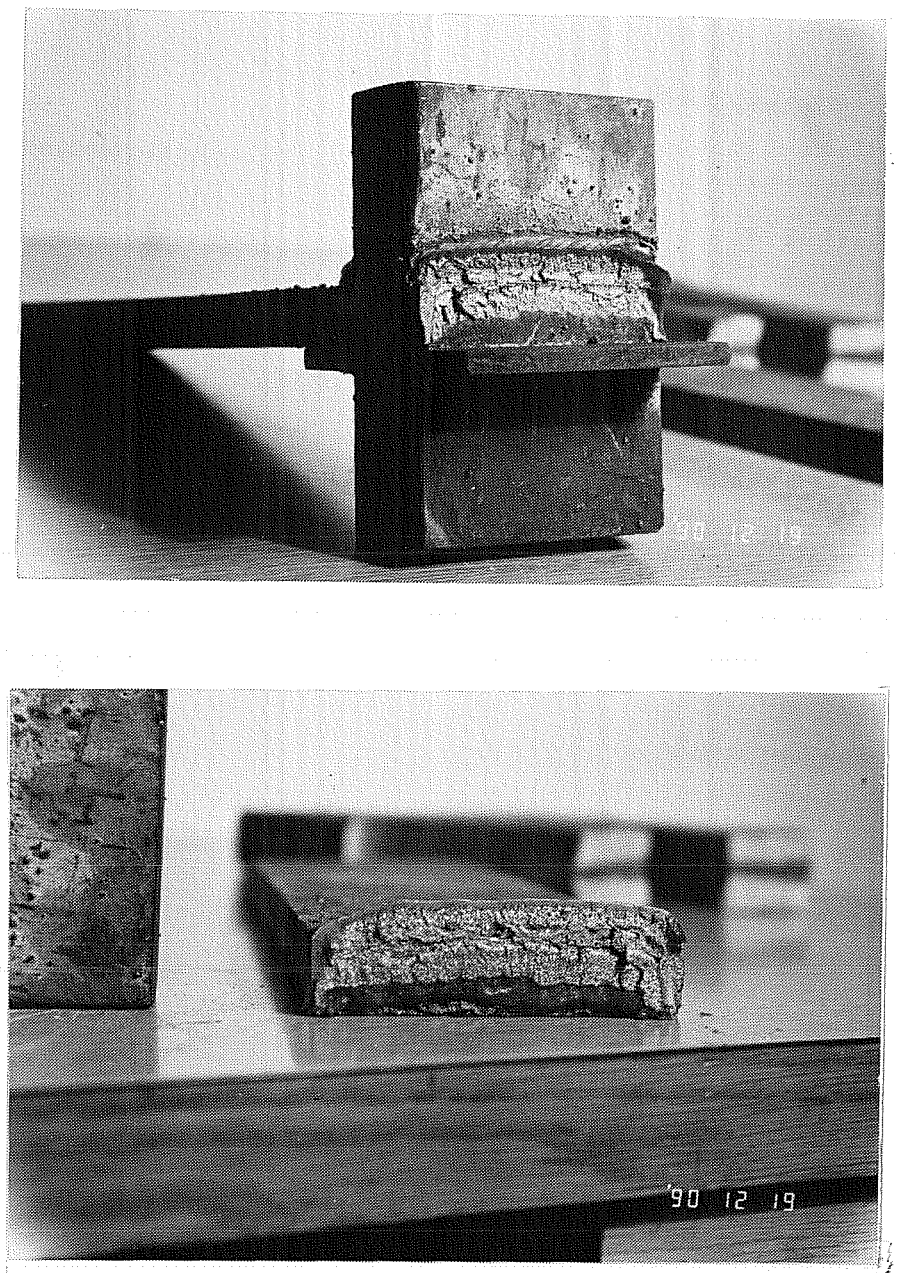

Figure 4.13 - Through-Thickness Coupon 'A' After Failure

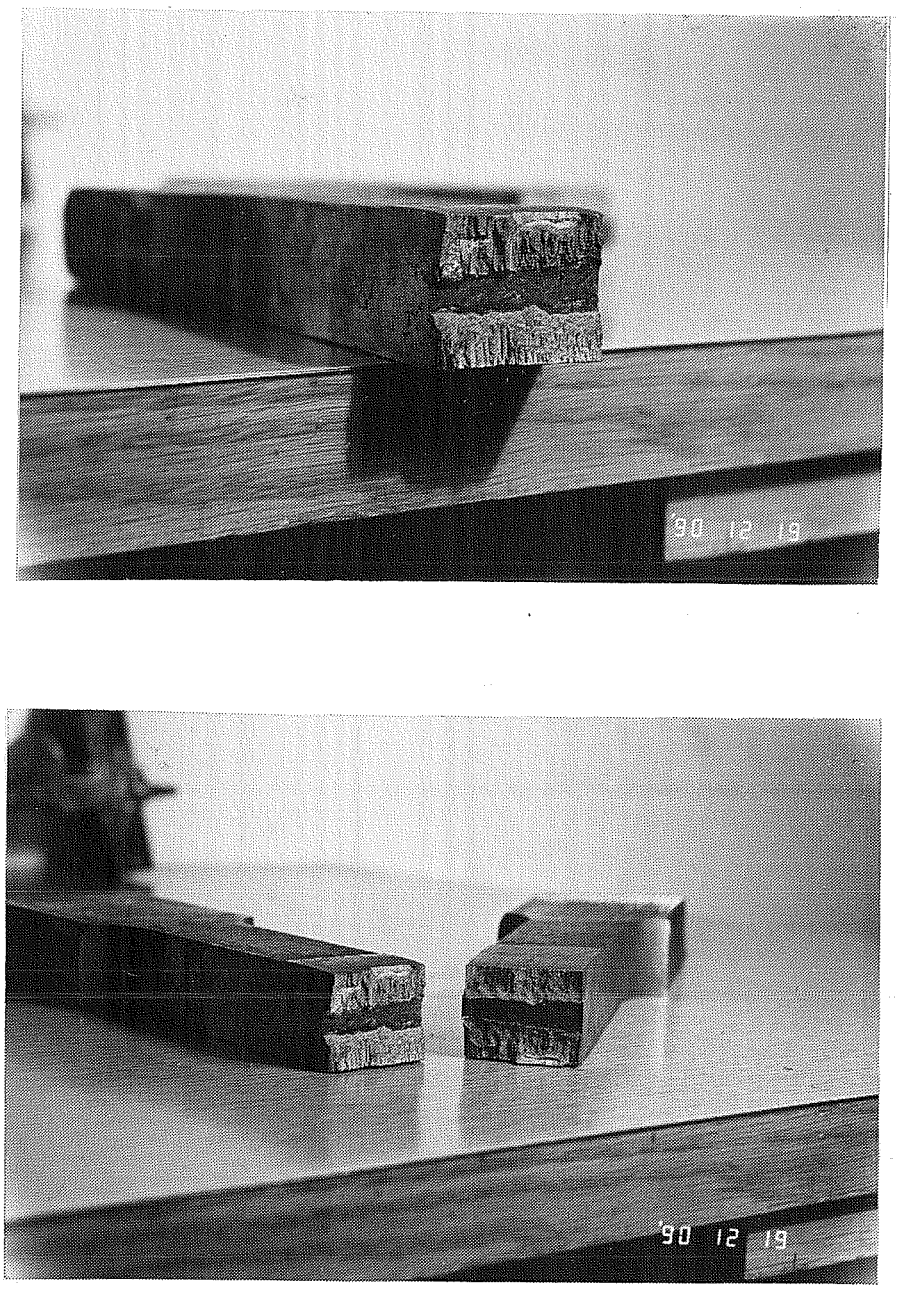

Figure 4.14 - Through-Thickness Coupon 'B' After Failure

about 2.5% compared to 27.3% in the regular coupon. Figure 4.14 shows the coupon after failure.

Both coupons failed after yielding occurred in the base metal, but prior to the development of significant strain hardening or inelastic deformation. These failures, similar to those observed in Specimens 1, 2, and 4, occurred even though the coupons were welded without the presence of significant shrinkage restraint. This suggests that the prime reason for the early failures witnessed on these coupons, as well as on Specimens 1, 2, and 4, was the quality of the welds rather than lamellar tearing related to weld shrinkage restraint. This again pointed out the crucial and vulnerable role of welds in the overall performance of the connection.

4.6 STEEL CHEMICAL ANALYSIS

As noted in Section 3.3.2, a chemical analysis was conducted on the column steel by an independent testing laboratory. The purpose of this test was to confirm the chemical analysis of the mill certificate. The results of the independent chemical analysis are shown in Table 4.5, for a sample taken from a column flange. The results are within specified limits of A572 Gr. 50, and agreed closely with the mill certificate for those elements reported on the mill certificate.

An independent chemical analysis was also conducted on a sample of steel taken from the flange of an A36 W21x57 beam used in this test program. The results are shown in Table 4.5, and are within specified limits for A36 steel.

Also shown in Table 4.5 is the carbon equivalent for each sample. According to information provided in Ref. 19, minimum AWS D1.1 preheat requirements should be adequate for the groove welds on the test specimens, based on the chemical analysis reported in Table 4.5.

TABLE 4.5

Chemical Analysis of Steel

Element	W12x136 Flange A572 Gr. 50	W21x57 Flange A36
carbon	.19 %	.08 %
manganese	1.26	.65
phosphorus	.013	.005
sulfur	.023	.027
silicon	.04	.18
nickel	.03	.12
chromium	.05	.10
molybdenum	.01	.03
copper	.11	.33
niobium	< .005	< .005
titanium	< .005	< .005
vanadium	.056	< .005
zirconium	< .005	< .005
aluminum	< .005	< .005
boron	< .0005	< .0005
CE (carbon equivalent)	.44	.28

$$CE = C + \frac{(Mn+Si)}{6} + \frac{(Cr+Mo+V)}{5} + \frac{(Ni+Cu)}{15}$$

5 - CONCLUSIONS AND RECOMMENDATIONS

5.1 GENERAL

All collected data and relevant information was provided in Chapters 3 and 4. This final chapter provides a discussion of that data. In addition, results from this testing program are compared with the results of previous testing programs in order to arrive at some general conclusions and recommendations.

5.2 DISCUSSION OF EXPERIMENTAL RESULTS

5.2.1 Review of Failure Modes

A study of Chapter 3 reveals two basic modes of failure in all of the specimens. The first was a sudden fracture at the weld-column interface across the entire width of the weld. This occurred at the bottom flange connection of Specimens 1, 2, and 4. The second mode was a gradual fracture in the beam flange, initiating typically at the edge of the flange, at or near the flange-weld interface. This occurred at the bottom flange of Specimens 3, 5, 6, and 8 and at the top flange of Specimen 7. In a few specimens, this fracture propagated further into the flange metal. On others, the fracture followed the flange-weld interface straight across the width of the flange.

As is noted in Chapter 3, the primary reason for the abrupt failures seen on Specimens 1, 2, and 4 was most likely the poor quality welds on the bottom flange. The major defect appeared to be lack of fusion of the weld into the column flange in a small region at the root of the weld. A subsequent review of the test results by a welding specialist further supported this conclusion [11]. The problem may have been aggravated by the small size of the web copes, making it more difficult for the welder to make a weld at the bottom flange. Concerns have been raised in the past [14] that increasing the

web cope size may lead to premature failures of beam flanges. No such direct effect was, however, observed. In all of the last four specimens provided with larger copes, the crack in the beam flange initiated at the flange edge and not at or near the web cope. Thus the most important effect of web cope size appeared to be increased difficulty of welding, leading to increased likelihood of weld defects.

Failures in Specimens 5 to 8 were observed at the weld-beam interface. These failures occurred after the beams had achieved substantially higher moments and plastic rotations as compared to Specimens 1, 2, and 4. Clearly, the welds were of higher quality in these later specimens. There were no obvious defects in the groove welds for Specimens 5 to 8. Nonetheless, these welds must still be viewed with suspicion. The fractures always appeared to initiate at the weld-beam interface, and in Specimens 5 and 8, propagated along the interface over almost the full width of the weld. After failure, the bottom beam flange of Specimens 5 and 8 appeared much the same as before welding, with the shape of the original bevel clearly visible. This suggests the possibility of defects at the weld-beam interface.

It is important to recall that all test specimens in this program were constructed by a commercial structural steel fabricator. All welders were qualified, and all complete penetration groove welds were ultrasonically tested by an independent welding inspection firm. Nonetheless, a number of welds were found to be inadequate when the connections were tested to destruction. This suggests the possibility that current industry practices for welding and quality control may not be adequate for this moment connection detail when subject to large cyclic deformations. Based on the very poor performance of Specimens 1, 2, and 4, which failed to achieve their estimated actual M_p, the adequacy of this detail for monotonic loading applications is also unclear.

5.2.2 Performance Criteria

Perhaps the most difficult part of this testing program is to develop criteria for evaluating the performance of the specimens. Strength and stiffness are important, but in the case of a severe earthquake, the most important issue is that of ductility. Different measures of ductility have been used in the past. These include ductility ratios, plastic rotation angles, and energy dissipation (calculated as the area enclosed by the hysteretic loops). Whatever measure is chosen to judge ductility, an estimate for actual ductility demands on connections in actual earthquakes is needed. Unfortunately, this information is rather limited.

A review of the limited analytical work done in this context, as well as the past experimental programs, suggest the plastic rotation capacity of a joint in a frame to be an appropriate measure of ductility. In this testing program, where the column panel zone did not undergo any significant plastic rotations, essentially all the plastic rotation came from the beam at the connection.

The question of selecting a minimum acceptable level of plastic beam rotation is a crucial one. No definite level can be set off-hand. One means for estimating plastic rotation demands at joints is to conduct inelastic dynamic frame analyses using past earthquake records. The plastic rotations can then be derived from the analyses. Unfortunately, this is not an easy task and very limited data is actually available. Two well documented inelastic analyses found were conducted by Tsai and Popov [24] and Roeder, Carpenter, and Taniguchi [21]. These references will be examined in the context of plastic rotation demands.

It should be remembered at this stage that the difficulties involved with comparing the available analytical data with the experimental results are also substantial. For one, the symmetric loading cycles used in the experiments are not usually seen in the analyses.

The plastic rotation at joints as determined from the analyses can actually be the result of a big rotation in just one direction or a number of inelastic cycles leaning to one side. Also to be realized is the fact that predicted rotation demands depend on the selected earthquake records. There is considerable uncertainty on what earthquake records should be used as a basis for establishing required plastic rotation capacities.

Tsai and Popov [24] analyzed a series of 6 story and 20 story MRFs under a variety of ground motion records, in order to study the effect of panel zone design on frame response. They report maximum beam plastic rotations on the order of 0.015 radian measured from the initial undeformed position. These maximum beam plastic rotations occurred in the 6 story frame under the unscaled 1966 Parkfield and 1985 Mexico City records. Further, they occurred in the frame in which the panel zone was designed for the shear produced by M_p of the beams. In frames designed with weaker panel zones, as permitted by the 1988 Blue Book and the 1988 UBC, beam plastic rotation demands were significantly reduced, as most of the plastic rotation occurred in the panel zone.

Roeder, Carpenter, and Taniguchi [21] analyzed 8 Story MRFs subjected to various earthquakes, primarily to assess the difference in performance of strong column-weak girder designs versus weak column-strong girder designs. Results of the analyses are also reported by Schneider, Roeder and Carpenter [22]. Their model apparently did not include a panel zone element, and therefore all plastic rotations are reported as flexural rotations occurring either in the column or in the beam. They report maximum beam plastic rotations for the strong column design, when the frame was subjected to the Imperial College Valley record of the 1979 Imperial Valley earthquake. For this case, a maximum beam plastic rotation of approximately .042 radian is developed, measured from the initial undeformed position, and occurs primarily as a single large cyclic of plastic rotation in one direction only.

Based on examination of the inelastic analyses noted above, it is believed that ± 0.015 radian constitutes a reasonable estimate of beam plastic rotation demand in MRFs subject to severe earthquakes. It is clear from a study of available inelastic dynamic analyses that actual beam plastic rotation demands are quite sensitive to frame design assumptions, frame inelastic modelling assumptions, and chosen earthquake records. Further, large inelastic deformation demands typically occur at only a limited number of joints within the frame. Thus the choice of ± 0.015 radian is based on judgement and interpretation of available data. Past experimental programs appear to have used similar levels of plastic rotation to evaluate performance of specimens [15,24].

Tsai and Popov [24] have shown that at joints in which the panel zone can effectively take part in developing inelastic action, the plastic rotation demand on the beam can be relaxed. However, significant panel zone participation cannot always be assured at all joints in a frame. Frames with very large and heavy columns may preclude panel zone yielding at some joints. Similarly, panel zone participation is not possible at connections to a column's weak axis, nor typically at connections to box columns. It should also be noted that some researchers have expressed the concern that large angular distortions of the panel zone may adversely affect the beam flange groove welds [15,18].

5.2.3 Performance of Specimens

Based on the criterion of ± 0.015 radian of beam plastic rotation at the connection measured from the original undeformed position, the performance of the specimens has been variable. It can be seen in Table 3.4 that the performance of Specimens 1, 2, and 4 was decidedly poor. All other specimens performed significantly better. However, Specimen 7 was the only one to achieve ± 0.015 radian. All others were judged as marginally acceptable, with plastic rotations varying from ± 0.009 radian to ± 0.013 radian.

5.2.4 Influence of Web Connection Details

As noted in Chapter 1, the project objectives were to investigate the relationship between bolt tensioning and supplementary web welds and whether one can be substituted for the other. It was also desired that a Z_f/Z ratio be determined above which supplementary welds between the beam web and shear tab need not be provided. The tests, however, revealed no clear influence of Z_f/Z or web connection details on ductility.

The web connection details showed an influence on the strength characteristics of the specimens as indicated by Table 4.1. This trend is not apparent for the first five specimens because of the poor quality flange welds on Specimens 1, 2, and 4, making comparisons with Specimens 3 and 5 difficult. However, Specimens 6, 7, and 8 do indicate that increased strength is achieved by increased participation of the beam web in resisting moments.

Although the tests showed some evidence of the effect of web connection details on strength, there was no clear evidence that the Z_f/Z ratio or the web connection details have a significant influence on ductility. Specimens 5 and 6, for example, both had bolted webs, but had different Z_f/Z ratios (0.75 for Specimen 5 and 0.67 for Specimen 6). Yet, the plastic rotation was nearly identical for these two specimens. Compare also Specimens 6, 7, and 8. These specimens had the same Z_f/Z ratio, but had increasing degrees of web participation. Specimen 7, with the supplemental web welding, did develop greater plastic rotation than Specimen 6, which had only a bolted web. However, Specimen 8, with a fully welded web, developed less plastic rotation than either Specimens 6 or 7. The reasoning developed in Chapter 1 that increased web participation would improve strength and consequently, ductility characteristics therefore turned out to be only partially correct based on these tests, with the effect of web connection details on ductility still unclear.

The most important observation on the behavior of the specimens was the

variability found in the flange weld performance. Not only did it obscure the influence of web connection details and Z_f/Z ratio, but also turned out to be the single most influential parameter in dictating the behavior of specimens. The potential amount of variability is clearly understood when the performance of Specimens 4 and 5 is taken into account. Although nominally identical, and both welded and ultrasonically inspected by AWS certified welders and an ASNT and AWS certified inspector, one achieved almost 6 times the inelastic deformations of the other.

The main question addressed by this program was about a possible relaxation in the 1988 UBC requirement for supplementary web welds to nominally develop 20% of web plastic moment if $Z_f/Z \leq 0.70$. In this testing program, Specimens 3 and 7 were provided with the supplementary welds. These specimens performed somewhat better than specimens without these welds. Realizing that the reason for the better performance may not be directly related to the presence of the web welds, the fact remains that these specimens did perform somewhat better. Also, there is no contrary evidence to show that any specimen without these welds would have shown equivalent performance. Consequently, based on these tests, there appears to be no justification to relax the UBC detailing requirement pertaining to supplementary web welds as given in Section 2722 (f) 2B of the 1988 edition.

5.3 COMPARISON WITH EARLIER TESTS

It is always beneficial to compare the test results with results of similar work done elsewhere. A logical question arises after going through this report of whether or not these results are in general conformity with what has been reported in the past. If the answer is no, then an effort is needed to assess the reasons for the apparent differences. The intent of this section is to provide some comparisons with past tests, as well as to make some general observations on the performance of the welded flange-bolted web detail.

Results of this investigation were compared with results of tests conducted by Popov and Stephen [16], Popov, Amin, Louie and Stephen [15], Tsai and Popov [24], and Anderson and Linderman [8,9]. Although this is not an exhaustive database, it is believed to represent a significant portion of cyclic tests performed on large scale specimens in the U.S. Table 5.1 provides a brief summary of test specimens and test results from these investigations. Only beam-to-column flange connections with bolted webs, with or without supplemental web welds, are included in the table. The beam plastic rotations, θ_p, reported in the table were calculated as one-half of the maximum plastic rotations measured from the total width of the hysteretic loops, as a basis for comparing results from many different tests. The tests by Popov, Amin, Louie and Stephen [15] included significant inelastic panel zone deformations. However, only the plastic rotation attributable to the beam is included in the θ_p as listed in the table.

Figure 5.1 graphically displays the beam plastic rotations in the form of bar charts. Plastic beam rotations for specimens listed in Tables 5.1 as well as for specimens from the present investigation are included in the bar charts. Specimen Nos. 1 and 3 from the investigation by Popov, Amin, Louie and Stephen [15] have been excluded from the bar charts, as these specimens violate current code requirements for continuity plates.

Several observations can be made from the data in Table 5.1 and Figure 5.1:

1. The results of the present test program, in terms of the magnitude and variability of beam plastic rotations and in terms of the types of failures observed, are similar to previous test programs.
2. There is a large variability in performance of test specimens in both the current test program as well as in previous test programs.
3. Premature failures due to poor welds have been observed in both the current test program as well as in previous test programs. Note that *all* specimens listed in Table 5.1 and represented in Figure 5.1 were

constructed by commercial structural steel fabricators. All specimens, other than for the current test program, were constructed in California.

4. A significant number of specimens have not achieved beam plastic rotations of 0.015 radian. A rather large number have not even achieved 0.005 radian.
5. Specimens with $Z_f/Z > 0.70$ have shown better performance, on average, than those with $Z_f/Z \leq 0.70$. Both groups of specimens, however, show variable performance.
6. Specimens with supplemental web welds (all have been on beams with $Z_f/Z \leq 0.70$) have performed somewhat better on average than their counterparts with no web welding. There is again, however, considerable variability.

5.4 RECOMMENDATIONS

As noted in Section 5.2.4, the current UBC detailing requirement pertaining to supplementary web welds (Section 2722 (f) 2 B of the 1988 edition) should not, at present, be relaxed. Although there is no clear evidence that the supplemental web welds significantly influence ductility, specimens provided with these welds have, on average, shown somewhat better performance.

An important observation from this and previous test programs is that the welded flange - bolted web connection detail has shown highly variable performance. While some specimens have performed satisfactorily, a significant number have demonstrated poor or marginal performance in cyclic test programs. Some of this variability can be attributed to the influence of the Z_f/Z ratio and web connection details. However, a great deal of the variability also appears to be related to the performance of the beam flange groove welds.

The final recommendation of this investigation calls for a thorough review of current U.S. industry practice for seismic steel moment connections. The results of this and previous test programs leads to questions on the reliability of the welded flange - bolted web detail for severe seismic applications. A careful review of design and detailing practices, as well as welding and quality control issues is needed.

Table 5.1
Beam Plastic Rotations - Results of Other Investigations
(Welded Flange - Bolted Web Connections to Column Flange)

Investigators	Spec. No.	Beam	Z_f/Z	Column	Web Connection	θ_p (rad)	Failure Description	Comments
Popov and Stephen [Ref. 16]	1	W18x50	0.74	W12x106 (A36)	5 - 7/8" A325	0.016	sudden fracture at weld-column interface at bottom flange	
	3	W18x50	0.74	"	5 - 3/4" A325	0.021	fracture in top beam flange	±0.013 rad of cyclic load, followed by monotonic load to failure
	4	W18x50	0.74	"	4 - 3/4" A325	0.017	sudden fracture at weld-column interface at bottom flange	
	5	W24x76	0.71	"	7 - 7/8" A325	0.030+	no failure	±.017 rad of cyclic load, followed by monotonic load
	6	W24x76	0.71	"	7 - 1" A325	0.012	fracture at weld-column interface at bottom flange	
	8	W18x50	0.74	"	no web connection	0.011	fracture in bottom beam flange initiating at cope	
Popov, Amin, Louie and Stephen [Ref. 15]	1	W18x40	0.70	welded W-shape: .625"x8.25" flgs. .375"x16.75" web with 3/16" doubler (A572 Gr. 50)	5 - 3/4" A325	0.005	sudden fracture at weld-beam interface at top flange	no continuity plates (does not satisfy 1988 UBC continuity plate req'ts) total plastic rotation (beam + panel zone) =.009 rad
	2	W18x40	0.70	"	5 - 3/4" A325	0.004	fracture at weld-beam interface at bottom flange	same as Spec. 1, except 1/4" continuity plates provided total plastic rotation (beam + panel zone) =.027 rad

continued

Table 5.1 (continued)

Investigators	Spec. No.	Beam	Z_f/Z	Column	Web Connection	θ_p (rad)	Failure Description	Comments
Popov, Amin, Louie and Stephen [Ref. 15] (continued)	3	welded W-shape: 1"x8.375" flgs. .56"x16.75" web	0.79	welded W-shape: 1.25"x8.5" flgs. .69"x16.625" web with 3/8" doubler (A572 Gr. 50)	5 - 1" A325	0.002	sudden fracture at weld-column interface at bottom flange	no continuity plates (does not satisfy 1988 UBC continuity plate req'ts) total plastic rotation (beam + panel zone) =.013 rad
	4	"	0.79	"	"	0	fracture at continuity plate weld, followed by fracture at weld-column interface at beam flange	same as Spec. 3, except 1/2" continuity plates provided total plastic rotation (beam + panel zone) =.014 rad
	5	"	0.79	"	"	0	sudden fracture at weld-column interface at beam flange; evidence of lamellar tearing at fracture	repaired version of Spec. 4 total plastic rotation (beam + panel zone) =.002 rad
	6	"	0.79	same as above, except no doubler plate	"	0	fracture at weld-column interface at beam flange	similar to Spec. 4, except no doubler plate total plastic rotation (beam + panel zone) =.012 rad

continued

Table 5.1 (continued)

Investigators	Spec. No.	Beam	Z_f/Z	Column	Web Connection	θ_p (rad)	Failure Description	Comments
Popov, Amin, Louie and Stephen [Ref. 15] (continued)	7	W18x71	0.75	W21x93 with 3/8" doubler (A572 Gr. 50)	4 - 1" A490	0.007	fracture of beam flange outside of weld	total plastic rotation (beam + panel zone) =.027 rad
	8	"	0.75	"	"	0.008	fracture of beam flange outside of weld	same as Spec. 7, except different flange weld root opening total plastic rotation (beam + panel zone) =.029 rad
Tsai and Popov [Ref. 24]	3	W18x35	0.66	W12x133	4 - 1" A325	0.008	fracture at bottom beam flange initiating at web cope	
	5	W21x44	0.62	W14x176	5 - 1" A325 + 10% web weld	0.007	fracture at weld-beam interface at top flange	
	13	W18x35	0.66	W14x159	4 - 1" A325 + 20% web weld	0.012	fracture of top flange outside of weld, initiating at web cope	
	14	W21x44	0.62	W14x159	5 - 1" A325 + 20% web weld	0.020	fracture of top flange outside of weld, initiating at web cope	
	15	W18x35	0.66	W14x159	4 - 1" A325 (twist-off bolts)	0	sudden fracture at top flange weld	

Table 5.1 (continued)

Investigators	Spec. No.	Beam	Z_f/Z	Column	Web Connection	θ_p (rad)	Failure Description	Comments
Tsai and Popov [Ref. 24] (continued)	16	W21x44	0.62	W14x159	5 - 1" A325 (twist-off bolts)	0.003	sudden fracture at weld-beam interface at top flange	
	17	W18x35	0.66	W14x159	4 - 1" A325 (twist-off bolts)	0.013	fracture initiating at weld-beam interface at edge of flange	
	18	W21x44	0.62	W14x159	5 - 1" A325 (twist-off bolts)	0.013	fracture of top flange away from weld, initiating at web cope	
Anderson and Linderman [Refs. 8,9]	13	W16x40	0.75	W12x136	4 - 7/8" A325	0.015	fracture of bottom beam flange, initiating at web cope	some panel zone yielding noted
	20	W16x40	0.75	W12x65 with 3/8" doubler	4 - 7/8" A325	0.010	fracture of top beam flange	

Notes for Table 5.1: All members A36, except where noted
All specimens constructed by structural steel fabricators

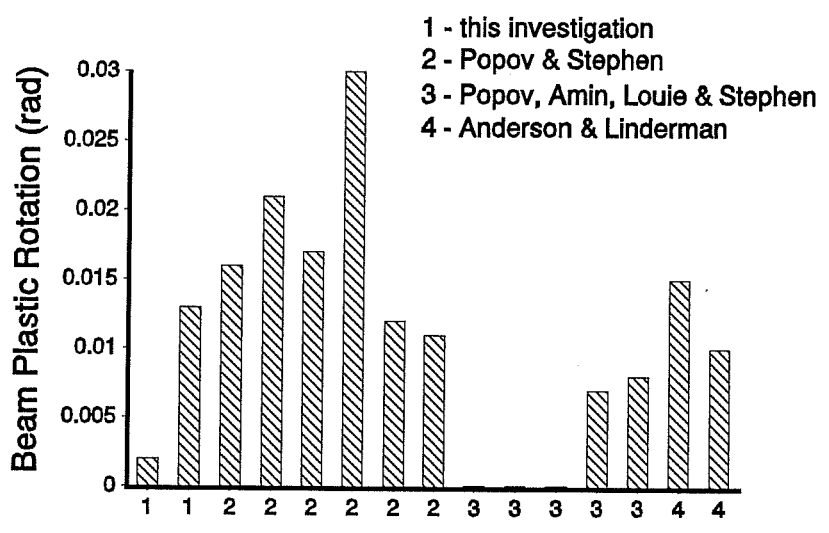

(a) Specimens with $Z_f/Z > 0.70$

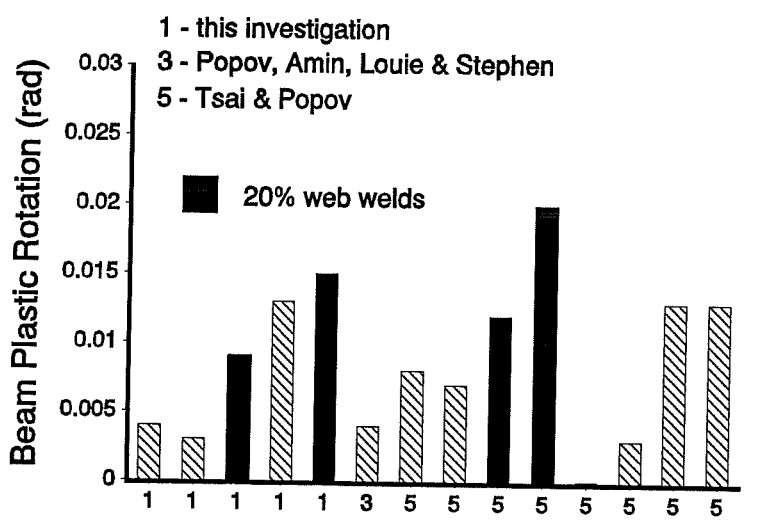

(b) Specimens with $Z_f/Z \leq 0.70$

Figure 5.1 - Comparison of Beam Plastic Rotations with Past Tests

REFERENCES

1. American Institute of Steel Construction, Inc., "Commentary on Highly Restrained Welded Connections," *Engineering Journal*, 3rd Quarter 1973.

2. American Institute of Steel Construction, Inc., *Manual of Steel Construction - Allowable Stress Design*, 9th Edition, Chicago, Illinois, 1989.

3. American Institute of Steel Construction, Inc, *Seismic Provisions for Structural Steel Buildings, Load and Resistance Factor Design*, Chicago, Illinois, 1990.

4. American Institute of Steel Construction, Inc, *Supplement 1 to the LRFD Specification for Structural Steel Buildings*, Chicago, Illinois, 1989.

5. American Society for Nondestructive Testing, *Recommended Practice No. SNT-TC-1A*, Columbus, Ohio, 1988.

6. American Welding Society, *Standard for AWS Certification of Welding Inspectors*, AWS QC-1-88, Miami, Florida, 1988.

7. American Welding Society, *Structural Welding Code - Steel*, AWS D1.1-88, Miami, Florida, 1988.

8. Anderson, J. C. and Linderman, R. R., "Steel Beam to Box Column Connections," *Report No. CE 91-03,* Department of Civil Engineering, University of Southern California, Los Angeles, California, December 1991.

9. Anderson, J. C. and Linderman, R. R., "Post Earthquake Repair of Welded

Moment Connections," *Report No. CE 91-04,* Department of Civil Engineering, University of Southern California, Los Angeles, California, May 1991.

10. Building Seismic Safety Council, *NEHRP Recommended Provisions for the Development of Seismic Regulations for New Buildings,* Federal Emergency Management Administration, 1988.

11. Collin, A. L., personnel communication

12. International Conference of Building Officials, *Uniform Building Code*, Whittier, California, 1988.

13. Krawinkler, H., "Shear in Beam-Column Joints in Seismic Design of Steel Frames," *Engineering Journal,* American Institute of Steel Construction, Inc., 3rd Quarter, 1978.

14. Lee, S.J. and Lu, L. W., "Cyclic Tests of Full-Scale Composite Joint Subassemblages," *Journal of Structural Engineering,* ASCE, Vol. 115, No. 8, August 1989.

15. Popov, E. P., Amin, N. R., Louie, J. and Stephen, R. M., "Cyclic Behavior of Large Beam-Column Assemblies," *Engineering Journal,* American Institute of Steel Construction, Inc., 1st Quarter, 1986.

16. Popov, E. P. and Stephen, R. M., "Cyclic Loading of Full-Size Steel Connections," *Bulletin No. 21,*American Iron and Steel Institute, February 1972.

17. Popov, E. P. and Tsai, K. C., "Performance of Large Seismic Steel Moment

Connections Under Cyclic Loads," *Proceedings, Structural Engineers Association of California 1987 Annual Convention,* San Diego, California, 1987.

18. Popov, E. P., Tsai, K. C. and Engelhardt, M. D., "On Seismic Steel Joints and Connections," *Proceedings, Structural Engineers Association of California 1988 Annual Convention,* Hawaii, 1988.

19. Preece, F. R. and Collin, A. L., "Structural Steel Construction in the '90's," *Steel Tips,* Structural Steel Education Council, Walnut Creek, California, September 1991.

20. Research Council on Structural Connections, *Specification for Structural Joints Using A325 or A490 Bolts,* 1985.

21. Roeder, C. W., Carpenter, J. E. and Taniguchi, H., "Predicted Ductility Demands for Steel Moment Resisting Frames," *Earthquake Spectra,* Earthquake Engineering Research Institute, May 1989.

22. Schneider, S. P., Roeder, C. W. and Carpenter, J. E., "Seismic Performance of Weak-Column Strong-Beam Steel Moment Resisting Frames," Department of Civil Engineering, University of Washington, Seattle, Washington, September 1991.

23. Structural Engineers Association of California, *Recommended Lateral Force Requirements,* San Francisco, California, 1988.

24. Tsai, K. C. and Popov, E. P., "Steel Beam-Column Joints in Seismic Moment Resisting Frames," *Report No. UCB/EERC - 88/19,* Earthquake Engineering Research Center, University of California, Berkeley, California, 1988.